Cell and Material Specific Dual-Functional Peptides for Enhancing Mesenchymal Stem Cell Migration for Bone Tissue Engineering

by

Eric Madsen

A dissertation submitted in partial fulfillment
of the requirements for the degree of
Doctor of Philosophy
(Oral Health Sciences)
in the University of Michigan
2023

Doctoral Committee:

Professor David Kohn, Chair
Professor Renny Franceschi
Associate Professor Darnell Kaigler
Professor Yuji Mishina
Professor Jan Stegemann

Eric J. Madsen

ericmads@umich.edu

ORCID iD: 0009-0003-0550-5163

Dedication

For all my friends and family who helped me along the way.

Acknowledgements

This work would not have been possible without the support of my advisor David Kohn. He has provided me excellent mentorship and encouraged me to pursue my own scientific ideas. Throughout my time in his lab, he has constantly challenged me to become an independent investigator, and I wouldn't be where I am today without his guidance. I would also like to thank my committee members, Yuji Mishina, Renny Franceschi, Jan Stegemann, and Darnell Kaigler who provided important feedback to help guide my research.

I would also like to thank the members of the Kohn Lab: Genny Romanowicz, Gurjit Mandair, Thomas Davidson, Morgan Bolger, Sam McGoldrick, Merjem Mededovic, Benjamin Sexton, and Carlos Urrego. They have all been excellent colleagues and have provided so much support over the years. I would also like to thank the undergraduate students who have assisted me in my many experiments over the years: Tia Calabrese, Madison Wahlsten, and Seungmeen Rhee. Many thanks to the staff of the Office of Research, the Biologic and Materials Sciences and Prosthodontics Department, and Grants and Contracts for helping with the logistical difficulties of my program. Also thank you to my fellow OHS buddies in the Oral Health Sciences program. Our comradery over the years has given me the motivation to keep going even through difficult times, and we will remain lifelong friends.

I am very thankful for all my friends and family who have supported me along the way. I would not have been able to complete this challenging program without their love and encouragement.

Table of Contents

List of Tables

List of Figures

Abstract

Millions of bone grafting procedures are performed annually to repair bone defects. While autografts and allografts are used clinically for such purposes, their limitations have motivated research into synthetic graft materials. Although numerous biocompatible materials have been developed, lack of bioactivity often results in suboptimal results. The use of bioactive peptides on the surface of a material can help create an interface between materials and specific cells in living tissue. Using phage-display technology, a dual-functional peptide DPI-VTK (GG**DPI**YALSWSGMAGGGS**VTK**HLNQISQSY) that contains both a mesenchymal stem cell (MSC) binding domain **DPI**YALSWSGMA (DPI) and a hydroxyapatite binding domain **VTK**HLNQISQSY (VTK) was developed. Because of the importance of adhesion molecules for cellular migration, such a peptide could not only enhance the adhesion of MSCs to hydroxyapatite but could also promote the specific migration of host MSCs, bypassing the need for cell transplantation. Additionally, this peptide could be combined with BMP peptides to create dual-functional osteoconductive and osteoinductive interfaces that encourage the homing of MSCs along with their subsequent differentiation. **The overall hypothesis of this dissertation is that dual-functional MSC and apatite binding peptide DPI-VTK along with a dual-functional BMP and apatite binding peptide KIP-VTK will increase bone regeneration with mineralized scaffolds by increasing the migration of MSCs and their subsequent osteogenic differentiation.**

This dissertation proposed the following aims to test this hypothesis: 1) determine if peptide DPI-VTK can increase MSC specific migration *in vitro and in vivo* to support bone formation; 2)

determine if peptide DPI-VTK has a synergistic effect with BMP derived peptide KIP-VTK to increase osteogenic differentiation.

In transwell assays, human iPS-MSCs showed significantly greater migration (6-fold increase) over no peptide controls when DPI-VTK was used as a chemoattractant. Non-MSC controls such as MC3T3 cells and mouse dermal fibroblasts (MDFs) showed no statistically significant effect on migration from DPI-VTK. When MSCs were incubated in transwells with peptides DPI-VTK, DPI, and VTK, migration was equivalent for DPI-VTK and DPI, while VTK had no difference from the control, demonstrating that the DPI peptide, but not VTK, can induce migration. Primary calvarial cells had a significant increase in migration (>2-fold increase) when exposed to DPI-VTK. After 1 week in-vivo, immunohistochemical staining for MSC markers demonstrated increased migration of CD90 and CD200 positive cells. After 8 weeks, micro-CT demonstrated a significant increase in regenerated bone volume in the DPI-VTK group versus no peptide control. Coupling peptide VTK to BMP derived peptide KIP increased absorption to mineral. When co-absorbed with DPI-VTK, KIP-VTK failed to generate a synergistic effect on osteogenic differentiation.

In conclusion, this research has demonstrated that targeting specific cell populations with cell and material binding peptides such as DPI-VTK is possible. Due to the widespread use of hydroxyapatite-based biomaterials in craniofacial bone grafting, DPI-VTK could be useful clinically for enhancing their ability to promote migration of host MSCs. Developing dual-functional material that both recruits host cells and induces differentiation could be a key strategy for regenerating large-volume defects without the need for exogenous cells or autografts.

Chapter 1: Introduction

1.1 Clinical Significance

Despite bone's regenerative properties, bone grafting is often necessary to heal defects and restore function. Millions of bone grafts are performed annually for various purposes such as non-union fractures, spinal fusion, alveolar ridge augmentation, and restoration of large defects following cancer resection [1–4]. Bone grafting is particularly important for oral and craniofacial applications, as the alveolar ridge bone that supports the teeth cannot regenerate on its own following bone loss due to periodontal disease or tooth loss [2]. When placing dental implants, it is critical that there is sufficient bone width and height to support the implant. A significant number of dental implants placed require bone augmentation prior to placement due to insufficient bone [5,6].

The current standard in bone grafting is to graft autogenous bone from another site to the defect. Sources of autogenous bone include the mandibular ramus, mandibular symphysis, the iliac crest, and fibula [1,2,7]. Autogenous bone is an ideal material for this purpose since it already contains the appropriate osteogenic cells, growth factors, extracellular matrix, and micro-environment to facilitate regeneration. A key limitation of autografts is donor site morbidity, which may include postoperative pain, infection, scarring, and increased surgical recovery time [1]. For example, with iliac crest grafting, as many as 91.3% of patients experience donor site pain, 54.6% have problems with ambulation after the surgery, and 34.8% have paresthesia [8].

Because of the risk of donor site morbidity, only a limited amount of tissue may be safely harvested at a time, and certain patients may not be appropriate candidates due to preexisting health conditions [8].

Allografting and xenografting, the grafting of donor human or animal bone respectively, are useful alternatives to autografting since they avoid donor site morbidity. These materials can take several forms such as block grafts, granulated grafts, cortical bone, trabecular bone, bone mineral, and demineralized bone matrix [2,9,10]. In order to render these graft materials safe for transplantation and avoid risks such as transmission of pathogens and immunogenic reactions, allografts/xenografts undergo extensive processing such as sterilization, decellularization, and demineralization which significantly decreases the bioactivity compared to autografts. [2,11,12]. Allografts/xenografts, however, are often used in combination with autografts to increase the total volume of the graft. Another option for bone grafting is to use alloplasts, which are synthetic graft materials. While these materials, such as tricalcium phosphate, do have some bioactivity, they are still not as osteogenic as autografts [9,10].

The disadvantages of autografting and allografting/xenografting have motivated tissue engineering approaches to regenerate bone. Tissue engineering is based on the principle that tissue regeneration can be achieved by combining the appropriate cells, signals, and biomaterials. Designing an appropriate biomaterial that can deliver the tissue-appropriate signals for cellular functions such as proliferation and differentiation is a key challenge for tissue engineering [13].

1.2 Bone Tissue Engineering

1.2.1 Biomaterials for Bone Tissue Engineering

In native tissues, cells are bound within a matrix of extracellular proteins called the extracellular matrix (ECM). The cells can interact with this matrix through a multitude of different receptors, most notably the integrins. Binding of the cells to the ECM not only allows for adhesion, but also stimulates signals for cellular functions such as survival, proliferation, and differentiation [14]. These connections also allow for the conduction of mechanical forces from the matrix to the cells, which is particularly important for bone physiology. While the ECM can be used as a biomaterial for bone regeneration in the form of either autografts (ECM with living cells) or allo/xenografts (processed ECM), the limitations of these techniques sometimes necessitate the use of other materials.

When foreign materials are implanted into the body, serum proteins rapidly adsorb onto the surface. Once cells begin to adhere to this layer, they begin to secrete ECM matrix proteins. Less biocompatible materials will be encapsulated within a thick fibrous capsule while more biocompatible materials will have a thin fibrous interface, as is the case in osseointegration [15,16]. In biomaterial design, it is important to consider the properties of the ECM. ECM properties such as stiffness and bioactivity should be recreated in the biomaterial to ensure proper functioning of the tissue's resident cells. The bone matrix is composed of proteins, most notably collagen, and bone mineral in the form of carbonated hydroxyapatite. The mineral

component of bone provides appropriate stiffness and strong resistance to compressive forces while the collagen component provides elasticity and toughness [17].

Being the key component of bone mineral, hydroxyapatite, has received much attention as a therapeutic biomaterial. Stoichiometric hydroxyapatite, however, is not suitable due to its non-resorbable nature. While non-resorbable materials may be appropriate for certain applications such as for biomedical implants, achieving true tissue regeneration requires a resorbable material that can be gradually replaced by native tissue. The hydroxyapatite in native bone mineral contains various ion substitutions such as carbonate and magnesium that modify the crystallinity and increase resorbability [18]. Biomimetic carbonated apatite that mimics the composition of bone mineral can be precipitated from simulated body fluid, a solution of various salts mimicking the ion composition of body fluid. This solution is useful for coating biodegradable polymers with a layer of bone like mineral to create scaffolds for bone regeneration [17]. Such biomimetic mineral scaffolds allow for delivery of mineralized biomaterials that have similar composition to native bone mineral while retaining control of characteristics such as degradation rate and porosity. Bone-like-mineral created with simulated body fluid also allows for the use of biomimetic mineral without the limitations associated with harvesting native bone mineral in the form of allo/xenografts.

1.2.2 Mesenchymal Stem Cells in Bone Regeneration

Mesenchymal stem cells (MSCs) are a classification of multi-potent stem/progenitor cells that exist in several different tissues. Originally identified in bone marrow as bone marrow

stromal cells, other cell types such as adipose stem cells, periosteal stem cells, and pericytes can also be considered as MSCs. A unifying definition of MSCs remains elusive, and some authors have argued that the term should be retired [19]. Various genetic and protein markers have been proposed to identify MSCs such as CD90, CD73, and CD105 [20]. The presence of these markers can vary depending on the tissue source of the MSCs, and many non-MSC cell types can also express these markers. The most definitive properties of MSCs are their multipotent differentiation into bone, cartilage, and adipose tissue. These facts suggest that MSCs should be considered as a broad category of many different cells sharing a similar phenotype rather than a discreet cell type. In bone healing, MSCs are critically important due to their ability to migrate into the wound, modulate the immune system, and differentiate into osteoblasts to secret new bone matrix.

MSCs have received much attention in the tissue engineering field due to their ability to regenerate multiple tissue types, particularly bone [21]. MSCs, typically bone marrow stromal cells, have been seeded onto various biomaterial scaffolds and transplanted into animal models and in human clinical trials to regenerate bone defects with much success. In animal studies involving mice, MSCs are typically harvested by flushing the marrow cavities of the femora and tibiae and culturing the resulting cell suspension on tissue culture polystyrene (TCPS). Since bone marrow stromal cells are known to have adherence to TCPS, expanding them on TCPS helps select for the BMSCs over the other cells present in the bone marrow. In human trials, BMSCs can be harvested by obtaining bone marrow aspirates from pelvis and purifying the BMSCSs through FACS [22]. Unlike pluripotent stem cells which can only be obtained from embryos or genetic induction, multipotent stem cells such as MSCs are present in the body

through adulthood. This allows for autogenous harvesting and transplantation of MSCs without any risks of immune rejection [23].

1.2.3 Cell-homing Approach to Tissue Engineering

While many tissue engineering approaches have focused on the transplantation of exogenous cells via biomaterial scaffolds, this approach is not always feasible due to logistical hurdles. For example, cells must be collected from patients ahead of time and expanded under sterile conditions, which requires expensive equipment and dedicated staff. As the number of clinics offering MSC based therapies increases, there is increasing concern about the safety and quality control practices [24]. Also, the survival rate of the transplanted cells may also be low [25]. The limitations of cellular transplantation have motivated alternative approaches to regenerate tissue. The presence of regenerative cells such as MSCs in bone and other tissues creates the possibility of regeneration utilizing only endogenous cells. By developing methods to specifically target and mobilize cells nearby a defect, the need for cellular transplantation could be bypassed. Cell-homing approaches to tissue engineering focus on the transplantation of acellular scaffolds to stimulate the migration and adhesion of host cells into the defect [21,26].

Induction of cellular migration can be accomplished by administering chemotactic factors into the defect along with the material. Such factors can include recombinant proteins such as PDGF, SDF-1, and BMP-2 [27]. Inducing host cell migration has the advantage of avoiding logistical difficulties with harvesting host cells prior to surgery and lowering healthcare costs. Cell specificity is important, and osteogenic cells such as MSCs should be targeted rather than other cells such as fibroblasts and epithelial cells which may form soft tissue rather than osseous

tissue. Encouraging early migration of MSCs into the defect is critical as they can direct the healing response by modulating immune cells and secreting chemotactic factors to drive the migration of other cell types [28]. While many types of cells are important for bone regeneration, specifically targeting MSCs in the early stages is critical since the presence of other cells could block the migration of MSCs, inhibit the regenerative process, and even form undesirable tissues such as fibrous or epithelial tissue rather than bone. Guided bone regeneration is a technique used clinically to regenerate bone defects that uses semi-permeable membranes that encourage migration of osteogenic cells while excluding epithelial cells [29]. Currently used chemotactic agents, however, lack cellular specificity and a MSC specific chemoattractant remains elusive.

1.2.4 BMP Therapies

In addition to promoting migration of MSCs, it is important to induce their differentiation into osteoblasts and stimulate secretion of new bone matrix. Some of the most powerful stimulators of osteogenic differentiation are the bone morphogenetic proteins (BMPs). While the many proteins in the BMP family play different roles in different tissue types, BMP-2 and BMP-7 both stimulate bone formation and are FDA approved for use in clinical bone grafting [30]. BMP-2 and BMP-7 both bind to the BMP type I and type II receptors, triggering the phosphorylation of Smad 1/5/8 which then translocate to the nucleus to activate osteogenic genes such as RUNX2, the master regulator of osteogenesis [31]. BMP-2 and BMP-7 are produced as recombinant proteins by Chinese Hamster Ovarian cells and sold commercially as a lyophilized powder. The proteins are reconstituted in saline solution before use and usually delivered along with a collagen sponge into the defect [32]. While BMPs have been successful in the clinic, there

are several downsides that have yet to be addressed. To drive the formation of bone as well as compensate for degradation in vivo, the BMPs must be delivered in supraphysiological doses. Typically, several milligrams of BMP are used at a time for each patient. At a cost of several thousand dollars per milligram, these high doses result in very high costs for treatment. Some patients may experience strong inflammatory responses to the BMP proteins, which may ironically lead to bone resorption. BMPs are also capable of forming ectopic bone in nearby soft tissue due to diffusion of the soluble BMPs from the site, thereby inhibiting their function [3]. These challenges have motivated the investigation of strategies to mitigate the negative effects of BMPs, including developing controlled release systems and deriving smaller molecular weight peptides from the BMP sequence [33,34].

1.2.5 Peptide Therapies

To improve the bioactivity of materials, functionalization with biomolecules is often necessary. Recombinant proteins have been used for this purpose, but are limited by their high cost of manufacture [35]. Globular proteins can also lose activity when absorbed or chemically coupled to biomaterial surfaces due to deformation of their complex higher-order structures and obscuring of the active site [36]. Another option to functionalize biomaterials is to use peptides, which are arbitrarily defined as having less than 50 amino acids per sequence. Peptides are an excellent alternative to large molecular weight proteins for several reasons. Since peptides can be chemically synthesized with solid phase peptide synthesis rather than being produced recombinantly by transgenic organisms, the manufacturing and purification process is simpler, resulting in significantly lower costs than recombinant proteins. Since the binding of peptide

sequences to their target is not dependent on having a stable tertiary structure like globular proteins, peptides are less susceptible to loss in activity from denaturation and have higher stability. The higher stability compared to proteins also allows peptides to be coupled to biomaterial surfaces with little loss in activity. Overall, the small sequence length of peptides also allows for more precise control of the conformation and specificity [37,38].

ECM proteins contain a multitude of binding sites that have different affinities for different types of integrins and other cell receptors. Many peptide sequences have been derived from the binding sites of native proteins. For example, the RGD sequence is a ubiquitous integrin binding sequence found in many ECM and serum proteins such as fibronectin and vitronectin [39]. Collagen also contains several cell binding sequences such as DGEA, GFOGER, and the P15 sequence [40–42]. The P15 peptide has been FDA approved for use in bone regeneration in the form of a product called Pepgen-P15, which consists of bovine derived bone granules with absorbed peptide [4,41]. These peptide epitopes not only allow for cellular adhesion but can also stimulate osteogenic differentiation of MSCs through the activation of FAK and MAPK pathways [43]. In addition to ECM proteins, attempts have been made to derive functional peptide sequences from the binding sites of growth factors. For example, KIPKASSVPTELSAISTLYL (KIP), is a sequence derived from the knuckle-epitope binding domain of the BMP-2 protein. This sequence can drive bone formation despite lacking the complex tertiary structure of the full BMP-2 protein [34].

There are several methods to deliver peptides, including bolus delivery, encapsulation within a material, covalent coupling to a material, and absorption to materials. Non-specific adsorption of peptides onto the surface of biomaterials can be a simple but sufficient method for

inducing a biological reaction [44]. An excellent example of this is the P15 peptide, a collagen derived peptide that supports bone formation when adsorbed onto HA. RGD peptides have also been adsorbed onto HA, but reduce cell adhesion due to competing interactions with serum proteins such as fibronectins [45].

1.2.6 Phage Display for Novel Peptide Discovery

While peptides derived from native proteins have proven useful for enhancing cellular adhesion to materials, naturally derived peptides have some limitations. Most notably, many of these sequences such as RGD lack specificity in binding [46]. To find peptides with high specificity for certain cells or materials, a different approach is needed. High throughput screening techniques such as phage display are useful for this purpose. Phage display involves the use of libraries composed of bacteriophages with random peptides sequences displayed on their surfaces. These phage libraries can be screened against various cells/materials to screen for high binding sequences. The high binding phages are isolated, amplified, and subjected to additional rounds of screening. The high binding phages are then sequenced to deduce the sequence of the high binding peptides. Phage display has been used extensively in the development of humanized monoclonal antibody drugs, and has utility in tissue engineering through the discovery of cell and material specific peptide sequences [18]. Using a commercially available M13 bacteriophage display kit with 10^9 sequences of 12-mers, this technique was used to discover the mesenchymal stem cell binding DPIYALSWSGMA (DPI) sequence and the mineral binding VTKHLNQISQSY (VTK) sequence. Combining these two sequences together

results in the dual-functional GGDPIYALSWSGMAGGGSVTKHLNQISQSY (DPI-VTK) peptide, which is designed to tether MSCs to mineralized biomaterials. DPI-VTK was found to increase the magnitude of adhesion of MSCs to BLM coated scaffolds and enhance bone regeneration and vascularization when used in a cell-seeded scaffolds ectopic transplantation model [47,48].

1.3 Hypothesis, Study Aims, and Organization of Dissertation

1.3.1 Study Rationale

The limitations of current grafting techniques (i.e. donor site morbidity) have motivated the use of tissue engineering approaches to regenerate bone tissue. Mesenchymal stem cells (MSCs) have shown promise for the regeneration of bone defects [14,49,50]. The complexity, unpredictable outcomes, regulatory hurdles, and expense of cell transplantation limits usage in the clinic. Therefore, research in this dissertation focused on developing biomaterials with host cell-homing capabilities.

Despite its extensive use as a bone grafting material, hydroxyapatite (HA) fails to completely bridge critical sized defects without exogenous cells [51,52]. HA enhances migration of host cells [61], but also promotes migration of non-MSC cell populations such as hematopoietic cells that cannot differentiate into osteoblasts [53]. Modifying HA with bioactive molecules that promote migration and differentiation of MSCs could overcome these limitations. Peptides can increase the migration and attachment of host cells into a scaffold but lack MSC

specificity and do not have high affinity for HA-based materials. These limitations motivated our laboratory to screen peptide libraries to discover novel sequences. This work culminated in the discovery of the VTK sequence, an HA binding peptide, and the DPI sequence, an MSC specific sequence. By combining these sequences into the dual-peptide DPI-VTK, it is possible to create an interface between HA biomaterials and mesenchymal stem cells in order to promote the regeneration of bone tissue [47,48,54,55].

While enhancing the osteoconductivity of materials can enhance bone formation through the recruitment of osteogenic cells, osteoinductive signals can further enhance regeneration by promoting differentiation and up-regulation of osteogenic genes. BMPs are examples of osteoinductive agents and are one of the most effective acellular bone regeneration therapies but are limited by high cost and side effects. Peptide sequences have been derived from BMP-2 that mimic the function of the native protein [34]. By combining a BMP sequence with mineral binding sequence VTK, it could be possible to deliver BMP in a less expensive and controlled manner. Preliminary research shows that DPI-VTK binds integrins, which is important due to the synergistic effects of integrin activation and BMP signaling on osteogenesis. Therefore, it was hypothesized that the combination of the osteoconductive DPI-VTK peptide with the osteoinductive BMP peptides on biomaterial scaffolds can promote bone formation without exogenous cells.

These studies will also provide more mechanistic information regarding the MSC specific homing and attachment to peptide-enhanced materials. Understanding how stem cells attach and

differentiate on the biomaterials introduced to the defect is critical to the ability to create better clinical outcomes for treating bone defects.

1.3.2 Aims and Hypothesis

The overall aim of this thesis is to demonstrate the advantages of using combination chemotactic and adhesion peptides to promote cell specific migration into a bone defect for conductive tissue engineering approaches. The primary aims of this dissertation were to: 1) Determine if peptide DPI-VTK can enhance MSC specific migration *in vitro and in vivo* to support bone formation; 2) determine if peptide DPI-VTK has a synergistic effect with BMP derived peptide KIP-VTK to enhance MSC osteogenic differentiation

Global hypothesis: The use of a dual-functional MSC and apatite binding peptide DPI-VTK along with a dual-functional BMP and apatite binding peptide KIP-VTK will support bone regeneration with mineralized scaffolds by supporting the cell-specific migration of MSCs and their subsequent differentiation.

Aim 1: Determine if DPI-VTK can specifically induce migration of MSCs for bone regeneration
Hypothesis: DPI-VTK will act as an MSC-specific chemotactic agent in vitro and in vivo

Aim 1.1: Determine effect of DPI-VTK on MSC migration in vitro using transwell assays

Hypothesis: DPI-VTK will improve migration of MSCs in vitro in an MSC specific manner

Aim 1.2: Determine target cell population of DPI-VTK using flow cytometry and immunostaining

Hypothesis: DPI-VTK will bind cells expressing known MSC markers

Aim 1.3: Quantify effect of DPI-VTK on migration of MSCs in vivo using a mouse calvarial defect model

Hypothesis: DPI-VTK will increase the quantity of MSCs migrating into a bone defect in vivo.

Aim 1.4: Determine effect of DPI-VTK on bone formation in vivo.

Hypothesis: DPI-VTK will increase bone formation in a calvarial defect model in vivo

Aim 2: Determine if DPI-VTK and KIP-VTK have a synergistic effect on osteogenic differentiation of MSCs.

Hypothesis: The combination of DPI-VTK and KIP-VTK will increase expression of osteogenic factors of MSCs versus either alone.

Aim 2.1: Quantify the binding of KIP-VTK to BLM mineral

Hypothesis: The addition of VTK to the KIP sequence will enhance the binding affinity to bone like mineral

Aim 2.2: Determine effect of DPI-VTK and KIP-VTK on osteogenic differentiation

Hypothesis: MSCs cultured on BLM films functionalized with both DPI-VTK and KIP-VTK will have enhanced expression of osteogenic factors

Aim 2.3: Determine effect of DPI-VTK and BMP-2 on osteogenic differentiation

Hypothesis: MSCs cultured on BLM films functionalized with DPI-VTK and stimulated with soluble BMP-2 will have increased expression of osteogenic factors

1.3.3 Summary and Organization of Dissertation

Chapter 1 discussed the clinical need for new bone grafting materials and methods using the principles of tissue engineering. Chapter 2 is a published review article that gives thorough overview of cell-biomaterial interactions. Chapter 3 presents data demonstrating that DPI-VTK can act as an MSC-specific chemoattractant in vitro and in vivo, demonstrating DPI-VTK's utility in the cell-homing approach of tissue engineering. Chapter 4 presents and discusses data testing the synergy between DPI-VTK and BMP derived peptides as well as recombinant BMP-2 protein. Chapter 5 discusses some pilot studies related to the binding mechanism of DPI-VTK. Finally, Chapter 6 summarizes the key findings of the thesis, and proposes future directions for the research. Overall, this work sought to investigate the ability of a dual-functional cell-binding and material-adhesive peptide to target a specific population of cells for the purposes of tissue engineering. Building on this work could lead to new techniques for designing and utilizing cell specific biomaterials to advance bone tissue engineering.

1.4 References

[1] L.M.E. Scheerlinck, M.S.M. Muradin, A. van der Bilt, G.J. Meijer, R. Koole, E.M. Van Cann, Donor site complications in bone grafting: comparison of iliac crest, calvarial, and mandibular ramus bone., Int. J. Oral Maxillofac. Implants. 28 (2013) 222–7. https://doi.org/10.11607/jomi.2603.

[2] N. Toscano, D. Holtzclaw, Z. Mazor, P. Rosen, R. Horowitz, M. Toffler, Horizontal ridge augmentation utilizing a composite graft of demineralized freeze-dried allograft, mineralized cortical cancellous chips, and a biologically degradable thermoplastic carrier combined with a resorbable membrane: a retrospective evaluation o, J. Oral Implantol. 36 (2010) 467–474. https://doi.org/10.1563/AAID-JOI-D-09-00100.

[3] N.E. Epstein, Pros, cons, and costs of INFUSE in spinal surgery, Surg. Neurol. Int. 2 (2011) 10. https://doi.org/10.4103/2152-7806.76147.

[4] F. Gomar, R. Orozco, J.L. Villar, F. Arrizabalaga, P-15 small peptide bone graft substitute in the treatment of non-unions and delayed union. A pilot clinical trial, Int. Orthop. 31 (2007) 93–99. https://doi.org/10.1007/s00264-006-0087-x.

[5] H.-S. Cha, J.-W. Kim, J.-H. Hwang, K.-M. Ahn, Frequency of bone graft in implant surgery, Maxillofac. Plast. Reconstr. Surg. 38 (2016) 19. https://doi.org/10.1186/s40902-016-0064-2.

[6] R. Zhao, R. Yang, P.R. Cooper, Z. Khurshid, A. Shavandi, J. Ratnayake, Bone grafts and substitutes in dentistry: A review of current trends and developments, Molecules. 26 (2021) 1–27. https://doi.org/10.3390/molecules26103007.

[7] D. Dolanmaz, A. Esen, G. Yıldırım, Ö. İnan, The use of autogeneous mandibular bone block grafts for reconstruction of alveolar defects, Ann. Maxillofac. Surg. 5 (2015) 71–76. https://doi.org/10.4103/2231-0746.161070.

[8] R. Pollock, I. Alcelik, C. Bhatia, G. Chuter, K. Lingutla, C. Budithi, M. Krishna, Donor site morbidity following iliac crest bone harvesting for cervical fusion: A comparison between minimally invasive and open techniques, Eur. Spine J. 17 (2008) 845–852. https://doi.org/10.1007/s00586-008-0648-3.

[9] V. Campana, G. Milano, E. Pagano, M. Barba, C. Cicione, G. Salonna, W. Lattanzi, G. Logroscino, Bone substitutes in orthopaedic surgery: from basic science to clinical practice, J. Mater. Sci. Mater. Med. 25 (2014) 2445–2461. https://doi.org/10.1007/s10856-014-5240-2.

[10] B.L. Eppley, W.S. Pietrzak, M.W. Blanton, Allograft and alloplastic bone substitutes: a review of science and technology for the craniomaxillofacial surgeon., J. Craniofac. Surg. 16 (2005) 981–989. https://doi.org/10.1097/01.scs.0000179662.38172.dd.

[11] E.J. Kubosch, A. Bernstein, L. Wolf, T. Fretwurst, K. Nelson, H. Schmal, Clinical trial and in-vitro study comparing the efficacy of treating bony lesions with allografts versus synthetic or highly-processed xenogeneic bone grafts., BMC Musculoskelet. Disord. 17 (2016) 77. https://doi.org/10.1186/s12891-016-0930-1.

[12] M. Krasny, K. Krasny, A. Kamiński, M. Zadurska, P. Piekarczyk, P. Fiedor, Evaluation of safety and efficacy of radiation-sterilized bone allografts in reconstructive oral surgery., Cell Tissue Bank. 14 (2013) 367–374. https://doi.org/10.1007/s10561-012-9348-7.

[13] S.P. Pilipchuk, A.B. Plonka, A. Monje, A.D. Taut, A. Lanis, B. Kang, W. V Giannobile,

Tissue engineering for bone regeneration and osseointegration in the oral cavity, Dent. Mater. 31 (2015) 317–338. https://doi.org/http://dx.doi.org/10.1016/j.dental.2015.01.006.
[14] P.T. Brown, A.M. Handorf, W.B. Jeon, W.-J. Li, Stem cell-based tissue engineering approaches for musculoskeletal regeneration., Curr. Pharm. Des. 19 (2013) 3429–45. https://doi.org/10.1016/j.biotechadv.2011.08.021.Secreted.
[15] J.M. Anderson, A. Rodriguez, D.T. Chang, Foreign body reaction to biomaterials, Semin. Immunol. 20 (2008) 86–100. https://doi.org/10.1016/j.smim.2007.11.004.
[16] R. Trindade, T. Albrektsson, S. Galli, Z. Prgomet, P. Tengvall, A. Wennerberg, Osseointegration and foreign body reaction: Titanium implants activate the immune system and suppress bone resorption during the first 4 weeks after implantation, Clin. Implant Dent. Relat. Res. 20 (2018) 82–91. https://doi.org/10.1111/cid.12578.
[17] J. Ramaswamy, H. Ramaraju, D.H. Kohn, Bone-like mineral and organically modified bone-like mineral coatings, Biol. Biomed. Coatings Handb. Process. Charact. (2011) 1–27.
[18] S.J. Segvich, D.H. Kohn, Phage Display as a Strategy for Designing Organic/Inorganic Biomaterials, in: B. R, D.A. Puleo (Eds.), Biol. Interact. Mater. Surfaces Underst. Control. Protein, Cell, Tissue Responses, Springer, New York, 2009: pp. 115–132.
[19] P. Robey, "Mesenchymal stem cells": Fact or fiction, and implications in their therapeutic use, F1000Research. 6 (2017) 1–8. https://doi.org/10.12688/f1000research.10955.1.
[20] C.-S. Lin, Z.-C. Xin, J. Dai, T. F. Lue, Commonly Used Mesenchymal Stem Cell Markers and Tracking, Histol Histopathol. 28 (2013) 1109–1116. https://doi.org/10.14670/HH-28.1109.
[21] M. Herrmann, S. Verrier, M. Alini, Strategies to stimulate mobilization and homing of endogenous stem and progenitor cells for bone tissue repair, Front. Bioeng. Biotechnol. 3 (2015) 1–11. https://doi.org/10.3389/fbioe.2015.00079.
[22] D. Kaigler, G. Avila-Ortiz, S. Travan, A.D. Taut, M. Padial-Molina, I. Rudek, F. Wang, A. Lanis, W. V. Giannobile, Bone Engineering of Maxillary Sinus Bone Deficiencies Using Enriched CD90+ Stem Cell Therapy: A Randomized Clinical Trial, J. Bone Miner. Res. 30 (2015) 1206–1216. https://doi.org/10.1002/jbmr.2464.
[23] G. Li, X. Wang, J. Cao, Z. Ju, D. Ma, Y. Liu, J. Zhang, Coculture of peripheral blood CD34+ cell and mesenchymal stem cell sheets increase the formation of bone in calvarial critical-size defects in rabbits, Br. J. Oral Maxillofac. Surg. (2014). https://doi.org/10.1016/j.bjoms.2013.10.004.
[24] P. Jayaraman, R. Lim, J. Ng, M.C. Vemuri, Acceleration of Translational Mesenchymal Stromal Cell Therapy Through Consistent Quality GMP Manufacturing, Front. Cell Dev. Biol. 9 (2021) 1–19. https://doi.org/10.3389/fcell.2021.648472.
[25] L. Li, X. Chen, W.E. Wang, C. Zeng, How to Improve the Survival of Transplanted Mesenchymal Stem Cell in Ischemic Heart?, Stem Cells Int. 2016 (2016). https://doi.org/10.1155/2016/9682757.
[26] W. Lin, L. Xu, S. Zwingenberger, E. Gibon, S.B. Goodman, G. Li, Mesenchymal stem cells homing to improve bone healing, J. Orthop. Transl. 9 (2017) 19–27. https://doi.org/10.1016/j.jot.2017.03.002.
[27] G. Chen, Y. Lv, Matrix elasticity-modified scaffold loaded with SDF-1α improves the in situ regeneration of segmental bone defect in rabbit radius, Sci. Rep. 7 (2017) 1–12. https://doi.org/10.1038/s41598-017-01938-3.
[28] O.I. Eseonu, C. De Bari, Homing of mesenchymal stem cells: mechanistic or stochastic?

Implications for targeted delivery in arthritis, Rheumatol. (United Kingdom). 54 (2015) 210–218. https://doi.org/10.1093/rheumatology/keu377.
[29] C. Dahlin, A. Linde, J. Gottlow, S. Nyman, Dahlin 1988 Healing of bone defects by guided tissue.pdf, Plast. Reconstr. Surg. 81 (1988) 672–676.
[30] W.F. McKay, S.M. Peckham, J.M. Badura, A comprehensive clinical review of recombinant human bone morphogenetic protein-2 (INFUSE?? Bone Graft), Int. Orthop. 31 (2007) 729–734. https://doi.org/10.1007/s00264-007-0418-6.
[31] K. Miyazono, Bone Morphogenetic Protein Receptors and Actions: BMPs, in: Princ. Bone Biol., 3rd ed., Academic Press, 2003: pp. 1177–1196.
[32] K.W.H. Lo, B.D. Ulery, K.M. Ashe, C.T. Laurencin, Studies of bone morphogenetic protein-based surgical repair, Adv. Drug Deliv. Rev. 64 (2012) 1277–1291. https://doi.org/10.1016/j.addr.2012.03.014.
[33] G.T.S. Kirby, L.J. White, C. V. Rahman, H.C. Cox, F.R. a J. Rose, D.W. Hutmacher, K.M. Shakesheff, M. a. Woodruff, PLGA-based microparticles for the sustained release of BMP-2, Eur. Cells Mater. 22 (2011) 24. https://doi.org/10.3390/polym3010571.
[34] A. Saito, Y. Suzuki, S.I. Ogata, C. Ohtsuki, M. Tanihara, Activation of osteo-progenitor cells by a novel synthetic peptide derived from the bone morphogenetic protein-2 knuckle epitope., Biochim. Biophys. Acta. 1651 (2003) 60–67. https://doi.org/10.1016/S1570-9639(03)00235-8.
[35] L.A. Palomares, S. Estrada-Moncada, O.T. Ramírez, Production of Recombinant Proteins BT - Recombinant Gene Expression: Reviews and Protocols, in: P. Balbás, A. Lorence (Eds.), Humana Press, Totowa, NJ, 2004: pp. 15–51. https://doi.org/10.1385/1-59259-774-2:015.
[36] P. Roach, D. Farrar, C.C. Perry, Interpretation of Protein Adsorption: Surface-Induced Conformational Changes, J. Am. Chem. Soc. 127 (2005) 8168–8173. https://doi.org/10.1021/ja042898o.
[37] C. Lamers, Overcoming the shortcomings of peptide-based therapeutics, Futur. Drug Discov. 4 (2022). https://doi.org/10.4155/fdd-2022-0005.
[38] K. Fosgerau, T. Hoffmann, Peptide therapeutics: Current status and future directions, Drug Discov. Today. 20 (2015) 122–128. https://doi.org/10.1016/j.drudis.2014.10.003.
[39] C.H. Damsky, Extracellular matrix-integrin interactions in osteoblast function and tissue remodeling, Bone. 25 (1999) 95–96. https://doi.org/10.1016/S8756-3282(99)00106-4.
[40] I. Pountos, M. Panteli, A. Lampropoulos, E. Jones, G.M. Calori, P. V Giannoudis, The role of peptides in bone healing and regeneration: a systematic review., BMC Med. 14 (2016) 103. https://doi.org/10.1186/s12916-016-0646-y.
[41] K.M. Hennessy, B.E. Pollot, W.C. Clem, M.C. Phipps, A. a. Sawyer, B.K. Culpepper, S.L. Bellis, The effect of collagen I mimetic peptides on mesenchymal stem cell adhesion and differentiation, and on bone formation at hydroxyapatite surfaces, Biomaterials. 30 (2009) 1898–1909. https://doi.org/10.1016/j.biomaterials.2008.12.053.
[42] B.K. Culpepper, M.C. Phipps, P.P. Bonvallet, S.L. Bellis, Enhancement of peptide coupling to hydroxyapatite and implant osseointegration through collagen mimetic peptide modified with a polyglutamate domain, Biomaterials. 31 (2010) 9586–9594. https://doi.org/10.1016/j.biomaterials.2010.08.020.
[43] Z. Saidak, C. LeHenaff, S. Azzi, C. Marty, S. Da Nascimento, P. Sonnet, P.J. Marie, Wnt/β-catenin signaling mediates osteoblast differentiation triggered by peptide-induced α5β1 integrin priming in mesenchymal skeletal cells, J. Biol. Chem. 290 (2015) 6903–

6912. https://doi.org/10.1074/jbc.M114.621219.
[44] B.J. Bruno, G.D. Miller, C.S. Lim, Basics and recent advances in peptide and protein drug delivery., Ther. Deliv. 4 (2013) 1443–67. https://doi.org/10.4155/tde.13.104.
[45] K.M. Hennessy, W.C. Clem, M.C. Phipps, A. a. Sawyer, F.M. Shaikh, S.L. Bellis, The effect of RGD peptides on osseointegration of hydroxyapatite biomaterials, Biomaterials. 29 (2008) 3075–3083. https://doi.org/10.1016/j.biomaterials.2008.04.014.
[46] E. Ruoslahti, The RGD Story: a personal account, Matrix Biol. 22 (2003) 1–7. https://doi.org/10.1016/S0945-053X.
[47] H. Ramaraju, S.J. Miller, D.H. Kohn, Dual-functioning peptides discovered by phage display increase the magnitude and specificity of BMSC attachment to mineralized biomaterials, Biomaterials. 134 (2017) 1–12. https://doi.org/10.1016/j.biomaterials.2017.04.034.
[48] H. Ramaraju, D.H. Kohn, Cell and Material-Specific Phage Display Peptides Increase iPS-MSC Mediated Bone and Vasculature Formation In Vivo, Adv. Healthc. Mater. 1801356 (2019) 1–11. https://doi.org/10.1002/adhm.201801356.
[49] P. Lin, Y. Lin, D.P. Lennon, D. Correa, M. Schluchter, A.I. Caplan, Efficient Lentiviral Transduction of Human Mesenchymal Stem Cells That Preserves Proliferation and Differentiation Capabilities, Stem Cells Transl. Med. 1 (2012) 886–897. https://doi.org/10.5966/sctm.2012-0086.
[50] A.-L. Gamblin, M.A. Brennan, A. Renaud, H. Yagita, F. Lézot, D. Heymann, V. Trichet, P. Layrolle, Bone tissue formation with human mesenchymal stem cells and biphasic calcium phosphate ceramics: The local implication of osteoclasts and macrophages, Biomaterials. 35 (2014) 9660–9667. https://doi.org/10.1016/j.biomaterials.2014.08.018.
[51] L. Oliveira, W.L.O. Da, R. Carlos, F. Silva, T.N. Guim, N.L. V Carren, Histological Evaluation of Bone Repair with Hydroxyapatite : A Systematic Review, (2017) 341–354. https://doi.org/10.1007/s00223-017-0294-z.
[52] W. Wang, K.W.K. Yeung, Bioactive Materials Bone grafts and biomaterials substitutes for bone defect repair : A review, Bioact. Mater. 2 (2017) 224–247. https://doi.org/10.1016/j.bioactmat.2017.05.007.
[53] M. Tommila, A. Jokilammi, P. Terho, T. Wilson, R. Penttinen, E. Ekholm, Hydroxyapatite coating of cellulose sponges attracts bone-marrow-derived stem cells in rat subcutaneous tissue, (2009) 873–880. https://doi.org/10.1098/rsif.2009.0020.
[54] S. Segvich, S. Biswas, U. Becker, D.H. Kohn, Identification of peptides with targeted adhesion to bone-like mineral via phage display and computational modeling, Cells Tissues Organs. 189 (2008) 245–251. https://doi.org/10.1159/000151380.
[55] H. Ramaraju, S.J. Miller, D.H. Kohn, Dual-functioning phage-derived peptides encourage human bone marrow cell-specific attachment to mineralized biomaterials., Connect. Tissue Res. 55 Suppl 1 (2014) 160–3. https://doi.org/10.3109/03008207.2014.923868.

Chapter 2: Review on Material Parameters to Enhance Bone Cell Function *in vitro* and *in vivo*[1]

2.1 Abstract

Bone plays critical roles in support, protection, movement, and metabolism. Although bone has an innate capacity for regeneration, this capacity is limited, and many bone injuries and diseases require intervention. Biomaterials are a critical component of many treatments to restore bone function and include non-resorbable implants to augment bone and resorbable materials to guide regeneration. Biomaterials can vary considerably in their biocompatibility and bioactivity, which are functions of specific material parameters. The success of biomaterials in bone augmentation and regeneration is based on their effects on the function of bone cells. Such functions include adhesion, migration, inflammation, proliferation, communication, differentiation, resorption, and vascularization. This review will focus on how different material parameters can enhance bone cell function both *in vitro* and *in vivo*.

2.2 Introduction

Bone is a rigid tissue which provides structural support, facilitates locomotion, serves as a reservoir for mineral storage, and protects internal organs and soft tissue. Bone is also an

[1] Published as E. Madsen, M. Mededovic, D.H. Kohn, Review on material parameters to enhance bone cell function in vitro and in vivo, Biochem. Soc. Trans. (2020) 1–12. https://doi.org/10.1042/bst20200210.

endocrine organ, which serves as a niche for bone marrow and a source of stem cells. This complex tissue consists of an organic component, an inorganic, mineral component and water. The organic component is primarily type I collagen, but also consists of protein polysaccharides, glycosaminoglycans (GAGs) and other non collagenous proteins. Together, the organic constituents are responsible for the toughness of bone [1] which is important to prevent propagation of microfractures. The organic material serves as a template for the nucleation and formation of the inorganic material [2] into both needle and platelet shaped crystals [3] of non-stoichiometric hydroxyapatite (HA), which contains carbonate substitutions. The mineral components give bone its hardness, rigidity and strength [4]. Multiple factors affect bone strength, including the composition, of both the organic and inorganic phases, their arrangement and microarchitecture, and cell presence [5]. Bone fulfils its functions by adapting to its environment across dimensional scale, such as modeling to alter the morphology of thick walled long bones to support mechanical demands, and chemical components, such as the mineral/collagen ratio, which affects physical properties.

Many materials have been used either as permanent prosthetic replacements for bone, or as transient scaffolds to promote bone regeneration. Bone-based biomaterials fall into three broad categories: metals, ceramics, and polymers. Metals used for bone anchored prostheses such as total hip replacements, are primarily cobalt-chromium, and titanium-based alloys [6]. Titanium is notable for its high biocompatibility and ability to form close to direct contact with bone (an interfacial zone of ~100μm) which is called osseointegration. The ability to achieve osseointegration is commonly exploited in anchoring dental implants to alveolar bone [7]. While metals have favorable mechanical properties for prosthetics, such as high strength and fatigue

resistance, titanium is subject to high wear and all metals release metal ions (corrosion), which is more pronounced when concomitant with wear [6,8]. Bioceramics used in bone reconstruction and regeneration includes non-resorbable, “bioinert” ceramics that elicit a minimal biological response and are held in bone by mechanical means (press fit, rough surfaces, grouting agents, or tissue ingrowth), surface active ceramics that form chemical bonds with bone, and resorbable ceramics that are gradually replaced by host bone [9]. “Inert” ceramics are typically used in orthopedic prostheses, particularly the acetabular bearing surface of hip prostheses, as well as endosseous dental implants, and include alumina, zirconia, and silicon nitride [6]. Although ceramics have a low friction coefficient and wear rate, their brittle nature and low fatigue resistance are potential limitations to use in load-bearing applications [8]. Resorbable ceramics includes calcium phosphate ceramics, such as apatites. The solubility and resorbility of apatites vary based on their chemistry and crystallinity. Highly crystalline, stoichiometric HA has poor solubility while biomimetic carbonated apatites similar to native bone mineral are more easily resorbed [10]. Like ceramics, polymers can be divided into resorbable and non-resorbable categories. Non-resorbable polymers include poly-methyl methacrylate which is used as bone cement and grouting agent for anchoring prostheses into bone, and ultra high molecular weight polyethylene which is used as a bearing surface in hip prostheses [6]. Biodegradable polymers such as poly-lactic acid and poly-caprolactone are used as porous scaffolds for bone tissue engineering. While these polymers’ tunable degradation rates and ease of functionalization are advantageous for directing cell adhesion and differentiation, their low strength and stiffness limits their use in load-bearing applications [11]. The goal of this paper is to review how material parameters affect functions of bone cells.

The success of implanted biomaterials is based on their effects on the myriad of different bone cells. Primarily four cell types reside in bone: osteoblasts, osteocytes, bone lining cells, and osteoclasts, which work together to grow, remodel and maintain bone volume and function. Osteoblasts are formed from stem cells recruited by cytokines from the bone marrow to the bone surface at sites of growth and remodeling. They are tightly connected to neighboring cells, via gap junctions and adherens. Osteoblasts are active bone cells with a myriad of activities, including secretion and assembly of the organic matrix, and directing mineralization of the matrix by secreting promoters such as alkaline phosphate (ALP). In addition to mineralization, osteoblasts secrete paracrine factors, such as bone morphogenenetic proteins (BMPs), which regulate osteoblast and chondrocyte differentiation [12]. Once the organic matrix is mineralized, most osteoblasts undergo apoptosis, but some become entrapped within the new bone and become osteocytes. Osteocytes are differentiated and encased osteoblasts which live in well ordered lacunae, and communicate via dendritic processes which form complex networks within the canaliculi [13]. Osteocytes are mechanoreceptive cells, can sense mechanical strain in bone, and respond to the physical stimuli by paracrine [14] ,gap junction communication and focal adhesions. Osteocyte death is caused by natural physiological processes, such as aging and menopause, but also due to microcracks, as they form due to failure of plastic deformation and cause mechanical damage to the osteocytes [15]. Osteoblasts which remain on the bone surface become bone lining cells and become inactive [16]. These cells act as a barrier between bone marrow and bone and digest collagen protruding from Howship's lacunae [17].

Mesenchymal stem cells (MSCs) are a heterogenous population of stem/progenitor cells capable of differentiating into bone, cartilage, and adipose. Originally identified in bone marrow

as bone marrow stromal cells (BMSCs), these cells can also be found in periosteum, the perivascular niche, and other tissues; although the extent to which these populations converge/diverge from each other as well as their classification as MSCs is still under debate [18–20]. Additionally, Hematopoietic stem cells (HSCs) regulate osteoblast lineage and support bone marrow vasculature, while circulating cells, which circulate throughout the body and arrive to bone via the vasculature, can help regulate mesenchymal and osteoblastic cells in coordinating hematopoiesis [21]. The main function of osteoclasts is bone resorption, which is vital for bone maintenance, the remodeling stage of bone healing and tooth eruption. These cells are enzymatically active and produce tartrate-resistant acid phosphatase (TRAP), calcitonin receptor (CTR) and matrix metalloproteinases (MMPs), which degrade the matrix**.** To resorb local areas of bone, osteoclasts form a resorption lacuna within which they release protons to acidify and dissolve mineral in a sealed area and proteases to degrade the bone matrix [22]. Osteoclasts can be activated and recruited to resorb multiple times, before undergoing apoptosis [23].

2.3 Inflammation

Inflammation is critical for proper healing of bone injuries and the implantation of foreign materials typically initiates an inflammatory response. Materials are classified by their biocompatibility into biotolerant, biocompatible, and bioactive categories. Biotolerant materials have low toxicity, but often initiate formation of a fibrous capsule or foreign body giant cell reaction [24]. While biocompatible materials were initially believed to trigger minimal or no inflammatory response, inflammation is critical for proper integration of implants.
Upon exposure to blood *in vivo*, plasma proteins and platelets are quickly absorbed onto the biomaterial surface and activated. Activated platelets initiate the clotting cascade, fibrin forms a

provisional matrix, and thrombosis is achieved. Chemokines such as PDGF recruit leukocytes such as neutrophils (initially) and monocytes/macrophages (later). Mast cells also release histamine to mediate the immune response. After the acute inflammation phase, the chronic inflammation phase is characterized by the presence of lymphocytes and plasma cells, but this typically resolves quickly for biocompatible materials. Macrophages remodel the provisional matrix and fibroblasts and endothelial cells are also recruited to form granulation tissue around the implant [24].

In osseointegration, both M1 (pro-inflammatory) and M2 (anti-inflammatory) macrophages are recruited to the peri-implant tissue [25]. Polarization of macrophages towards the M2 phenotype is critical for implant integration and maintenance [26,27]. M2 macrophages secrete BMP-2 to recruit osteoblasts to form new bone around the implant surface [28].

Surface modifications can modulate the inflammatory response of biomaterials. Coating titanium implants with bioglass increases macrophage adhesion while reducing secretion of pro-inflammatory cytokines [29]. Other surface treatments can modulate the inflammatory response. For example, surface hydrophobicity down-regulates proinflammatory cytokines such as TNFa and IL1a [30]. Although many materials provoke only minimal inflammation in bulk form, biocompatible materials can become inflammatory when in micro/nano particle form. Such particles can be released as prosthetic debris into the surrounding tissue during wear, contributing to inflammation, osteolysis, and implant failure [31]. Macrophages will attempt to phagocytize these particles and secrete proinflammatory cytokines including TNF-a, IL-1a, IL-1B, IL-6, IL-8, IL-11, IL-15, TGF-a, GM-CSF, M-CSF, and PDGF. Osteoclast formation is

subsequently stimulated through the RANKL pathway, contributing to peri-implant bone resorption and osteolysis [32].

2.4 Adhesion

One of the first steps for biomaterial-cell interactions is cellular adhesion. Cellular adhesion is mediated by integrins, heterodimeric membrane proteins that facilitate attachment of cells to the extracellular matrix as well as biomaterials. It is important to recognize that cells do not attach to "naked" materials. Material surfaces are conditioned by the surrounding fluid/serum. Upon immersion in biological fluids, the material surface is quickly saturated with proteins. Surface energy influences protein adsorption [33], but the relationship is not simple, as other material parameters including hydrophilicity, stiffness, charge and topography also direct protein adsorption. Serum proteins such as vitronectin and fibronectin are important for osteoblast adhesion to materials [34]. These proteins contain adhesive peptide sequences such as RGD that form attachments with integrins [35]. Fibronectin supports the survival of attached osteoblasts [36] and vitronectin is critical for cell attachment and spreading *in* [37]. Osteopontin is another matrix protein present at the bone-biomaterial interface. Osteopontin quickly accumulates at the tissue-implant interface to form a cement line. This osteopontin rich layer helps support cell adhesion, regulates mineralization, and may play a vital role in anchoring the implant to the surrounding tissue. Materials found to accumulate an osteopontin coating include HA, titanium, and cell culture dishes [38].

Physical properties of the bulk material and surface also influence cellular adhesion. For example, fibroblasts spread more, form stress fibers, and increase integrin expression when on

stiffer substrates [39]. Surface roughness and topography can have effects on the magnitude of cell adhesion, which is often exploited when designing dental/orthopedic implants to enhance osseointegration. For example, sand blasting, acid etching, and anodization enhances cell adhesion and osseointegration of titanium implants [40], and greater numbers of osteoblasts attached to grooved titanium than rough titanium because of patterning and alignment [41]. The influence of topography on cell adhesion extends to the nanoscale [42] and nanoporous titanium promotes maturation of focal adhesion and filopodia in osteogenic cells compared to polished titanium [43]. Cell adhesion, however, can be reduced on rough titanium surfaces in some situations. Human osteoblast-like MG63 cells have lower attachment to grit-blasted titanium (roughness 2.0-3.3 μm) versus machined titanium (0.2 μm roughness) [44]. The seemingly contradictory information regarding the effect of roughness on cell attachment illustrates the complex relationship between roughness and surface topography. Definitions of "rough" surfaces vary from study to study and many studies do not characterize surface topography, or do so only with qualitative techniques [45].

Surface chemistry of materials also directs cell adhesion. Cells typically have greater adhesion on hydrophilic surfaces [37]. Contamination of titanium surfaces with hydrocarbons has a negative effect on adhesion, whereas UV photofunctionalization enhances osteoblast adhesion by catalyzing the oxidation of hydrocarbon contaminants, increasing hydrophilicity and surface energy [46]. There is much interest in engineering material surfaces with specific ligands to influence cell attachment. One of the most common ligands is the RGD peptide sequence, which is found in extracellular matrix proteins such as collagen, fibronectin, and vitronectin. RGD can bind to integrins such as α5β1 and αVβ3 [35]. Cyclic RGD stimulates osteoblast

adhesion [47] and RGD helps osteoblasts attach to chitosan [48]. Since RGD binds integrins, it can have conflicting interactions with serum proteins, resulting in negative effects on cell adhesion. For example, RGD coating can enhance MSC attachment to HA depending on density, but can also interfere due to competing interactions with serum proteins [49,50]. *In vivo* studies on the effect of RGD coatings on osseointegration have had conflicting results, with RGD coating on hydroxyapatite inhibiting osseointegration [51] but stimulating bone formation when conjugated to titanium [52]. Other peptides have been used as well, including the P-15 collagen peptide (GTPGPQGIAGQRGW) that increases cell attachment to bovine anorganic bone mineral [53]. Dual-peptides containing material-binding domains and cell-binding domains have proven useful for creating adhesive interfaces between cells and materials. The Glu7-Pro-Arg-Gly-Asp-Thr peptide containing the mineral binding polyglutamate sequence as well as RGD facilitates attachment of osteoblasts to HA [54]. Phage display is a powerful tool that facilitates the discovery of novel sequences with specificity to certain cells or materials. This technique resulted in the discovery of the MSC-binding DPIYALSWSGMA (DPI) sequence and biomimetic mineral binding VTKHLNQISQSY (VTK) sequence. Combining these sequences into dual-peptide DPI-VTK increases the magnitude and specificity of MSC attachment to mineralized biomaterials [55]. *In vivo*, DPI-VTK functionalized scaffolds seeded with human MSCs resulted in greater volume of regenerated bone and vasculature [56].

2.5 Migration

Like adhesion, integrins play a critical role in cell migration. Cell migration requires that adhesions are dismantled on the back end of the cell while new ones are created on the leading edge. In order for this to occur, adhesion must be strong enough to facilitate attachment while

weak enough to allow detachment. Therefore, cell migration is greatest at intermediate ligand concentration/attachment strength [57]. Cells migrate at different rates on different materials. For example, bone marrow stromal cells have reduced motility on mineralized vs non-mineralized PLGA [58]**.** For directional migration to occur, cells must be able to sense a gradient. This can occur through two main modes, haptotaxis with surface-bound gradients of ligands, or chemotaxis with soluble gradients. Haptotaxis can be influenced by the hydrophilicity of a substrate, with bone cells migrating towards hydrophilic substrates due to increased vitronectin adsorption (Dalton 1998). Functionalization of scaffolds with ligands can increase migration *in vivo*. For example, α2β1 integrin specific peptides coupled to a hydrogel enhances migration of osteoprogenitors [59]. Growth factors adsorbed or encapsulated within materials can be released in a controlled manner, creating a soluble gradient to induce chemotaxis of osteogenic cells. For example, SDF-1 induces migration of MSCs when released from scaffolds [60], and calcium, released by certain ceramic materials, induces MSC migration [61] by increasing osteopontin expression [18].

2.6 Proliferation

Cell proliferation is necessary to replace cells lost from apoptosis during both bone homeostasis and regeneration. Of particular importance during bone healing is the proliferation of MSCs, which will subsequently differentiate into osteoblasts to form new bone [62]. Different material parameters can stimulate or inhibit this process. Chemical cues, such as extracellular calcium released from calcium containing bioceramics can stimulate proliferation of MSCs [18]. Integrins such as α5β1 regulate cell proliferation in osteoblasts. Blocking the α5 subunit in osteoblasts resulted in reduced proliferation [63]. In contrast, silencing integrin α2β1 in

osteoblast-like cells increased proliferation. Proliferation and differentiation are typically mutually exclusive processes, as evidenced by the pro-differentiation and anti-proliferation effects of α2β1 [64]**.** Micropatterning of surfaces can stimulate cell proliferation by directing mechanical strain along the axis of cell elongation [65]. Microroughness, in contrast, can reduce proliferation and induce differentiation of MSCs, and this general trend holds for many cell types [34,64]. Controlling protein adsorption can impact cell proliferation, with fibronectin stimulating proliferation [66]. Functionalizing surfaces with adhesive ligands such as RGD, rather than the whole protein, can also increase proliferation [48].

2.7 Communication

The complex and dynamic functions of bone tissue require cell coordination on a spatial and temporal level, which is regulated by cell communication. Gap junction communication between osteocytes coordinate mechanotransduction, mineral deposition and paracrine communication via BMPs, VEGF and RANKL. Paracrine communication via BMP-2 and osteocalcin coordinate osteogenic differentiation of stem cells [67], osteoclastogenesis, healing and other cell activities for bone. The most important function of gap junction communication in bone is mechanotransduction, allowing other functions of bone, such as remodeling, to occur.

Mechanical properties of the material, as well as the forces around the material affect gap junction communication. Permeability of bone, which allows for mechanotransduction, is a function of bone porosity and viscosity of the fluids within the pores. Mechanotransduction is mediated through gap junction communication and occurs by shear flow of the fluid in the pores caused by mechanical forces. Fluid shear directly triggers perturbation of α5β1 integrins [68], but also cadherins and caveolae [69] to activate the ERK1/2 pathway and open gap junction

hemichannels [70]. The reaction to mechanical stimulus is more complex than the proposed Mechanostat Theory, which indicated that at high mechanical stimuli bone mass is increased, at lower stimuli is decreased and an intermediate stimulus is maintained. Within the range of physiological strains, there is overlap in resorption and formation rates, which indicates that load is not the only factor controlling bone remodelling.

Although mediated through gap junction communication, mechanotransduction, through gap junction communication, can promote paracrine communication as a result. Mechanotransduction allows cells to create a biochemical signal within the cell from a mechanical signal from the surrounding matrix. The direct mechanical material-cell interaction prompts osteocytes to produce paracrine signals such as BMPs, Wnts, PGE2 and NO, which influence cell behavior such as recruitment, differentiation and activity of osteoblasts and osteoclasts [71–74]. The effect of gap junction communication on paracrine communication and other cell functions, such as differentiation, can be manipulated by micropatterning surfaces. Engineering patterns allows for contact between multiple cells and encourages gap junction communication increased differentiation [75]. Many studies do not delve beyond observing the effects certain biomaterials make on cell behavior. Understanding the underlying mechanisms may lead to better understanding the role of gap junction communication in cell behavior.

Cell communication is also modulated by surface chemistry. For example, cell attachment to calcium silicate induces cross-talk between osteocytes and endothelial cells, inducing paracrine communication of VEGF [76]. Col-I attachment can modulate [Ca^{2+}]- and cAMP-signaling pathways in osteoblasts [77]. Material characteristics, such as aligned pattern

and surface chemistry, can be used in tandem to affect cell behavior. For example, Xu et al [78] used aligned ECM and bioglass to increase Cx43 expression in MSCs, which has an important role in MSC differentiation. Biomaterials containing silica have been used for bone regeneration as the presence of silica increases Cx43 mediated gap junction communication [79,80], proliferation and differentiation in MSCs [81], while decreasing osteoclastogenesis [82]. Both paracrine and gap junction communication can modulate other cell functions, thus it is important to assess the effect of the material on cell communication.

2.8 Differentiation

Mesenchymal stem cells can be sourced from multiple locations, including the bone marrow**,** and are multipotent stem cells, which differentiate into osteoblasts, adipose cells, cartilage, neural or muscle cells [83]**.**

MSC differentiation can be directed by physical cues such as material stiffness and surface geometry, as MSCs are mechanotransductive and convert mechanical signals from the substrate surface into biochemical signals. Mechanical parameters such as fluid shear stress and substrate strain also provide cues for MSC differentiation, also through means of mechanotransduction [84]. The mechanical to chemical signal transduction can be observed by focal adhesion formation and the YAP gene program [85]. More specifically, α2β1 integrin binding [64] promotes osteogenic differentiation.

The mechanical property of surface stiffness particularly, affects MSC cell fate. MSCs on softer substrates, with elasticity mimicking brain elasticity (E~0.1-1kPa) have neuron-like morphology past 7 days, while stiffer matrices (25-40 kPa) results in polygonal MSC morphology, resembling osteoblasts [86–88]. Micropatterning regulates cell shape, which

determines fate and commitment of MSCs. [89,90] Convex geometries, such as pentagons, lead to an adipocyte lineage, while concave geometries, such as star shapes, lead to an osteogenic lineage [91]. Smaller micropatterns (1024 μm^2 islands) lead MSCs into chondrocyte lineage, while large micropatterns (10000 μm^2 islands) drive MSCs into myocytes [92].

2.9 Vascularization

Vascularization is necessary for bone survival, but also healing and endocrine signaling. Angiogenesis, formation of blood vessels from existing vessels, is tightly bound with osteogenesis and bone remodeling, and the collagen that is deposited by osteoblasts onto the surface of the new blood vessels is also a template for mineral deposition [93]**.** During bone development and healing, the processes of angiogenesis and osteogenesis are coupled, and together are regulated by vascular endothelial growth factor (VEGF) and BMP2 . Type H vessels, which are in the vicinity of bone growth plates direct bone growth by gap junction communication as well as paracrine communication, stimulating progenitor cells to proliferate and differentiate [93].

Multiple material parameters affect quality and quantity of newly formed vessels. For bone regeneration, both pore size and interconnection are important parameters. Interconnected pores between 100-150 μm are beneficial for vessel development [94]. β-TCP scaffolds made with larger pores implanted without cells lead to the formation of larger blood vessels, but scaffolds with larger interconnections result in both larger vessels and more vessels, with effect plateauing at pore size of 400μm [84].

Increased roughness and surface energy of both metal [95,96] and polymeric surfaces [97,98] improves cell adhesion by increasing adhesion density and cell aspect ratio, even on a

nanometer scale. To undergo angiogenesis, endothelial cells need to be adherent and motile, therefore increasing endothelial cell adhesion density is critical to induce angiogenesis and maintain the neovasculature. Surface stiffness also affects endothelial cell morphology, which affects angiogenic potential. Endothelial cells develop a spread morphology and have more actin fibers when seeded on stiffer surfaces. ($E > 2kPa$) [39,99]

2.10 Resorption

Bone remodeling is a dynamic process of replacing old bone matrix with new matrix, and maintaining bone volume. Bone resorption is an essential process for bone to adapt to physiological changes throughout life [100]. Resorption is a complex process including migration of osteoclasts to a focal site, followed by attachment and polarization, then dissolution of hydroxyapatite (HA) and degradation of the organic matrix. Once these steps are complete, the osteoclasts undergo apoptosis.

Resorption by osteoclasts can be modulated by altering surface parameters such as material surface chemistry and surface roughness. Resorption of calcium-phosphate ceramics is dependent on Ca/P ratio and crystallinity. For example, osteoclasts resorb more biphasic calcium phosphate when HA/β-tri calcium phosphate (β-TCP) ratio is 25/75 versus 75/25. [8] Strontium substituted calcium phosphate inhibits osteoclast resorption by delaying osteoclast differentiation [101,102]. Carbonated apatite has increased resorption [103]. The nature of organic materials also impacts resorption, as fibrinogen modified chitosan has greater osteoclastic resorption than on unmodified chitosan [104]. Besides surface chemistry, surface roughness affects osteoclast resorption. When on rough biomimetic hydroxyapatite, osteoclasts have reduced resorption

[105], but on rough titanium, there is no change in MMP expression or morphology [26,106]. This is due to surface wettability and surface energy. [107,108]

2.11 Conclusion

Cell functions can be stimulated or inhibited by choice of material, which guides surface chemistry, protein adsorption and material stiffness, and material surface and bulk modification, such as surface roughness, topography, porosity and strain. Additionally, modifications of many of these material properties can promote one cell function over another. Many cell functions can be modulated through modifying integrin binding and cell adhesion, as osteocytes and MSCs are mechanotransductive cells and sense surface stiffness, roughness and shear forces through focal adhesions which have cascade effects throughout the cell and tissue. An overview of the relationships between material parameters and cell functions can be seen in Figure 2.

Better understanding of the effect of how physical parameters drive bone cell function has allowed for improved therapy and implant design. As bone is a dynamic organ, which is interconnected with the immune system and vascular system, future material designs need to better account for not only osteogenic potential, but also vascular and immune potential. Additionally, most of the studies cited assessed the effect of one parameter on one cell action, which although informative, may be giving a limited image of the potential of manipulating a particular variable on effective tissue engineering strategies. The future of material design would encompass various cell functions and modulating material parameters to ensure not only one, but multiple cell functions are promoted in order to achieve optimal effects.

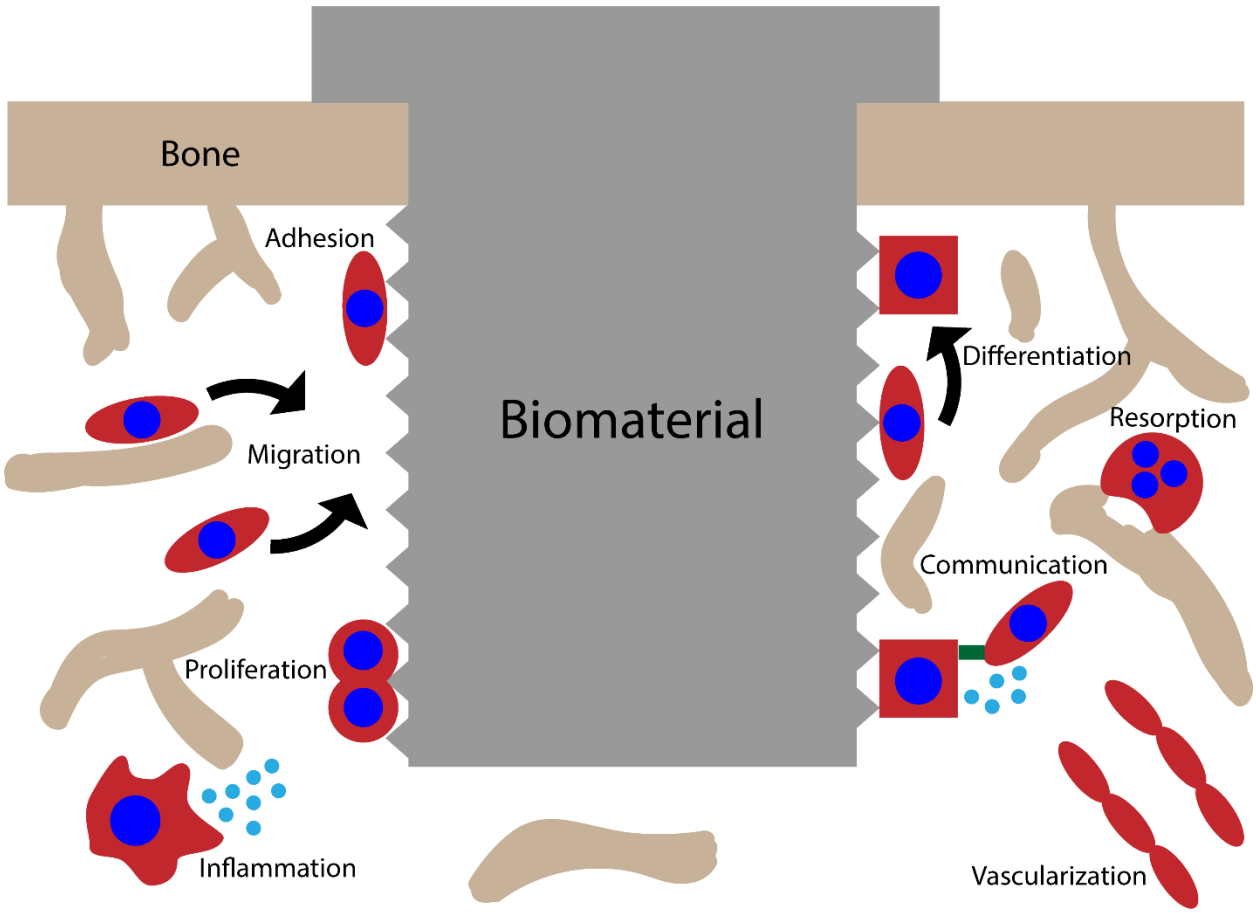

Figure 2.1 Visual representation of different cell functions affected by biomaterials in bone.

Upon implantation of a biomaterial in bone, an inflammatory response is initiated that stimulates the migration and subsequent adhesion of host cells to the material surface. Osteoprogenitors will then proliferate and later differentiate into osteoblasts to secrete new bone. Eventually new vasculature will form and osteoclasts begin to remodel/resorb the surrounding bone. Cellular communication will occur throughout this process contributing to multiple cell functions.

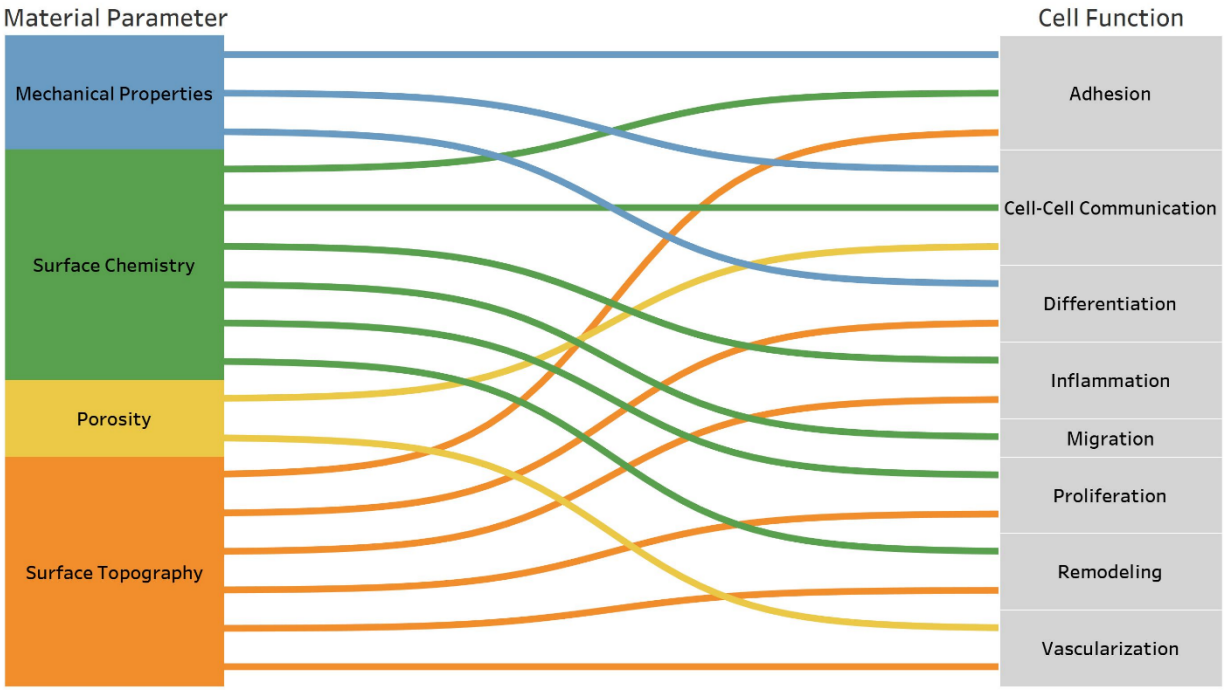

Figure 2.2 Relationship between most influential material parameters and impacted cell functions

The diagram highlights the connections between cell functions and material parameters discussed in the review paper.

2.12 References

[1] K.J. Jepsen, S.A. Goldstein, J.L. Kuhn, M.B. Schaffler, J. Bonadio, Type-I collagen mutation compromises the post-yield behavior of Mov13 long bone, J. Orthop. Res. 14 (1996) 493–499. https://doi.org/10.1002/jor.1100140320.

[2] M.A. Rubin, I. Jasiuk, J. Taylor, J. Rubin, T. Ganey, R.P. Apkarian, TEM analysis of the nanostructure of normal and osteoporotic human trabecular bone, Bone. 33 (2003) 270–282. https://doi.org/10.1016/S8756-3282(03)00194-7.

[3] N. Reznikov, M. Bilton, L. Lari, M.M. Stevens, R. Kröger, Fractal-like hierarchical organization of bone begins at the nanoscale, Science (80-.). 360 (2018). https://doi.org/10.1126/science.aao2189.

[4] I. Jäger, P. Fratzl, Mineralized collagen fibrils: A mechanical model with a staggered arrangement of mineral particles, Biophys. J. 79 (2000) 1737–1746. https://doi.org/10.1016/S0006-3495(00)76426-5.

[5] H. Fonseca, D. Moreira-Gonçalves, H.J.A. Coriolano, J.A. Duarte, Bone quality: The determinants of bone strength and fragility, Sport. Med. 44 (2014) 37–53. https://doi.org/10.1007/s40279-013-0100-7.

[6] C.Y. Hu, T.R. Yoon, Recent updates for biomaterials used in total hip arthroplasty, Biomater. Res. 22 (2018) 1–12. https://doi.org/10.1186/s40824-018-0144-8.

[7] D.D. Bosshardt, V. Chappuis, D. Buser, Osseointegration of titanium, titanium alloy and zirconia dental implants: current knowledge and open questions, Periodontol. 2000. 73 (2017) 22–40. https://doi.org/10.1111/prd.12179.

[8] C. Steffi, Z. Shi, C.H. Kong, W. Wang, Modulation of osteoclast interactions with orthopaedic biomaterials, J. Funct. Biomater. 9 (2018). https://doi.org/10.3390/jfb9010018.

[9] D.H. Kohn, P. Ducheyne, Materials for Bone, Joint and Cartilage Replacement, Med. Dent. Mater. (1992) 29–109.

[10] J. Ramaswamy, H. Ramaraju, D.H. Kohn, Bone-like mineral and organically modified bone-like mineral coatings, Biol. Biomed. Coatings Handb. Process. Charact. (2011) 1–27.

[11] P. Gentile, V. Chiono, I. Carmagnola, P. V Hatton, An Overview of Poly (lactic- co - glycolic) Acid (PLGA) -Based Biomaterials for Bone Tissue Engineering, (2014) 3640–3659. https://doi.org/10.3390/ijms15033640.

[12] M. Urist, B. Strates, Bone Morphogenic Protein, J. Dent. Res. 50 (1971) 1392–1406.

[13] E.M. Aarden, P.J. Nijweide, E.H. Burger, Function of osteocytes in bone, J. Cell. Biochem. 55 (1994) 287–299. https://doi.org/10.1002/jcb.240550304.

[14] J.M. Lean, A.G. Mackay, J.W. Chow, T.J. Chambers, Osteocytic expression of mRNA for c-fos and IGF-I: an immediate early gene response to an osteogenic stimulus, Am. J. Physiol. Endocriniology Metab. 270 (1995) E937–E945.

[15] B.S. Noble, J. Reeve, Osteocyte function, osteocyte death and bone fracture resistance, Mol. Cell. Endocrinol. 159 (2000) 7–13. https://doi.org/10.1016/S0303-7207(99)00174-4.

[16] S. Miller, L. de Saint-Georges, B. Bowman, J. W, Bone lining cells: structure and function, Scanning Microsc. 3 (1989) 953–60.

[17] V. Everts, J.M. Delaissié, W. Korper, D.C. Jansen, W. Tigchelaar-Gutter, P. Saftig, W. Beertsen, The bone lining cell: Its role in cleaning Howship's lacunae and initiating bone formation, J. Bone Miner. Res. 17 (2002) 77–90.

https://doi.org/10.1359/jbmr.2002.17.1.77.
[18] M.N. Lee, H.S. Hwang, S.H. Oh, A. Roshanzadeh, J.W. Kim, J.H. Song, E.S. Kim, J.T. Koh, Elevated extracellular calcium ions promote proliferation and migration of mesenchymal stem cells via increasing osteopontin expression, Exp. Mol. Med. 50 (2018). https://doi.org/10.1038/s12276-018-0170-6.
[19] S. Debnath, A.R. Yallowitz, J. McCormick, S. Lalani, T. Zhang, R. Xu, N. Li, Y. Liu, Y.S. Yang, M. Eiseman, J.-H. Shim, M. Hameed, J.H. Healey, M.P. Bostrom, D.A. Landau, M.B. Greenblatt, Discovery of a periosteal stem cell mediating intramembranous bone formation, Nature. (2018). https://doi.org/10.1038/s41586-018-0554-8.
[20] Y. Kfoury, D.T. Scadden, Mesenchymal cell contributions to the stem cell niche, Cell Stem Cell. (2015). https://doi.org/10.1016/j.stem.2015.02.019.
[21] A. ; Everaers, RalfRosa, 乳鼠心肌提取 HHS Public Access, Physiol. Behav. 176 (2017) 139–148. https://doi.org/10.1016/j.physbeh.2017.03.040.
[22] J. Parvizi, G. Kim, High Yield Orthopaedics, in: High Yield Orthop., 2010: pp. 337–339.
[23] J. Kanehisa, J.N.M. Heersche, Osteoclastic bone resorption: In vitro analysis of the rate of resorption and migration of individual osteoclasts, Bone. 9 (1988) 73–79. https://doi.org/10.1016/8756-3282(88)90106-8.
[24] J.M. Anderson, A. Rodriguez, D.T. Chang, Foreign body reaction to biomaterials, Semin. Immunol. 20 (2008) 86–100. https://doi.org/10.1016/j.smim.2007.11.004.
[25] R. Trindade, T. Albrektsson, S. Galli, Z. Prgomet, P. Tengvall, A. Wennerberg, Osseointegration and foreign body reaction: Titanium implants activate the immune system and suppress bone resorption during the first 4 weeks after implantation, Clin. Implant Dent. Relat. Res. 20 (2018) 82–91. https://doi.org/10.1111/cid.12578.
[26] A. Insua, A. Monje, H.L. Wang, R.J. Miron, Basis of bone metabolism around dental implants during osseointegration and peri-implant bone loss, J. Biomed. Mater. Res. - Part A. 105 (2017) 2075–2089. https://doi.org/10.1002/jbm.a.36060.
[27] R. Sridharan, A.R. Cameron, D.J. Kelly, C.J. Kearney, F.J. O'Brien, Biomaterial based modulation of macrophage polarization: A review and suggested design principles, Mater. Today. 18 (2015) 313–325. https://doi.org/10.1016/j.mattod.2015.01.019.
[28] H.P. Jennissen, A macrophage model of osseointegration, Curr. Dir. Biomed. Eng. 2 (2016) 53–56. https://doi.org/10.1515/cdbme-2016-0015.
[29] A. Scislowska-Czarnecka, E. Menaszek, B. Szaraniec, E. Kolaczkowska, Ceramic modifications of porous titanium: effects on macrophage activation., Tissue Cell. 44 (2012) 391–400. https://doi.org/10.1016/j.tice.2012.08.002.
[30] S. Hamlet, M. Alfarsi, R. George, S. Ivanovski, The effect of hydrophilic titanium surface modification on macrophage inflammatory cytokine gene expression., Clin. Oral Implants Res. 23 (2012) 584–590. https://doi.org/10.1111/j.1600-0501.2011.02325.x.
[31] D. Bitar, J. Parvizi, Biological response to prosthetic debris, World J. Orthop. 6 (2015) 172–189. https://doi.org/10.5312/wjo.v6.i2.172.
[32] J. Kzhyshkowska, A. Gudima, V. Riabov, C. Dollinger, P. Lavalle, N.E. Vrana, Macrophage responses to implants: prospects for personalized medicine, J. Leukoc. Biol. 98 (2015) 953–962. https://doi.org/10.1189/jlb.5vmr0415-166r.
[33] B.D. Boyan, T.W. Hummert, D.D. Dean, Z. Schwartz, Role of material surfaces in regulating bone and cartilage cell response, Biomaterials. 17 (1996) 137–146. https://doi.org/10.1016/0142-9612(96)85758-9.
[34] C.J. Wilson, R.E. Clegg, D.I. Leavesley, M.J. Pearcy, Mediation of biomaterial-cell

interactions by adsorbed proteins: A review, Tissue Eng. 11 (2005) 1–18. https://doi.org/10.1089/ten.2005.11.1.
[35] E. Ruoslahti, The RGD Story: a personal account, Matrix Biol. 22 (2003) 1–7. https://doi.org/10.1016/S0945-053X.
[36] R.K. Globus, S.B. Doty, J.C. Lull, E. Holmuhamedov, M.J. Humphries, C.H. Damsky, Fibronectin is a survival factor for differentiated osteoblasts, J. Cell Sci. 111 (1998) 1385–1393.
[37] K. Anselme, Osteoblast adhesion on biomaterials, Biomaterials. 21 (2000) 667–681. https://doi.org/10.1016/S0142-9612(99)00242-2.
[38] M.D. McKee, A. Nanci, Osteopontin at mineralized tissue interfaces in bone, teeth, and osseointegrated implants: Ultrastructural distribution and implications for mineralized tissue formation, turnover, and repair, Microsc. Res. Tech. 33 (1996) 141–164. https://doi.org/10.1002/(SICI)1097-0029(19960201)33:2<141::AID-JEMT5>3.0.CO;2-W.
[39] T. Yeung, P.C. Georges, L.A. Flanagan, B. Marg, M. Ortiz, M. Funaki, N. Zahir, W. Ming, V. Weaver, P.A. Janmey, Effects of substrate stiffness on cell morphology, cytoskeletal structure, and adhesion, Cell Motil. Cytoskeleton. 60 (2005) 24–34. https://doi.org/10.1002/cm.20041.
[40] M.H. Kim, K. Park, K.H. Choi, S.H. Kim, S.E. Kim, C.M. Jeong, J.B. Huh, Cell adhesion and in vivo osseointegration of sandblasted/acid etched/anodized dental implants, Int. J. Mol. Sci. 16 (2015) 10324–10336. https://doi.org/10.3390/ijms160510324.
[41] M. Jayaraman, U. Meyer, M. Bühner, U. Joos, H.P. Wiesmann, Influence of titanium surfaces on attachment of osteoblast-like cells in vitro, Biomaterials. 25 (2004) 625–631. https://doi.org/10.1016/S0142-9612(03)00571-4.
[42] G. Mendonça, D.B.S. Mendonça, F.J.L. Aragão, L.F. Cooper, Advancing dental implant surface technology - From micron- to nanotopography, Biomaterials. 29 (2008) 3822–3835. https://doi.org/10.1016/j.biomaterials.2008.05.012.
[43] D. Guadarrama Bello, A. Fouillen, A. Badia, A. Nanci, A nanoporous titanium surface promotes the maturation of focal adhesions and formation of filopodia with distinctive nanoscale protrusions by osteogenic cells, Acta Biomater. 60 (2017) 339–349. https://doi.org/10.1016/j.actbio.2017.07.022.
[44] Z. Schwartz, P. Raz, G. Zhao, Y. Barak, M. Tauber, H. Yao, B.D. Boyan, Effect of micrometer-scale roughness of the surface of Ti6Al4V pedicle screws in vitro and in vivo, J. Bone Jt. Surg. - Ser. A. 90 (2008) 2485–2498. https://doi.org/10.2106/JBJS.G.00499.
[45] A. Wennerberg, T. Albrektsson, Effects of titanium surface topography on bone integration: A systematic review, Clin. Oral Implants Res. 20 (2009) 172–184. https://doi.org/10.1111/j.1600-0501.2009.01775.x.
[46] M. Yamada, T. Miyauchi, A. Yamamoto, F. Iwasa, M. Takeuchi, M. Anpo, K. Sakurai, K. Baba, T. Ogawa, Enhancement of adhesion strength and cellular stiffness of osteoblasts on mirror-polished titanium surface by UV-photofunctionalization, Acta Biomater. 6 (2010) 4578–4588. https://doi.org/10.1016/j.actbio.2010.07.010.
[47] M. Kantlehner, P. Schaffner, D. Finsinger, J. Meyer, a Jonczyk, B. Diefenbach, B. Nies, G. Hölzemann, S.L. Goodman, H. Kessler, Surface coating with cyclic RGD peptides stimulates osteoblast adhesion and proliferation as well as bone formation., Chembiochem. 1 (2000) 107–114. https://doi.org/10.1002/1439-7633(20000818)1:2<107::aid-cbic107>3.0.co;2-4.
[48] W.B. Tsai, Y.R. Chen, H.L. Liu, J.Y. Lai, Fabrication of UV-crosslinked chitosan

scaffolds with conjugation of RGD peptides for bone tissue engineering, Carbohydr. Polym. 85 (2011) 129–137. https://doi.org/10.1016/j.carbpol.2011.02.003.
[49] a. a. Sawyer, K.M. Hennessy, S.L. Bellis, Regulation of mesenchymal stem cell attachment and spreading on hydroxyapatite by RGD peptides and adsorbed serum proteins, Biomaterials. 26 (2005) 1467–1475. https://doi.org/10.1016/j.biomaterials.2004.05.008.
[50] K.M. Hennessy, B.E. Pollot, W.C. Clem, M.C. Phipps, A. a. Sawyer, B.K. Culpepper, S.L. Bellis, The effect of collagen I mimetic peptides on mesenchymal stem cell adhesion and differentiation, and on bone formation at hydroxyapatite surfaces, Biomaterials. 30 (2009) 1898–1909. https://doi.org/10.1016/j.biomaterials.2008.12.053.
[51] K.M. Hennessy, W.C. Clem, M.C. Phipps, A. a. Sawyer, F.M. Shaikh, S.L. Bellis, The effect of RGD peptides on osseointegration of hydroxyapatite biomaterials, Biomaterials. 29 (2008) 3075–3083. https://doi.org/10.1016/j.biomaterials.2008.04.014.
[52] D. Ferris, RGD-coated titanium implants stimulate increased bone formation in vivo, Biomaterials. 20 (1999) 2323–2331. https://doi.org/10.1016/S0142-9612(99)00161-1.
[53] J.J. Qian, R.S. Bhatnagar, Enhanced cell attachment to anorganic bone mineral in the presence of a synthetic peptide related to collagen, J. Biomed. Mater. Res. 31 (1996) 545–554. https://doi.org/10.1002/(SICI)1097-4636(199608)31:4<545::AID-JBM15>3.0.CO;2-F.
[54] R. Fujisawa, M. Mizuno, Y. Nodasaka, K. Yoshinori, Attachment of osteoblastic cells to hydroxyapatite crystals by a synthetic peptide (Glu7-Pro-Arg-Gly-Asp-Thr) containing two functional sequences of bone sialoprotein, Matrix Biol. 16 (1997) 21–28. https://doi.org/10.1016/S0945-053X(97)90113-X.
[55] H. Ramaraju, S.J. Miller, D.H. Kohn, Dual-functioning peptides discovered by phage display increase the magnitude and specificity of BMSC attachment to mineralized biomaterials, Biomaterials. 134 (2017) 1–12. https://doi.org/10.1016/j.biomaterials.2017.04.034.
[56] H. Ramaraju, D.H. Kohn, Cell and Material-Specific Phage Display Peptides Increase iPS-MSC Mediated Bone and Vasculature Formation In Vivo, Adv. Healthc. Mater. 1801356 (2019) 1–11. https://doi.org/10.1002/adhm.201801356.
[57] P.A. DiMilla, J.A. Stone, J.A. Quinn, S.M. Albelda, D.A. Lauffenburger, Maximal migration of human smooth muscle cells on fibronectin and type IV collagen occurs at an intermediate attachment strength, J. Cell Biol. 122 (1993) 729–737. https://doi.org/10.1083/jcb.122.3.729.
[58] E. V Leonova, K.E. Pennington, P.H. Krebsbach, D.H. Kohn, Substrate mineralization stimulates focal adhesion contact redistribution and cell motility of bone marrow stromal cells., J. Biomed. Mater. Res. A. 79 (2006) 263–270. https://doi.org/10.1002/jbm.a.30786.
[59] A. Shekaran, J.R. García, A.Y. Clark, T.E. Kavanaugh, A.S. Lin, R.E. Guldberg, A.J. García, Bone regeneration using an alpha 2 beta 1 integrin-specific hydrogel as a BMP-2 delivery vehicle, Biomaterials. 35 (2014) 5453–5461. https://doi.org/10.1016/j.biomaterials.2014.03.055.
[60] G. Chen, Y. Lv, Matrix elasticity-modified scaffold loaded with SDF-1α improves the in situ regeneration of segmental bone defect in rabbit radius, Sci. Rep. 7 (2017) 1–12. https://doi.org/10.1038/s41598-017-01938-3.
[61] R. Aquino-martínez, A.P. Angelo, F.V. Pujol, Calcium-containing scaffolds induce bone regeneration by regulating mesenchymal stem cell differentiation and migration, (2017)

1–10. https://doi.org/10.1186/s13287-017-0713-0.
[62] G. Li, G. White, C. Connolly, D. Marsh, Cell proliferation and apoptosis during fracture healing, J. Bone Miner. Res. 17 (2002) 791–799. https://doi.org/10.1359/jbmr.2002.17.5.791.
[63] B.G. Keselowsky, L. Wang, Z. Schwartz, A.J. Garcia, B.D. Boyan, Integrin alpha(5) controls osteoblastic proliferation and differentiation responses to titanium substrates presenting different roughness characteristics in a roughness independent manner., J. Biomed. Mater. Res. A. 80 (2007) 700–710. https://doi.org/10.1002/jbm.a.30898.
[64] M. Lai, C.D. Hermann, A. Cheng, R. Olivares-Navarrete, R.A. Gittens, M.M. Bird, M. Walker, Y. Cai, K. Cai, K.H. Sandhage, Z. Schwartz, B.D. Boyan, Role of α2β1 integrins in mediating cell shape on microtextured titanium surfaces, J. Biomed. Mater. Res. - Part A. 103 (2015) 564–573. https://doi.org/10.1002/jbm.a.35185.
[65] M. Théry, Micropatterning as a tool to decipher cell morphogenesis and functions, J. Cell Sci. 123 (2010) 4201–4213. https://doi.org/10.1242/jcs.075150.
[66] A. Dolatshahi-Pirouz, T. Jensen, D.C. Kraft, M. Foss, P. Kingshott, J.L. Hansen, A.N. Larsen, J. Chevallier, F. Besenbacher, Fibronectin adsorption, cell adhesion, and proliferation on nanostructured tantalum surfaces, ACS Nano. 4 (2010) 2874–2882. https://doi.org/10.1021/nn9017872.
[67] F. Li, N. Whyte, C. Niyibizi, Differentiating multipotent mesenchymal stromal cells generate factors that exert paracrine activities on exogenous MSCs: Implications for paracrine activities in bone regeneration, Biochem. Biophys. Res. Commun. 426 (2012) 475–479. https://doi.org/10.1016/j.bbrc.2012.08.095.
[68] N. Batra, S. Burra, A.J. Siller-Jackson, S. Gu, X. Xia, G.F. Weber, D. DeSimone, L.F. Bonewald, E.M. Lafer, E. Sprague, M.A. Schwartz, J.X. Jiang, Mechanical stress-activated integrin α5β1 induces opening of connexin 43 hemichannels, Proc. Natl. Acad. Sci. U. S. A. 109 (2012) 3359–3364. https://doi.org/10.1073/pnas.1115967109.
[69] W.J. Nelson, R. Nusse, Convergence of Wnt, β-Catenin, and Cadherin pathways, Science (80-.). 303 (2004) 1483–1487. https://doi.org/10.1126/science.1094291.
[70] S. Burra, D.P. Nicolella, W.L. Francis, C.J. Freitas, N.J. Mueschke, K. Poole, J.X. Jiang, Dendritic processes of osteocytes are mechanotransducers that induce the opening of hemichannels, Proc. Natl. Acad. Sci. U. S. A. 107 (2010) 13648–13653. https://doi.org/10.1073/pnas.1009382107.
[71] A.G. Robling, A.B. Castillo, C.H. Turner, Biomechanical and Molecular Regulation of Bone Remodeling, Annu. Rev. Biomed. Eng. 8 (2006) 455–498. https://doi.org/10.1146/annurev.bioeng.8.061505.095721.
[72] S.D. Tan, T.J. de Vries, A.M. Kuijpers-Jagtman, C.M. Semeins, V. Everts, J. Klein-Nulend, Osteocytes subjected to fluid flow inhibit osteoclast formation and bone resorption, Bone. 41 (2007) 745–751. https://doi.org/10.1016/j.bone.2007.07.019.
[73] L. You, S. Temiyasathit, P. Lee, C.H. Kim, P. Tummala, W. Yao, W. Kingery, A.M. Malone, R.Y. Kwon, C.R. Jacobs, Osteocytes as mechanosensors in the inhibition of bone resorption due to mechanical loading, Bone. 42 (2008) 172–179. https://doi.org/10.1016/j.bone.2007.09.047.
[74] A. Santos, A.D. Bakker, J. Klein-Nulend, The role of osteocytes in bone mechanotransduction, Osteoporos. Int. 20 (2009) 1027–1031. https://doi.org/10.1007/s00198-009-0858-5.
[75] J. Tang, R. Peng, J. Ding, The regulation of stem cell differentiation by cell-cell contact

on micropatterned material surfaces, Biomaterials. 31 (2010) 2470–2476. https://doi.org/10.1016/j.biomaterials.2009.12.006.
[76] H. Li, K. Xue, N. Kong, K. Liu, J. Chang, Silicate bioceramics enhanced vascularization and osteogenesis through stimulating interactions between endothelia cells and bone marrow stromal cells, Biomaterials. 35 (2014) 3803–3818. https://doi.org/10.1016/j.biomaterials.2014.01.039.
[77] J. Green, S. Schotland, D.J. Stauber, C.R. Kleeman, T.L. Clemens, Cell-matrix interaction in bone: type I collagen modulates signal transduction in osteoblast-like cells, Am. J. Physiol. Cell Physiol. 268 (1995) C1090–C1103.
[78] Y. Xu, Z. Wu, X. Dong, H. Li, Combined biomaterial signals stimulate communications between bone marrow stromal cell and endothelial cell, RSC Adv. 7 (2017) 5306–5314. https://doi.org/10.1039/c6ra28101j.
[79] P. Uribe, A. Johansson, R. Jugdaohsingh, J.J. Powell, C. Magnusson, M. Davila, A. Westerlund, M. Ransjö, Soluble silica stimulates osteogenic differentiation and gap junction communication in human dental follicle cells, Sci. Rep. 10 (2020) 1–11. https://doi.org/10.1038/s41598-020-66939-1.
[80] J. Popara, L. Accomasso, E. Vitale, C. Gallina, D. Roggio, A. Iannuzzi, S. Raimondo, R. Rastaldo, G. Alberto, F. Catalano, G. Martra, V. Turinetto, P. Pagliaro, C. Giachino, Silica nanoparticles actively engage with mesenchymal stem cells in improving acute functional cardiac integration, Nanomedicine. 13 (2018) 1121–1138. https://doi.org/10.2217/nnm-2017-0309.
[81] J. Costa-Rodrigues, S. Reis, A. Castro, M.H. Fernandes, Bone anabolic effects of soluble si: In vitro studies with human mesenchymal stem cells and cd14+ osteoclast precursors, Stem Cells Int. 2016 (2016). https://doi.org/10.1155/2016/5653275.
[82] Ž. Mladenović, A. Johansson, B. Willman, K. Shahabi, E. Björn, M. Ransjö, Soluble silica inhibits osteoclast formation and bone resorption in vitro, Acta Biomater. 10 (2014) 406–418. https://doi.org/10.1016/j.actbio.2013.08.039.
[83] L. Moroni, P.M. Fornasari, Human mesenchymal stem cells: A bank perspective on the isolation, characterization and potential of alternative sources for the regeneration of musculoskeletal tissues, J. Cell. Physiol. 228 (2013) 680–687. https://doi.org/10.1002/jcp.24223.
[84] F. Bai, Z. Wang, J. Lu, J. Liu, G. Chen, R. Lv, J. Wang, K. Lin, J. Zhang, X. Huang, The correlation between the internal structure and vascularization of controllable porous bioceramic materials in vivo: A quantitative study, Tissue Eng. - Part A. 16 (2010) 3791–3803. https://doi.org/10.1089/ten.tea.2010.0148.
[85] N. Wang, J.D. Tytell, D.E. Ingber, Mechanotransduction at a distance: Mechanically coupling the extracellular matrix with the nucleus, Nat. Rev. Mol. Cell Biol. 10 (2009) 75–82. https://doi.org/10.1038/nrm2594.
[86] A.J. García, C.D. Reyes, CRITICAL REVIEWS IN ORAL BIOLOGY & MEDICINE Bio-adhesive Surfaces to Promote Osteoblast Differentiation and Bone Formation, (2004) 407–413.
[87] J. Xi, L. Kong, Y. Gao, Y. Gong, N. Zhao, X. Zhang, Properties of poly(3-hydroxybutyrate-co-3-hydroxyhexanoate) films modified with polyvinylpyrrolidone and behavior of MC3T3-E1 osteoblasts cultured on the blended films, J. Biomater. Sci. Polym. Ed. 16 (2005) 1395–1408. https://doi.org/10.1163/156856205774472344.
[88] A.J. Engler, S. Sen, H.L. Sweeney, D.E. Discher, Matrix Elasticity Directs Stem Cell

Lineage Specification, Cell. 126 (2006) 677–689. https://doi.org/10.1016/j.cell.2006.06.044.
[89] R. McBeath, D.M. Pirone, C.M. Nelson, K. Bhadriraju, C.S. Chen, Cell Shape, Cytoskeletal Tension, and RhoA Regulate Stem Cell Lineage Commitment, Dev. Cell. 6 (2004) 483–495.
[90] X. Wang, T. Nakamoto, I. Dulińska-Molak, N. Kawazoe, G. Chen, Regulating the stemness of mesenchymal stem cells by tuning micropattern features, J. Mater. Chem. B. 4 (2016) 37–45. https://doi.org/10.1039/c5tb02215k.
[91] K.A. Kilian, B. Bugarija, B.T. Lahn, M. Mrksich, Geometric cues for directing the differentiation of mesenchymal stem cells, Proc. Natl. Acad. Sci. U. S. A. 107 (2010) 4872–4877. https://doi.org/10.1073/pnas.0903269107.
[92] L. Gao, R. McBeath, C.S. Chen, Stem cell shape regulates a chondrogenic versus myogenic fate through rac1 and N-cadherin, Stem Cells. 28 (2010) 564–572. https://doi.org/10.1002/stem.308.
[93] C. Rot, T. Stern, S. Krief, A. Akiva, Deposition of collagen type I onto skeletal endothelium reveals a new role for blood vessels in regulating bone morphology, 2016. https://doi.org/10.1242/dev.139253.
[94] F.M. Klenke, Y. Liu, H. Yuan, E.B. Hunziker, K.A. Siebenrock, W. Hofstetter, Impact of pore size on the vascularization and osseointegration of ceramic bone substitutes in vivo, J. Biomed. Mater. Res. - Part A. 85 (2008) 777–786. https://doi.org/10.1002/jbm.a.31559.
[95] T. Raimondo, S. Puckett, T.J. Webster, Greater osteoblast and endothelial cell adhesion on nanostructured polyethylene and titanium, Int. J. Nanomedicine. 5 (2010) 647–652. https://doi.org/10.2147/IJN.S13047.
[96] D. Khang, J. Lu, C. Yao, K.M. Haberstroh, T.J. Webster, The role of nanometer and sub-micron surface features on vascular and bone cell adhesion on titanium, Biomaterials. 29 (2008) 970–983. https://doi.org/10.1016/j.biomaterials.2007.11.009.
[97] T.W. Chung, D.Z. Liu, S.Y. Wang, S.S. Wang, Enhancement of the growth of human endothelial cells by surface roughness at nanometer scale, Biomaterials. 24 (2003) 4655–4661. https://doi.org/10.1016/S0142-9612(03)00361-2.
[98] D.C. Miller, A. Thapa, K.M. Haberstroh, T.J. Webster, Endothelial and vascular smooth muscle cell function on poly(lactic-co-glycolic acid) with nano-structured surface features, Biomaterials. 25 (2004) 53–61. https://doi.org/10.1016/S0142-9612(03)00471-X.
[99] F.J. Byfield, R.K. Reen, T.P. Shentu, I. Levitan, K.J. Gooch, Endothelial actin and cell stiffness is modulated by substrate stiffness in 2D and 3D, J. Biomech. 42 (2009) 1114–1119. https://doi.org/10.1016/j.jbiomech.2009.02.012.
[100] P. Proff, P. Römer, The molecular mechanism behind bone remodelling: A review, Clin. Oral Investig. 13 (2009) 355–362. https://doi.org/10.1007/s00784-009-0268-2.
[101] M. Schumacher, A.S. Wagner, J. Kokesch-Himmelreich, A. Bernhardt, M. Rohnke, S. Wenisch, M. Gelinsky, Strontium substitution in apatitic CaP cements effectively attenuates osteoclastic resorption but does not inhibit osteoclastogenesis, Acta Biomater. 37 (2016) 184–194. https://doi.org/10.1016/j.actbio.2016.04.016.
[102] E. Bonnelye, A. Chabadel, F. Saltel, P. Jurdic, Dual effect of strontium ranelate: Stimulation of osteoblast differentiation and inhibition of osteoclast formation and resorption in vitro, Bone. 42 (2008) 129–138. https://doi.org/10.1016/j.bone.2007.08.043.
[103] G. Spence, N. Patel, R. Brooks, W. Bonfield, N. Rushton, Osteoclastogenesis on hydroxyapatite ceramics: The effect of carbonate substitution, J. Biomed. Mater. Res. -

Part A. 92 (2010) 1292–1300. https://doi.org/10.1002/jbm.a.32373.
[104] A.L. Torres, S.G. Santos, M.I. Oliveira, M.A. Barbosa, Fibrinogen promotes resorption of chitosan by human osteoclasts, Acta Biomater. 9 (2013) 6553–6562. https://doi.org/https://doi.org/10.1016/j.actbio.2013.01.015.
[105] D.O. Costa, P.D.H. Prowse, T. Chrones, S.M. Sims, D.W. Hamilton, A.S. Rizkalla, S.J. Dixon, The differential regulation of osteoblast and osteoclast activity bysurface topography of hydroxyapatite coatings, Biomaterials. 34 (2013) 7215–7226. https://doi.org/10.1016/j.biomaterials.2013.06.014.
[106] J. Brinkmann, T. Hefti, F. Schlottig, N.D. Spencer, H. Hall, Response of osteoclasts to titanium surfaces with increasing surface roughness: An in vitro study, Biointerphases. 7 (2012) 1–9. https://doi.org/10.1007/s13758-012-0034-x.
[107] S.C. Sartoretto, A.T.N.N. Alves, R.F.B. Resende, J. Calasans-Maia, J.M. Granjeiro, M.D. Calasans-Maia, Early osseointegration driven by the surface chemistry and wettability of dental implants, J. Appl. Oral Sci. 23 (2015) 272–278. https://doi.org/10.1590/1678-775720140483.
[108] K. Breding, R. Jimbo, M. Hayashi, Y. Xue, K. Mustafa, M. Andersson, The effect of hydroxyapatite nanocrystals on osseointegration of titanium implants: An in vivo rabbit study, Int. J. Dent. 2014 (2014). https://doi.org/10.1155/2014/171305.

Chapter 3: Dual-Functional Peptide DPI-VTK Promotes Mesenchymal Stem Cell Migration Towards Biomimetic Apatite Scaffolds for Bone Regeneration

3.1 Abstract

Targeting specific populations of cells with chemotactic and adhesion factors is a promising strategy for bone regeneration. Previously, our laboratory identified two peptide sequences: the mesenchymal stem cell (MSC) binding DPI (DPIYALSWSGMA) sequence, and the apatite binding VTK (VTKHLNQISQSY) sequence. When combined into the dual-functional DPI-VTK sequence, DPI-VTK enhances the adhesion strength of MSCs to apatite surfaces. We hypothesize that DPI-VTK, in addition to supporting adhesion, can act as a soluble chemotactic agent. In this study, we test DPI-VTK as an MSC-specific chemotactic factor in the context of supporting bone regeneration. In transwell assays, induced pluripotent stem cell derived human MSCs ($p<0..0001$) and primary mouse calvarial cells ($p<0.0001$) showed significantly increased migration *in vitro* when DPI-VTK was used as a chemoattractant. Further characterization of DPI-VTK binding cells from mouse calvaria using flow cytometry showed specificity towards cells expressing MSC markers. When administered along with a mineralized scaffold *in vivo,* DPI-VTK increased the migration of CD90 and CD200 positive cells ($p<0.05$) and increased bone formation versus no peptide controls ($p<0.05$). This study is significant in showing the ability of phage-display derived peptides to act as both cell-specific chemotactic agents and cell-specific adhesive agents for bone tissue engineering. These results demonstrate

the utility of creating multi-functional peptides that can influence both migration and adhesion; a strategy that could be applied to numerous different cell types and systems.

3.2 Introduction

Despite bone's regenerative properties, bone grafting is often necessary to heal defects and restore function. The current standard is to graft autogenous bone from another site to the defect. However, donor site morbidity such as postoperative pain, infection, scarring, and increased surgical recovery time occur[1]. For example, with iliac crest grafting, as many as 91.3% of patients experience donor site pain, 54.6% have problems with ambulation after the surgery, and 34.8% have paresthesia[2]. Allografting is a useful alternative to autografting, but results in inferior bone regeneration compared to autografting [3,4]. The disadvantages of autografting and allografting have motivated tissue engineering approaches to regenerate bone. For example, transplantation of mesenchymal stem cells (MSCs) on a biomaterial scaffold increases bone regeneration versus acellular scaffolds [5]. However, outcomes from MSC transplantation therapies are not always predictable and cell transplantation is not always clinically practical due to the complexity, time, regulatory hurdles, and high cost involved. An alternative is to use a "cell homing" strategy to promote host cell migration into a defect. Increased cell migration has been accomplished using soluble factors such as stromal cell-derived factor 1 (SDF-1), but the short half-life of growth factors and lack of specificity in cells targeted by the factors results in variability in healing[6]. An alternative to homing via growth factors is to engineer a conducting material to facilitate the migration and attachment of host cells. For bone regeneration, homing MSCs is critical due to their bone progenitor capabilities and promotion of angiogenesis[7].

Hydroxyapatite (HA) and other calcium-phosphate ceramics have been used extensively as osteoconductive materials due to their similar mechanical properties to native bone mineral and high level of protein absorption that enhances cell attachment[8]. Although apatites and calcium phosphate based materials have been used clinically, they fail to catalyze complete bridging of critical sized defects and lack specificity in the cell populations that they recruit[9]. Specificity towards osteogenic cells is critical as migration of epithelial/connective tissue cells may result in unwanted soft tissue growth [10]. While cell matrix proteins have been used to enhance cell adhesion on HA, the high cost and complexity of producing and purifying proteins has motivated research to derive peptide sequences from proteins that mediate cell adhesion[11].

Peptides are advantageous for biomaterial functionalization because they have higher stability and reduced cost compared to higher molecular weight proteins[12]. Peptides derived from matrix proteins can enhance the adhesion and differentiation of MSCs on biomaterials, but lack specificity for MSCs and do not have high affinity for HA-based materials[8]. Materials that target MSCs are important because an increased number of MSCs in a defect likely results in increased bone formation, and other cell populations may compete for cell binding sites in the case of non-specific cell homing to materials[13]. These limitations of using peptides derived from known ECM sequences motivated the screening of peptide libraries to discover novel sequences. Screening techniques such as phage display have made it possible to discover sequences that are not obvious or known candidates for binding to a particular substrate[14]. Phage display was used to discover the HA mineral binding sequence VTK (**VTK**HLNQISQSY), and the MSC binding sequence DPI (**DPI**YALSWSGMA)[8,12]. The fusion of these two domains into the dual peptide DPI-VTK (GG**DPI**YALSWSGMAGGGS**VTK**HLNQISQSY) presents a tool for enhancing the attachment of MSCs to mineralized materials. The use of this dual peptide has several advantages

over other peptides, such as strong affinity for HA, specificity for MSCs, and presenting the cell binding domain away from the surface and more accessible for cell binding. DPI-VTK increases the strength of adhesion and promotes bone and vascular regeneration in an ectopic transplantation model [8,12].

Peptide DPI-VTK adhesion is mediated by integrins α5, αV, β1, β3, β5, and α2β1 [15]. Due to the importance of integrins in cellular migration, it follows that DPI-VTK can influence cellular migration. Further, since many ECM proteins such as fibronectin and peptide derivatives can act as chemoattractants [16], we hypothesize that peptide DPI-VTK can specifically recruit MSCs towards mineralized materials and subsequently increase bone regeneration when using acellular scaffolds. To test this hypothesis, transwell migration assays were first conducted with human MSCs to determine the chemotactic effects of DPI-VTK. In order to better understand the cells recruited by DPI-VTK in vivo, transwell assays were conducted with heterogenous populations of primary cells from calvaria and bone marrow. Further characterization of the DPI-VTK binding cell population was conducted using flow cytometry to look at which MSC markers DPI-VTK binding cells expressed. To see if this cell population could be recruited using DPI-VTK in combination with scaffolds, an *in vivo* migration experiment was conducted using the mouse calvarial defect model. Mineralized scaffolds administered either with DPI-VTK or no peptide were placed in the calvarial defects for 1 week before analysis with immunohistochemistry to quantify migration of cells expressing various MSC markers. To see if peptide DPI-VTK could increase bone regeneration, a longer term calvarial defect experiment was conducted for 8 weeks with scaffolds containing no peptide, DPI-VTK, P15 as a peptide comparison, SDF-1 as a positive

control, and BMP-2 as a positive control. Micro-CT was used to determine BV/TV values of the regenerated defects.

3.3 Materials and Methods

***3.3.1 Peptide Synthesis*:** Peptides used included DPIYALSWSGMA (DPI), VTKHLNQISQSY (VTK), GGDPIYALSWSGMAGG GSVTKHLNQISQSY (DPI-VTK), and GTPGPQGIAGQRGVV (P15). Peptides were synthesized by the University of Michigan Peptide Core using solid phase peptide synthesis. All peptides were verified at >95% purity with HPLC. Peptides were stored lyophilized at -20 C until use. Stock solutions were obtained by dissolving lyophilized peptides in ddH20 followed by dilution with PBS. FITC tagged peptides were obtained by reacting FITC with peptides in pH 9 carbonate buffer overnight and then dialyzing for 48 hours. FITC peptides were lyophilized, dissolved in DMSO, and diluted in PBS before use. All peptides were sterile filtered before use in cell and animal studies.

3.3.2 Cell Culture: Clonally derived human bone marrow stromal cells (HBMSCs, provided by NIH) [17,18], human induced pluripotent stem cell derived MSCs (iPS-MSCs, provided by Dr. Paul Krebsbach and Dr. Luis Villa) [19], MC3T3 cells, C3H10 cells, and mouse dermal fibroblasts (MDFs, provided by Dr. Renny Frenceschi) were maintained in aMEM with 10% HI FBS and antibiotics. Cells were expanded until 80-90% confluent before passaging. iPS-MSC

cells and HBMSCs were used from passages 5-10, C3H10 cells were used from passages 10-15, MC3t3s were used from passages 10-20, and MDFs were used from passages 25-30.

3.3.3 Transwell Migration Assay: Migration assays were performed by seeding human iPS-MSCs, HBMSCs, C3H10, MC3T3s, and MDFs in transwell inserts (8-micron pore size) (20,000 per well) with differing concentrations of peptide in the lower chamber. Cells were expanded, trysanized, and resuspended in serum-free alpha-MEM with 0.1% BSA. 100 uL of cell suspension containing 20,000 cells was placed in the upper transwell chamber and incubated for 10 minutes. Then 600 uL of serum-free alpha-MEM with 0.1% BSA media with or without chemoattractant was added to the lower chamber and the plate was placed in the incubator at 37^{o}C with 5% CO_2. After different timepoints, the media was aspirated from the transwells, they were washed 3x with PBS, and the transwell membranes were fixed with 4% PFA for 15 minutes at room termpature. Using a cotton swab, the cells were carefully removed from the upper membrane to leave only the migrated cells on the lower membrane. The membranes were then stained with crystal violet solution for 1 hour, washed with distilled water three times, and dried. The dried membranes were removed from the transwells using a scalpel blade and mounted on glass slides with permount. The mounted slides were then imaged at 200x magnification with an Olympus BX51 microscope with brightfield. Cell counting was done manually using 5 fields per membrane. Average cells/field were obtained and used to calculate the percentage of migrated cells from the initial seeded population. Samples were run with 3 replicates per condition.

***3.3.4 Primary Cell Harvesting for transwell assay*:** To determine the effect of DPI-VTK on primary mouse cell migration, mouse cells were harvested and tested in the transwell assay. All animal procedures were approved by the Institutional Animal Care and Use Committee (IACUC) at the University of Michigan. 4–5-week-old male C57/BL6 mice (n=7) were sacrificed. For calvaria cells, the calvaria were removed, minced, and digested in a collagenase solution for 1 hour followed by filtering through a cell strainer to remove bone fragments. For bone marrow cells, the tibiae and femora were removed, both epiphyses of each bone were cut, and then the marrow removed through centrifugation. The heterogenous primary cell suspensions were used directly in transwell assays as described above, without expansion.

3.3.5 Scaffold Fabrication: Scaffolds were fabricated from a solution of 85:15 PLGA in chloroform at 7.5% w/v using solvent casting/particulate leaching in a Delrin mold (5 mm diameter) with NaCL particles sieved to 250-425 microns. The mold was covered with aluminum foil and allowed to dry in a fumehood followed by transfer to a vacuum chamber. Once the chloroform was fully evaporated, the NaCL was leached from the scaffolds with double distilled water and the scaffolds were chemically functionalized with 0.5 M sodium hydroxide followed by rinsing with water. Molds containing the scaffolds were attached to a bioreactor and cycled through a solution of 4x modified simulated body fluid (mSBF) for 1 day changing the solution every 6 hours. This was followed by 4 days of 2x mSBF changing the solution every 12 hours. 1x mSBF contains 141 mM NaCl, 4.0 mM KCl, 0.5 mM $MgSO_4$, 1.0 mM $MgCl_2$, 4.2 mM $NaHCO_3$, 5.0 mM $CaCl_2 \cdot 2H_2O$, and 2.0 mM KH_2PO_4 at pH 6.8.

***3.3.6 Peptide absorption on scaffolds and controlled release measurements*:** To determine if DPI-VTK can be delivered using mineralized scaffold, DPI-VTK was dissolved in PBS buffer at a concentration of 100 μg/mL and incubated with scaffolds for 3 hours at 37°C. The remaining concentration of DPI-VTK in the solution was quantified using UV absorbance with a DPI-VTK standard curve and subtracted from the initial concentration to determine amount absorbed. For controlled release studies, DPI-VTK loaded scaffolds were incubated in PBS buffer at 37°C and samples (n=3) were taken at 1 hour, 2 hours, 24, hours, and 72 hours for measurement with UV absorbance (214 nm) with a DPI-VTK standard curve.

3.3.7 In-vivo migration: To determine the ability of DPI-VTK to promote migration of MSCs *in vivo*, 10-week-old male C57/BL6 mice (n=5) were anesthetized with isofluorane and an incision was made in the scalp to expose the calvarium. A 5 mm critical sized defect was made in the parietal bone with a trephine bur and the scaffold was placed within the defect along with a bolus of 50 μL of 1mg/mL DPI-VTK or PBS control. The surgical wounds were closed with 4-0 nylon simple-interrupted sutures. All surgical procedures were performed in accordance with NIH guidelines for the care and use of laboratory animals. The mice were allowed to heal for 1 week before sacrifice. Calvaria were then prepared for immunohistochemical staining.

***3.3.8 Immunohistochemistry*:** To determine the MSC marker expression of DPI-VTK attracted cells *in vivo*, calvaria were removed following sacrifice, fixed in 4% PFA for 24 hours and demineralized in 10% EDTA for 2 weeks. They were then embedded in paraffin and sectioned on slides. The slides were de-paraffinized with xylene followed by gradual rehydration with decreasing concentrations of ethanol/water solution. Antigen retrieval was performed by

incubation in pH 6 citrate buffer for 1 hour at 60 C. blocked, and stained with primary antibodies for CD31, CD90, CD73, CD105, CD29, CD106, CD45, CD200, CD44 or Sca-1 overnight. After incubation with secondary biotinylated antibodies, the sections were incubated with streptavidin HRP and developed with DAB. The slides were counterstained with hematoxylin and mounted before imaging. Images were obtained on an Olympus BX51 microscope at 200x magnification with 10 fields of view per sample. The images were analyzed and quantified in Image-J using a published protocol [20]. Briefly, intensity of the DAB stain was quantified for each field of view and normalized to the number of cellular nuclei. For CD31, vessels for each field of view were counted manually.

3.3.9 In-vivo Regeneration: To determine the effect of DPI-VTK in promoting bone regeneration, 10-week-old male C57/BL6 mice (n=7/condition) were anesthetized with isoflurane and an incision was made in the scalp to expose the calvarium. Scaffolds were prepared as previously described. For the DPI-VTK and P15 groups, scaffolds were incubated in 100 ug/mL peptide (in PBS) for 3 hours to saturate scaffold in peptide. The other scaffolds were incubated in PBS for 3 hours and all scaffolds were washed in PBS prior to transplant. A 5 mm critical sized defect was made in the parietal bone with a trephine bur and the scaffold was placed within the defect along with a bolus of 50 μL of 1mg/mL DPI-VTK, 1 mg/mL P15, 20μg/mL rhBMP-2, 20μg/mL rhSDF-1, or PBS control. The surgical wounds were closed with 4-0 nylon simple-interrupted sutures. The mice were allowed to heal for 8 weeks before sacrifice. Calvaria were removed and fixed in 4% PFA for 24 hours followed by transfer to 70% ethanol.

***3.3.10 Micro-CT*:** Mineralized scaffolds and calvaria were analyzed using a Scanco μCT 100 at 10 μm voxel size and 10 μm slice increments. MicroCT scans were obtained at 70 kV, 114 A using a 0.5 Al filter. Reconstructed images of all scaffolds and bones were analyzed using the Scanco μCT evaluation tool with a threshold of 180 to calculate mineral volume fractions. Circular regions of interest of concentric circles (5, 4, 3, 2, and 1 mm diameter) were traced around the calvaria defects throughout the thickness of the scaffolds and used to calculate the BV/TV values of the volumes of interest. BV/TV values of concentric rings were determined by subtracting the BV and TV values from the inner portion from the total BV and TV values and determining the new BV/TV value. The threshold used was able to filter out the majority of the starting mineral from the initial mineralized scaffolds. Values are presented unadjusted since the scaffold mineral constituted approximately only 1% of the total mineral volume on average at the selected threshold.

***3.3.11 Immunofluorescence*:** To determine the localization and MSC marker expression of DPI-VTK binding cells *in* vivo, calvaria from 4-5 week old male C57/BL6 mice (n=3) were fixed in 4% PFA for 24 hours and demineralized in 10% EDTA for 2 weeks. They were then embedded in paraffin and sectioned on slides. The slides were de-paraffinized with xylene followed by gradual rehydration with decreasing concentrations of ethanol/water solution. Antigen retrieval was performed by incubation in pH 6 citrate buffer for 1 hour at 60 C. blocked, and stained with primary antibodies for CD31, CD90, CD73, CD105, CD29, CD106, CD45, CD200, CD44, Sca-1, CD146, or Cathepsin K along with FITC-DPI-VTK (10 μg/mL) overnight. Unstained tissue sections were used as controls. The sections were incubated with secondary antibodies, stained with DAPI, and then mounted with Vectashield and imaged with a Nikon Eclipse Ti confocal

microscope to determine the localization of DPI-VTK binding cells and marker positive cells within the calvarium.

3.3.12 Flow Cytometry: To determine the specificity of DPI-VTK towards MSCs *in vivo*, calvaria were dissected from 4–5-week-old male C57/BL6 mice (n=7) and digested in collagenase solution to yield a heterogenous cell suspension. The cells were resuspended in flow cytometry buffer and stained with primary antibodies for MSC markers CD29, CD45, CD73, CD90, CD105, CD106, Sca-1, CD31, CD44, and CD200 followed by APC tagged secondary antibodies and FITC tagged DPI-VTK. The stained cells were submitted to the University of Michigan Flow Cytometry core for analysis on a BD LSRFortessa Cell Analyzer.

3.3.13 Statistics: Two-way ANOVA with multiple comparison was used to determine differences for transwell migration assays with multiple cell types. One-way ANOVA and t-tests were used for other studies.

3.4 Results

3.4.1 DPI-VTK promotes migration of MSCs

In the transwell studies, iPS-MSCs showed significantly greater migration over no peptide controls at DPI-VTK concentrations of 50ug/mL or above. HBMSCs showed increasing trend that was not statistically significant. C3H10s showed no difference at highest dose of DPI-VTK. MC3T3 migration was inhibited at the highest dose. MDFs showed no statistically significant effect (Fig 3.1A). When iPS-MSCs were incubated in transwells with peptides DPI-VTK, DPI,

and VTK, migration was equivalent for DPI-VTK and DPI while VTK had no difference from the control, demonstrating that the DPI peptide, but not VTK, can induce migration (Fig 3.1B). Primary calvarial cells had a >2-fold increase in migration when exposed to peptide ($p < 0.0001$). Primary BMSC migration was also increased but non-significantly (Fig 3.1C).

3.4.2 Delivery of DPI-VTK with scaffolds

Controlled release studies with scaffolds saturated with DPI-VTK showed that after 72 hours, the DPI-VTK concentration was only approximately 3 ug/mL (Figure 3.2A). This is less than the minimum significant concentration of DPI-VTK for inducing migration (Figure 3.2C). Adding a bolus of 50 ul of 1 mg/mL DPI-VTK to scaffolds does induce a significant effect (Figure 3.2B).

3.4.3 Peptide specificity data with flow cytometry

When the flow cytometry data was analyzed as the fold change of marker positive cells in the peptide binding population compared to the total populations, all markers except CD44 were significantly increased compared to the negative control CD45, with CD90, CD31, and CD200 having the greatest magnitude difference.

3.4.4 In vivo migration experiment

H and E staining of scaffolds in calvarial defect 1 week following implantation (N=5) demonstrated 3/5 DPI-VTK samples formed cellular bridge across defect compared to 0/5 in the control group. The mean cell count was higher in the DPI-VTK group, but this was not

statistically significant. CD200 and CD90 positive cells were increased in the DPI-VTK group compared to the no-peptide control group. Negative MSC marker CD45 was not increased relative to control.

3.4.5 In vivo regeneration experiment

After 8 weeks post-transplantation, scaffolds delivered with DPI-VTK had significantly increased BV/TV ($P<0.5$) compared to the no-peptide control scaffold group when the whole 5 mm defect region was analyzed. Analysis of the inner 4 mm, and 3 mm regions of the defects showed no significant difference between groups for 4mm, but the rhBMP-2 group was significantly increased from the control group in the inner 3 mm. Analysis of the 5 concentric rings of the defects showed that DPI-VTK was significantly increase compared to the control in the 3-4 mm ring, and BMP-2 was significantly increased in the 2-3 mm ring compared to control. Analysis of the distribution of bone mineral demonstrated the majority of the bone volume came from the outer 2 mm of the defect for all groups.

3.4.6 Co-staining of FITC-DPI-VTK with MSC markers

Merged images of calvarial suture with FITC-DPI-VTK, various MSC markers (Alexa-Fluor 594), and DAPI. Co-staining of peptide with markers was noted for CD90, CD105, CD106, CD 146, CD200, Sca1, and CD31, but not CD44, CD45, CD72, Cathepsin K, and Gli1 (Figure 3.6A). Merged images of calvarium periosteum showed co-staining of peptide with marker for

Cathepsin K and CD200 (3.6B). Staining of calvaria with FITC-DPI, FITC-DPI (scrambled), and FITC-DPI-VTK showed weak staining of scrambled peptide compared to DPI and DPI-VTK (Figure 3.7C).

3.5 Discussion

This work presents the use of a dual-functional mineral binding and MSC binding peptide, DPI-VTK, to stimulate chemotaxis of MSCs and enhance MSC migration in vivo into a mineralized scaffold. This peptide increases regeneration of bone and vasculature when MSCs are transplanted on a mineralized scaffold [15]. The increased migratory capacity supports a long-term goal of bypassing cell transplantation and relying on host cells to catalyze bone regeneration. The use of peptide DPI-VTK is significant in several aspects. While most chemotactic agents are naturally derived, DPI-VTK demonstrates that techniques such as phage display can be used to discover novel chemoattractants. Although ECM proteins such as fibronectin induce chemotaxis in addition to promoting adhesion, the coupling of a combination chemotactic/cell adhesion domain to a specific material binding domain is a novel concept that has applications in recruiting specific cells to specific material chemistries. Additionally, the discovery of an MSC specific chemo-attractant/adhesion molecule could be used as a probe to identify specific MSC populations that are critical for healing.

DPI-VTK demonstrates an effect on MSC migration in a transwell assay (Figure 2C). This was not seen in non-MSC cells such as MC3T3s and MDFs (Figure 1a). MC3T3s are not affected by DPI-VTK despite being part of the MSC lineage. This is consistent with previous work studying the adhesion of cells to DPI-VTK [8]. It is possible that the binding targets of the

peptide stop being expressed as the MSCs differentiate into osteoblasts. Also, certain MSCs, such as the iPS-MSCs, exhibited a greater chemotactic response compared to the HBMSCs and C3H10 cells (Figure 1A), indicating that the peptide may target specific sub-populations of MSCs. A possible explanation for the differential effect of DPI-VTK on iPS-MSCs versus HBMSCs is that the iPS-MSCs may be more homogenous than the HBMSCs, resulting in a greater proportion of cells that are attracted to DPI-VTK. Both DPI-VTK and DPI have an equivalent effect on migration versus the negative control and VTK, suggesting that the DPI domain on its own is able to induce chemotaxis, although only DPI-VTK was significantly different from the control so the presence of the VTK anchor may modulate the effect (Figure 1B). Due to the strong affinity of DPI-VTK to apatite, relying on diffusion of the peptide from the surface alone is unable to induce an effect, necessitating the bolus delivery approach used during the in vivo studies (Figure 2).

In order to better understand the effect of DPI-VTK on *in* vivo cell populations, transwell assays were conducted with heterogenous populations of primary mouse calvarial and bone marrow cells. When tested with primary cells, the peptide had a more significant effect on the calvarial population versus the bone marrow population, suggesting the calvaria may contain a greater proportion of DPI-VTK sensitive cells (Figure 1C). Due to the different embryonic origins of the craniofacial and axial bones, the resident mesenchymal stem cell populations are distinct [21]. Preferential targeting of the calvarial cells suggests that DPI-VTK may have particular use for tissue engineering of craniofacial bone.

Flow cytometry with a panel of MSC markers showed a significant increase of all but one marker compared to the negative marker CD45 (Figure 3). The most notable MSC marker was CD90, with the peptide-binding cell population having 5-fold as many CD90 positive cells as the non-peptide binding cell population. CD90 cells were also increased in the in vivo migration experiment, suggesting that DPI-VTK is actively recruiting this sub-population of cells (Figure 4). Although CD90 is associated with several cell types, this marker has been used in clinical trials to isolate MSCs from autogenously harvested bone marrow aspirates. For example, in a clinical trial utilizing autogenous MSCs for maxillary sinus augmentation, higher proportions of CD90 cells were associated with increased bone volume fractions [22]. In human MSCs derived from adipose tissue, CD90 is associated with a more osteogenic phenotype [23]. CD90 interacts with different integrins and regulates migration in several types of cancer cells[24]; this suggests that CD90 and integrins could play a role in the specificity and chemotactic effects of DPI-VTK. To differentiate these CD90 positive MSCs from other cell types, absence of CD45 is often used [25]. CD45 did not appear as a positive marker in any of the experiments (Figures 3, 4, 6). There was a decrease in CD45 cells in migration experiment although it was not significant (Figure 4). The flow cytometry data and immunostaining data showing absence of CD45 supports idea that these cells are CD45 negative. CD200 was another marker highly expressed in the peptide binding group and significantly increased for the DPI-VTK group in the in vivo migration experiment (Figure 4). While not a traditional marker for MSCs, CD200 has been found in a population of periosteal stem cells that are present in the calvaria [26]. Additionally, CD200 expression in MSCs has been associated with an osteogenic phenotype [27].

CD31, a marker of endothelial cells that was initially used as a negative control, was highly expressed in the peptide binding population (Figure 3). Despite not being an intended target of peptide DPI-VTK, e recruitment of CD31 positive endothelial cells could have a positive effect on bone regeneration through the formation of new vasculature, although a significant increase in CD31 cells was not seen in the in vivo migration experiment (Figure 4). DPI-VTK increases vasculature in a cell transplantation ectopic model [15]. Staining of calvarium histological sections with FITC tagged DPI-VTK demonstrated that the peptide binds clusters of cells within the sagittal suture (Figure 6). These peptide binding cells co-stain for CD90, CD105, CD106, CD 146, CD200, Sca1, and CD31. The proximity of these cells to the blood vessels suggests these cells exist as pericytes in the perivascular niche. This is supported by these cells co-staining for pericyte marker CD146. Within the calvarial periosteum, the peptide also binds Cathepsin K and CD200 positive cells, which are known markers for periosteal stem cells [26].

With evidence that DPI-VTK induces migration of MSCs with osteogenic markers such as CD90 and CD200, we hypothesized that DPI-VTK could enhance bone regeneration *in* vivo. When delivered along with an acellular scaffold, DPI-VTK resulted in increased regenerated bone volume versus the scaffold alone, demonstrating that the peptide can enhance bone regeneration even without the addition of exogenous cells (Figure 5). In the DPI-VTK group, bone regeneration occurred at the margins of the defect in an orthotopic manner, suggesting that peptide is enhancing bone formation throughout the recruitment of osteogenic cells rather than inducing ectopic induction of bone formation as seen in BMP-2. This is supported by analysis of

the inner portions of the defects. When the inner 3 mm of the defect is analyzed, BV/TV of the BMP-2 group is significantly increased compared to the control (Figure 5).

There are some limitations to the *in vivo* study. The BMP-2 group was not statistically different from the scaffold-only control and the standard deviation was high for the full defect analysis as wells as the inner 4 mm of the defect. There was, however, a significant increase in BV/TV in the inner 3 mm of the defects. Some of the animals had a large response in terms of bone formation, and some had minimal to no response. In the bolus delivery model, some of the solution could migrate out of the defect, resulting in some animals receiving a higher dose than others. DPI-VTK, because of its affinity for apatite, could be binding to some of the surrounding calvarial bone, preventing it from being washed away like some other factors.

This chapter demonstrates that peptide DPI-VTK enhances MSC-specific chemotaxis in vitro, binds to cells expressing MSC markers, recruits cells expressing MSC markers in vivo, and enhances bone formation of acellular scaffolds in vivo. Discovering a cell specific chemotactic factor is an important step in developing more sophisticated tissue engineering techniques for bone regeneration.

3.6 Acknowledgments

Thank you to the University of Michigan Peptide Core for helping with peptide synthesis for the peptides used in this study. Thank you to Michelle Lynch from the Micro-CT Core for assisting with Micro-CT scanning and providing guidance on the analysis. Thank you to Chris Strayhorn from the Histology Core for assisting with histological processing. Thank you to the

UM Flow Cytometry core for assisting with the flow cytometry analysis. Thank you to Dr. Paul Krebsbach for providing the iPS-MSCs and Renny Franceschi for providing the MC3T3s.

Table 1 Peptides used in Chapter 3

Peptide	Sequence	Description	MW (g/mol)	Net Charge	Acidic Residues
DPI	DPIYALSWSGMA	MSC-binding peptide	1310.49	-1	3
VTK	VTKHLNQISQSY	Mineral-binding Peptide	1417.59	1	2
DPI-VTK	GGDPIYALSWSGMAGGGSVTKHLNQISQSY	Dual-functional MSC and mineral binding peptide	3025.35	0	5
P15	GTPGPQGIAGQRGVV	Col1a1 derived peptide	1393.57	1	0

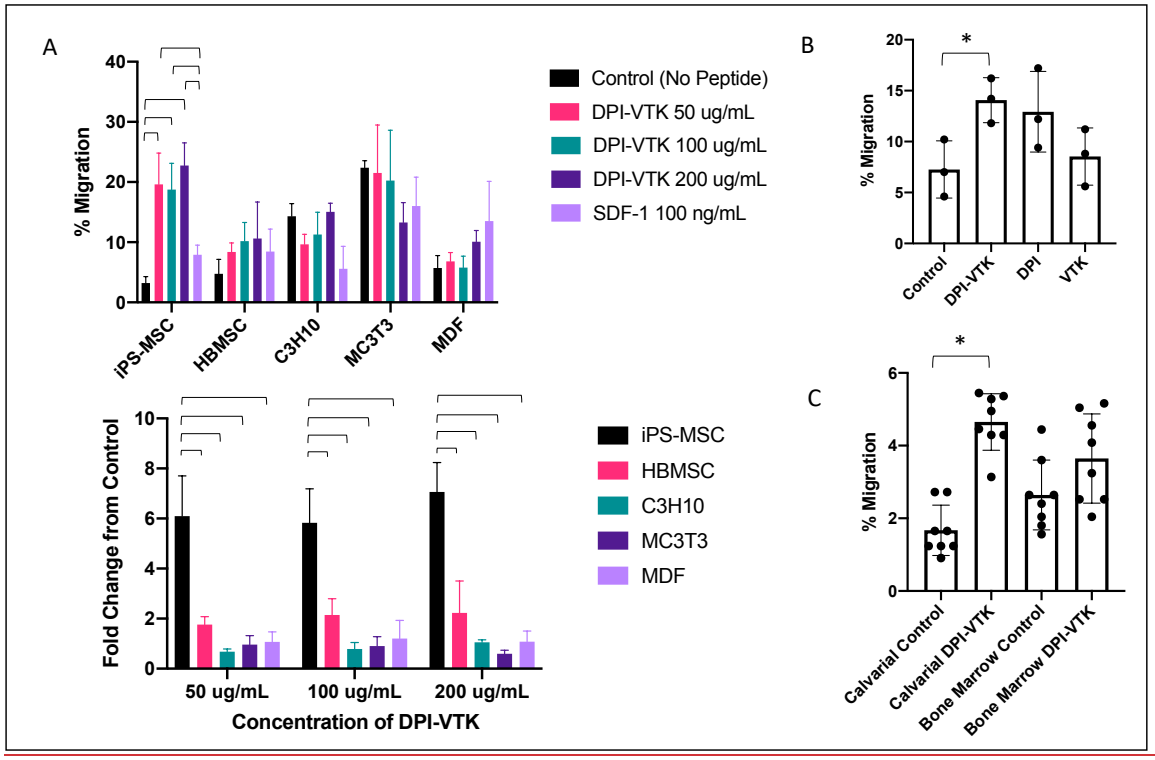

Figure 3.1 DPI-VTK promotes migration of MSCs

A: Quantification of cell migration in transwell assay with different concentrations of DPI-VTK as chemoattractant. SDF-1 served as positive control. iPS-MSCs showed significant increase over control at all DPI-VTK doses tested ($p<0.0001$). HBMSCs showed increasing trend that was not statistically significant ($p=0.2256$). C3H10s showed no difference at highest dose of DPI-VTK. MC3T3 migration was inhibited ($p=0.0251$) at the highest dose. MDFs showed no statistically significant effect ($p=0.4723$).

B: DPI domain is responsible for migratory effect. iPS-MSCs were tested in transwells with DPI-VTK, DPI, and VTK peptides. Migration was equivalent for DPI-VTK and DPI while VTK had no difference from the control, demonstrating that the DPI peptide, but not VTK, can induce migration.

C: DPI-VTK promotes migration of mouse primary cells

Primary calvarial cells and bone marrow cells were isolated from 4-5-week-old C57BL/6 mice and tested in transwell assay with DPI-VTK (100 ug/mL) and no-peptide controls. Primary calvarial cells had a >2-fold increase in migration with a p value <0.0001. Primary bone marrow migration was also increased but this was not statistically significant.

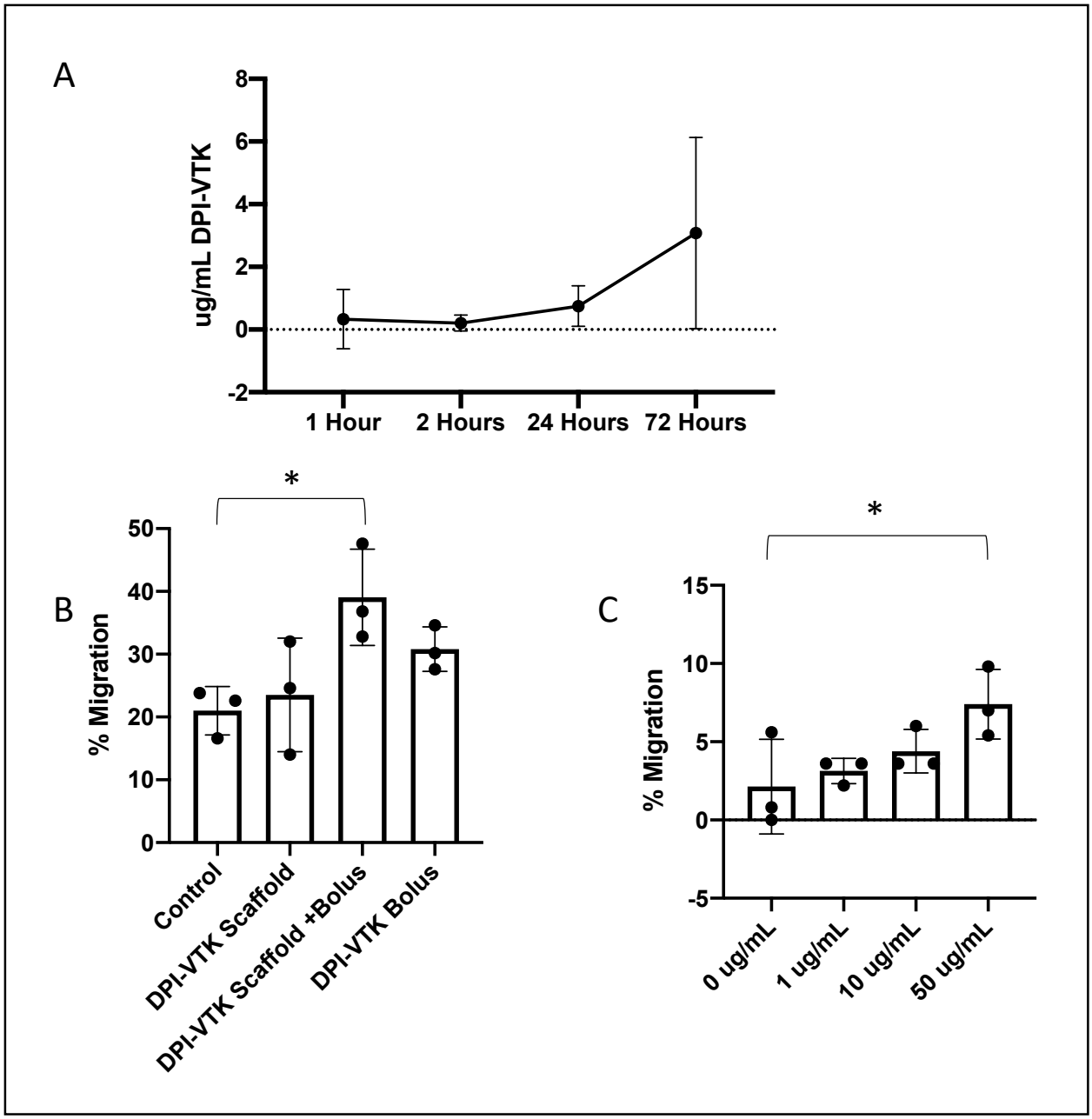

Figure 3.2 Delivery of DPI-VTK with scaffolds

A: Peptide release from scaffold. Scaffolds were saturated with DPI-VTK and placed in PBS. After 72 hours, the maximum peptide concentration achieved was approximately 3 ug/mL, far lower than the minimum concentration (50 ug/mL) necessary to induce migration.
B: Bolus delivery with scaffold. Scaffolds without peptide, scaffolds with absorbed peptide, and scaffolds with absorbed peptide with a bolus of 50 uL of 1 mg/mL solution DPI-VTK were placed in transwells. Migration experiments with iPS-MSCs were conducted and demonstrated significant difference between control scaffold and the scaffold with a bolus of DPI-VTK.

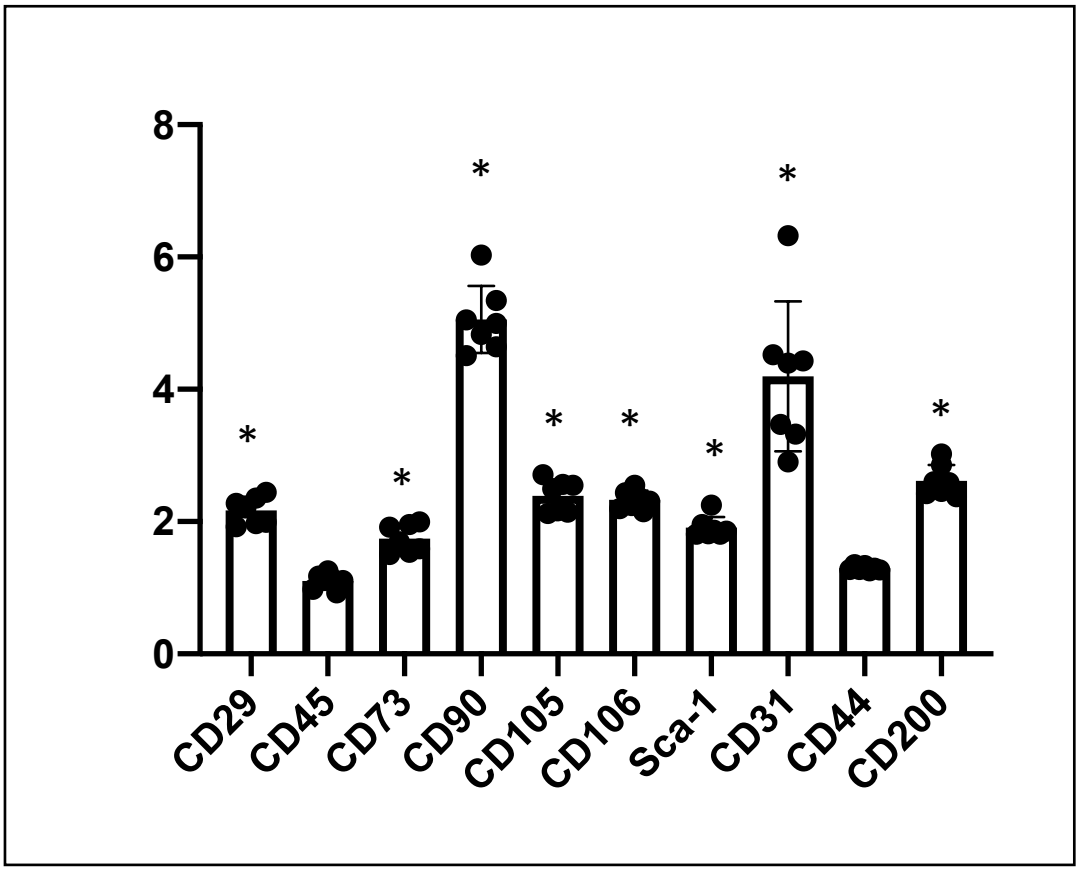

Figure 3.3 Flow Cytometry Data

Fold change of marker positive cells in peptide binding population compared to total population. All markers except CD44 were significantly increased compared to the negative control CD45, with CD90, CD31, and CD200 having the greatest magnitude difference.

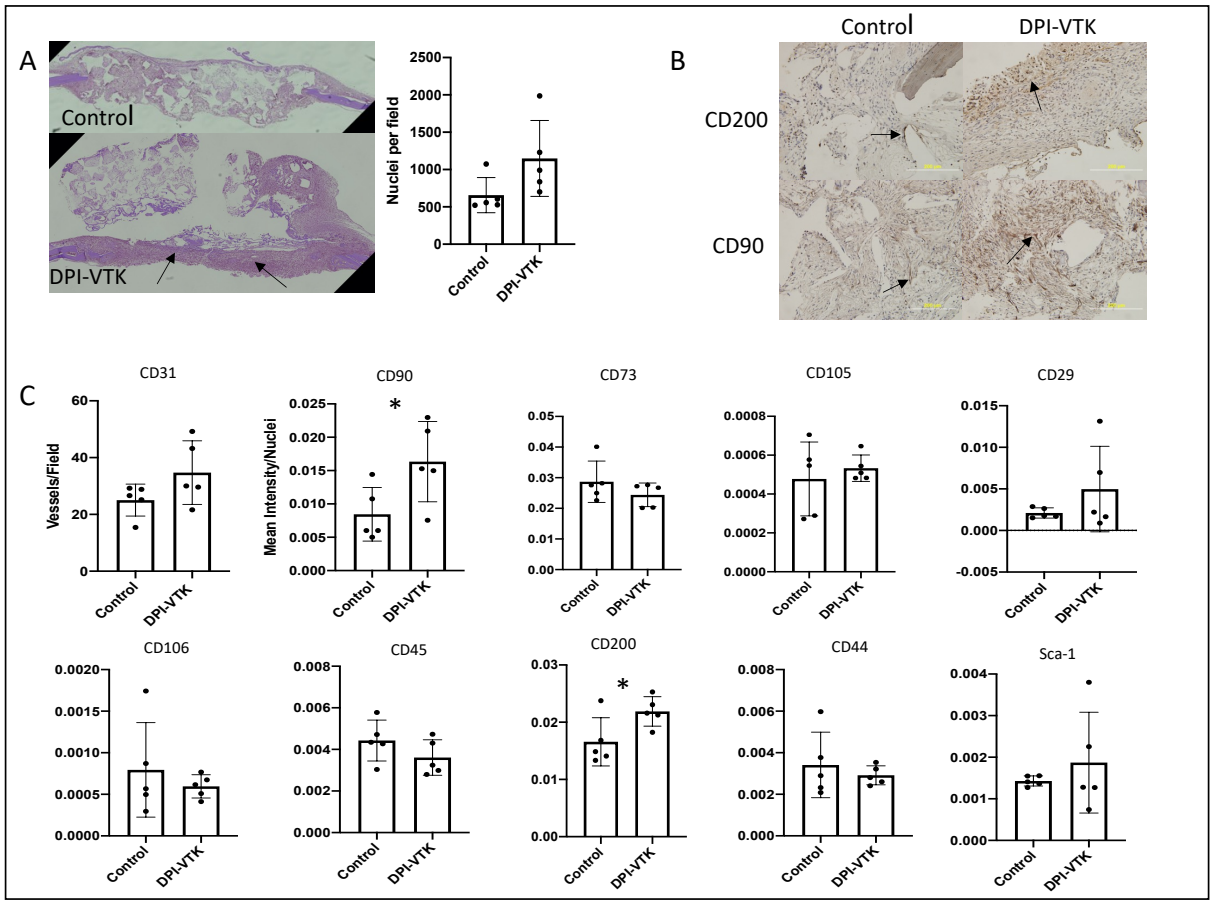

Figure 3.4 In vivo migration experiment

A: H and E staining of scaffolds in calvarial defect 1 week following implantation (N=5). 3/5 DPI-VTK samples formed cellular bridge across defect compared to 0/5 in the control group. The mean cell count was higher in the DPI-VTK group, but this was not statistically significant.
B: Representative immunohistochemical images from *in vivo* migration study. CD200 and CD90 positive cells were increased in the DPI-VTK group compared to the control
C: Quantification of migration of MSC marker positive cells into defect. Samples were stained with antibodies for different MSC markers. 10 images per section were imaged and quantified by taking the mean intensity of staining and dividing it by the number of cells. CD31 was quantified by counting the number of CD31 positive vessels per field. MSC markers CD90 and CD200 showed a statistically significant increase in the DPI-VTK group. Negative MSC marker CD45 did not increase, suggesting that DPI-VTK does promote specific migration of MSCs.

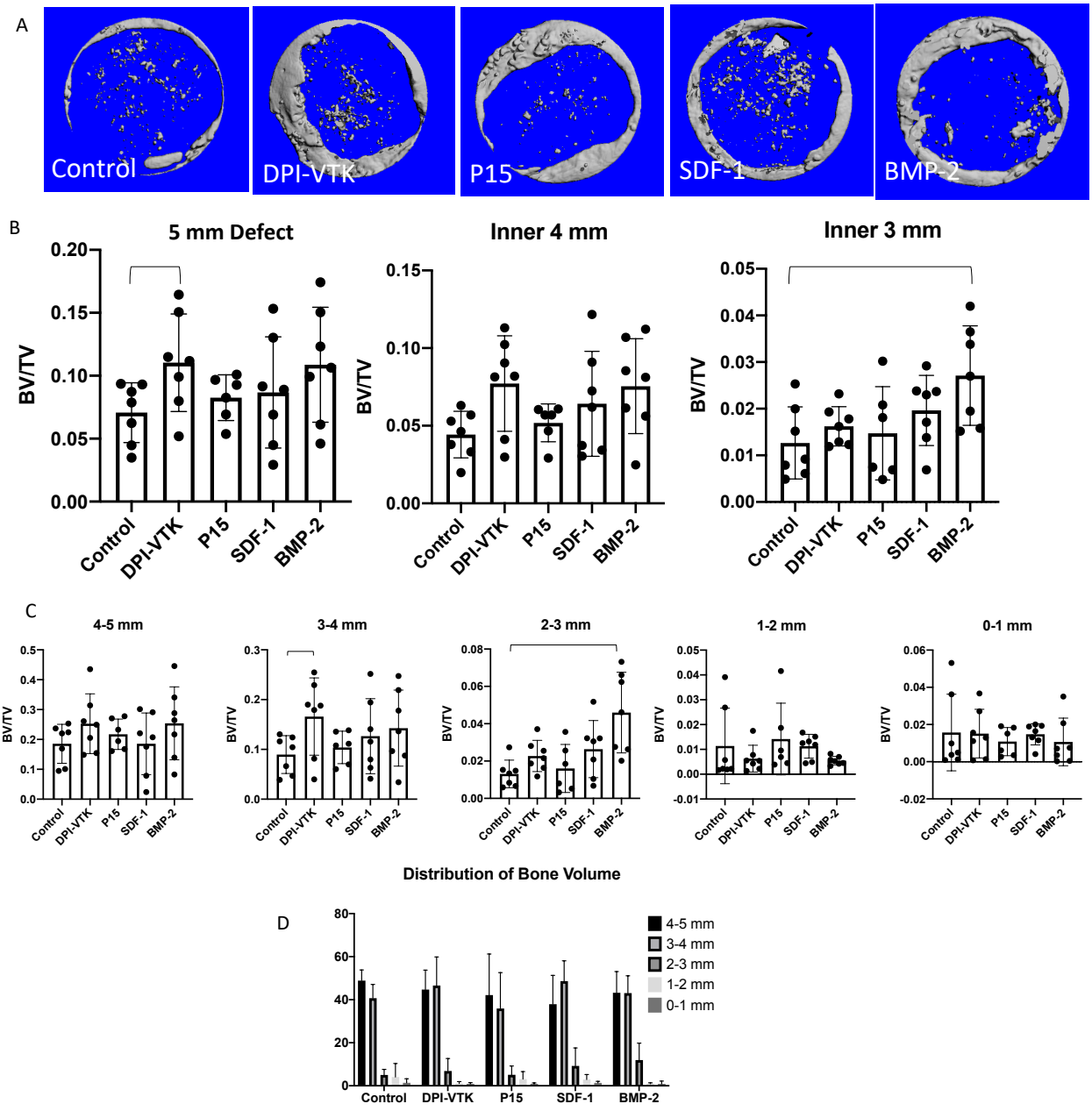

Figure 3.5 In vivo regeneration experiment

A: 3D renders of 5 mm calvarial defect 8 weeks post-surgery
B: Quantification of BV/TV in 5 mm calvarial defects 8 weeks post-surgery. DPI-VTK was significantly increased ($P<0.5$) compared to no peptide control with Welch's t-test when analyzing full 5 mm defect. Analysis of the inner 4 mm of the defect showed no significant effect between groups. In the inner 3 mm of the defect, there was a significant difference between the BMP-2 group and the control.
C: BV/TV of concentric circles in defect
D: Distribution of bone mineral

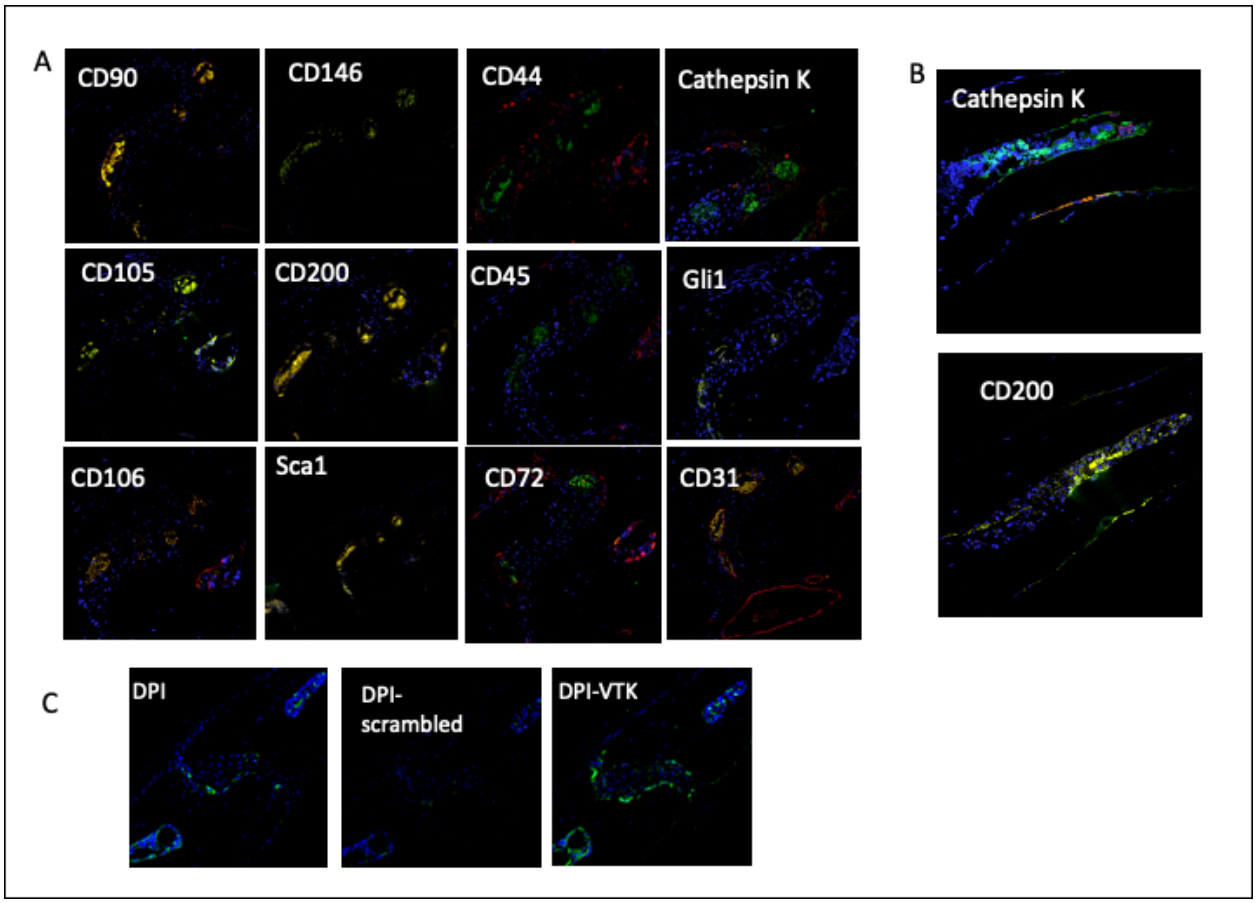

Figure 3.6 Co-localization of peptide with MSCs – co-staining of FITC-DPI-VTK with MSC markers

A: Merged images of calvarial suture with FITC-DPI-VTK, various MSC markers (Alexa-Fluor 594), and DAPI. Co-staining of peptide with markers was noted for CD90, CD105, CD106, CD 146, CD200, Sca1, and CD31, but not CD44, CD45, CD72, Cathepsin K, and Gli1.
B: Merged images of calvarium periosteum. Co-staining of peptide with marker was noted for Cathepsin K and CD200 in periosteum.
C. Images of calvarial suture stained with DPI, DPI-Scrambled, or DPI-VTK.

3.7 References

[1] L.M.E. Scheerlinck, M.S.M. Muradin, A. van der Bilt, G.J. Meijer, R. Koole, E.M. Van Cann, Donor site complications in bone grafting: comparison of iliac crest, calvarial, and mandibular ramus bone., Int. J. Oral Maxillofac. Implants. 28 (2013) 222–7. https://doi.org/10.11607/jomi.2603.

[2] R. Pollock, I. Alcelik, C. Bhatia, G. Chuter, K. Lingutla, C. Budithi, M. Krishna, Donor site morbidity following iliac crest bone harvesting for cervical fusion: A comparison between minimally invasive and open techniques, Eur. Spine J. 17 (2008) 845–852. https://doi.org/10.1007/s00586-008-0648-3.

[3] N. Toscano, D. Holtzclaw, Z. Mazor, P. Rosen, R. Horowitz, M. Toffler, Horizontal ridge augmentation utilizing a composite graft of demineralized freeze-dried allograft, mineralized cortical cancellous chips, and a biologically degradable thermoplastic carrier combined with a resorbable membrane: a retrospective evaluation o, J. Oral Implantol. 36 (2010) 467–474. https://doi.org/10.1563/AAID-JOI-D-09-00100.

[4] E.J. Kubosch, A. Bernstein, L. Wolf, T. Fretwurst, K. Nelson, H. Schmal, Clinical trial and in-vitro study comparing the efficacy of treating bony lesions with allografts versus synthetic or highly-processed xenogeneic bone grafts., BMC Musculoskelet. Disord. 17 (2016) 77. https://doi.org/10.1186/s12891-016-0930-1.

[5] P.T. Brown, A.M. Handorf, W.B. Jeon, W.-J. Li, Stem cell-based tissue engineering approaches for musculoskeletal regeneration., Curr. Pharm. Des. 19 (2013) 3429–45. https://doi.org/10.1016/j.biotechadv.2011.08.021.Secreted.

[6] M. Herrmann, S. Verrier, M. Alini, Strategies to stimulate mobilization and homing of endogenous stem and progenitor cells for bone tissue repair, Front. Bioeng. Biotechnol. 3 (2015) 1–11. https://doi.org/10.3389/fbioe.2015.00079.

[7] J.Y. Lee, J.E. Choo, Y.S. Choi, J.S. Suh, S.J. Lee, C.P. Chung, Y.J. Park, Osteoblastic differentiation of human bone marrow stromal cells in self-assembled BMP-2 receptor-binding peptide-amphiphiles, Biomaterials. 30 (2009) 3532–3541. https://doi.org/10.1016/j.biomaterials.2009.03.018.

[8] J. Ramaswamy, H. Ramaraju, D.H. Kohn, Bone-Like Mineral and Organically Modied Bone-Like Mineral Coatings, Biol. Biomed. Coatings Handb. (2020) 15–50. https://doi.org/10.1201/b10870-6.

[9] H.L. Oliveira, W.L.O. Da Rosa, C.E. Cuevas-Suárez, N.L.V. Carreño, A.F. da Silva, T.N. Guim, O.A. Dellagostin, E. Piva, Histological Evaluation of Bone Repair with Hydroxyapatite: A Systematic Review, Calcif. Tissue Int. 101 (2017) 341–354. https://doi.org/10.1007/s00223-017-0294-z.

[10] C. Dahlin, A. Linde, J. Gottlow, S. Nyman, Healing of Bone Defects by Guided Tissue Regeneration, Plast. Reconstr. Surg. 81 (1988) 672–676.

[11] S.L. Bellis, Biomaterials Advantages of RGD peptides for directing cell association with

biomaterials q, Biomaterials. 32 (2011) 4205–4210. https://doi.org/10.1016/j.biomaterials.2011.02.029.

[12] S. Segvich, S. Biswas, U. Becker, D.H. Kohn, Identification of peptides with targeted adhesion to bone-like mineral via phage display and computational modeling, Cells Tissues Organs. 189 (2008) 245–251. https://doi.org/10.1159/000151380.

[13] H. Ramaraju, S.J. Miller, D.H. Kohn, Dual-functioning peptides discovered by phage display increase the magnitude and specificity of BMSC attachment to mineralized biomaterials, Biomaterials. 134 (2017) 1–12. https://doi.org/10.1016/j.biomaterials.2017.04.034.

[14] M. Mebarki, L. Coquelin, P. Layrolle, S. Battaglia, M. Tossou, Acta Biomaterialia Enhanced human bone marrow mesenchymal stromal cell adhesion on scaffolds promotes cell survival and bone formation, Acta Biomater. 59 (2017) 94–107. https://doi.org/10.1016/j.actbio.2017.06.018.

[15] S.J. Segvich, D.H. Kohn, Phage Display as a Strategy for Designing Organic/Inorganic Biomaterials, in: B. R, D.A. Puleo (Eds.), Biol. Interact. Mater. Surfaces Underst. Control. Protein, Cell, Tissue Responses, Springer, New York, 2009: pp. 115–132.

[16] H. Ramaraju, D.H. Kohn, Cell and Material-Specific Phage Display Peptides Increase iPS-MSC Mediated Bone and Vasculature Formation In Vivo, Adv. Healthc. Mater. 1801356 (2019) 1–11. https://doi.org/10.1002/adhm.201801356.

[17] A.E. Postlethwaite, J. Keski-Oja, G. Balian, A.H. Kang, Induction of fibroblast chemotaxis by fibronectin. Localization of the chemotactic region to a 140,000-molecular weight non-gelatin-binding fragment., J. Exp. Med. 153 (1981) 494–499. https://doi.org/10.1084/jem.153.2.494.

[18] S.A. Kuznetsov, M.H. Mankani, P.G. Robey, In vivo formation of bone and haematopoietic territories by transplanted human bone marrow stromal cells generated in medium with and without osteogenic supplements, J. Tissue Eng. Regen. Med. 7 (2013) 226–235. https://doi.org/https://doi.org/10.1002/term.515.

[19] S.A. Kuznetsov, P.H. Krebsbach, K. Satomura, J. Kerr, M. Riminucci, D. Benayahu, P.G. Robey, Single-colony derived strains of human marrow stromal fibroblasts form bone after transplantation in vivo, J. Bone Miner. Res. 12 (1997) 1335–1347. https://doi.org/10.1359/jbmr.1997.12.9.1335.

[20] L.G. Villa-Diaz, S.E. Brown, Y. Liu, a. M. Ross, J. Lahann, J.M. Parent, P.H. Krebsbach, Derivation of mesenchymal stem cells from human induced pluripotent stem cells cultured on synthetic substrates, Stem Cells. 30 (2012) 1174–1181. https://doi.org/10.1002/stem.1084.

[21] A. Crowe, W. Yue, Semi-quantitative Determination of Protein Expression Using Immunohistochemistry Staining and Analysis: An Integrated Protocol, Bio-Protocol. 9 (2019) 1–11. https://doi.org/10.21769/bioprotoc.3465.

[22] T. Maruyama, J. Jeong, T.J. Sheu, W. Hsu, Stem cells of the suture mesenchyme in craniofacial bone development, repair and regeneration, Nat. Commun. (2016). https://doi.org/10.1038/ncomms10526.

[23] D. Kaigler, G. Avila-Ortiz, S. Travan, A.D. Taut, M. Padial-Molina, I. Rudek, F. Wang,

A. Lanis, W. V. Giannobile, Bone Engineering of Maxillary Sinus Bone Deficiencies Using Enriched CD90+ Stem Cell Therapy: A Randomized Clinical Trial, J. Bone Miner. Res. 30 (2015) 1206–1216. https://doi.org/10.1002/jbmr.2464.

[24] M.T. Chung, C. Liu, J.S. Hyun, D.D. Lo, D.T. Montoro, M. Hasegawa, S. Li, M. Sorkin, R. Rennert, M. Keeney, F. Yang, N. Quarto, M.T. Longaker, D.C. Wan, CD90 (Thy-1)-positive selection enhances osteogenic capacity of human adipose-derived stromal cells, Tissue Eng. - Part A. 19 (2013) 989–997. https://doi.org/10.1089/ten.tea.2012.0370.

[25] L. Leyton, J. Díaz, S. Martínez, E. Palacios, L.A. Pérez, R.D. Pérez, Thy-1/CD90 a Bidirectional and Lateral Signaling Scaffold, Front. Cell Dev. Biol. 7 (2019) 1–11. https://doi.org/10.3389/fcell.2019.00132.

[26] C.-S. Lin, Z.-C. Xin, J. Dai, T. F. Lue, Commonly Used Mesenchymal Stem Cell Markers and Tracking, Histol Histopathol. 28 (2013) 1109–1116. https://doi.org/10.14670/HH-28.1109.

[27] S. Debnath, A.R. Yallowitz, J. McCormick, S. Lalani, T. Zhang, R. Xu, N. Li, Y. Liu, Y.S. Yang, M. Eiseman, J.-H. Shim, M. Hameed, J.H. Healey, M.P. Bostrom, D.A. Landau, M.B. Greenblatt, Discovery of a periosteal stem cell mediating intramembranous bone formation, Nature. (2018). https://doi.org/10.1038/s41586-018-0554-8.

[28] C. Pontikoglou, A. Langonné, M.A. Ba, A. Varin, P. Rosset, P. Charbord, L. Sensébé, F. Deschaseaux, CD200 expression in human cultured bone marrow mesenchymal stem cells is induced by pro-osteogenic and pro-inflammatory cues, J. Cell. Mol. Med. 20 (2016) 655–665. https://doi.org/10.1111/jcmm.12752.

Chapter 4: Investigation of Dual-Functional BMP-Binding and Mineral-Binding Peptide KIP-VTK and its Potential Synergy with DPI-VTK

4.1 Abstract

Recombinant bone morphogenetic proteins (BMPs) have seen extensive use in clinical bone grafting due to their high osteoinductive potential. While effective, these recombinant proteins have significant limitations such as high cost and side effects such as inflammation and ectopic bone formation. Peptides have been derived from sequences of BMP binding domains, including the BMP-2 knuckle-epitope derived peptide KIPKASSVPTELSAISTLYL (KIP). BMP peptides such as KIP have the potential to be cheaper, easer to manipulate, and have increased stability while retaining the osteoinductive effects of BMP-2. When combined with material-binding peptides, these peptides could be used to create BMP functionalized biomaterials. By combining the mineral binding peptide VTKHLNQISQSY (VTK) with KIP, a dual-functional BMP- and mineral- binding peptide GGKIPKASSVPTELSAISTLYLGGGSVTKHLNQISQSY (KIP-VTK) was created. We hypothesized that KIP-VTK could be co-adsorbed with mesenchymal stem cell (MSC) binding peptide DPI-VTK on mineralized biomaterials to enhance the osteogenic differentiation of MSCs. KIP-VTK had higher absorption to bone-like mineral than KIP alone and could be co-adsorbed to mineral with peptide DPI-VTK. When human mesenchymal stem cells were cultured on KIP-VTK and DPI-VTK co-functionalized mineral films, no synergistic interaction on osteogenic differentiation was found, possibly due to

the inability of the KIP domain to sufficiently activate BMP signaling. These results demonstrate the limitations of dual-functional peptides and the importance of understanding structure-function relationships in peptide design. Understanding such relationships can help guide the creation of peptide sequences that are optimized to bind and activate their receptors while tethered to a biomaterial.

4.2 Introduction

One strategy to repair bone defects without the use of cellular transplantation is to use osteoinductive agents such as the bone morphogenetic proteins (BMPs). BMP-2 and BMP-7 are both clinically approved for the treatment of certain bone defects such as open tibial fractures and lumbar spinal fusions, but have also been used off-label for other defects such as craniofacial bone grafting [1]. In order to compensate for the short half-life of recombinant growth factors, BMP-2 and BMP-7 are usually delivered in high doses (>1 mg) [2]. While effective in inducing bone formation, these treatments have been associated with side effects such as inflammation and ectopic bone formation. The high doses required, coupled with the high cost of recombinant BMP, means that a single treatment can cost thousands of dollars [2–4].

An approach to overcome these limitations in using recombinant proteins is to use peptides derived from the active sites of the proteins. Peptides are advantageous because they are typically less expensive to manufacture than recombinant proteins and the increased stability from being bound to a material surface provides longer half-life (thus requiring lower doses) [5–7]. Linking such peptides to biomaterials could reduce the side effects by requiring lower doses and providing for localized delivery [5]. While proteins can be chemically conjugated to

materials, this often results in loss of activity due to alteration of their fragile structures [8,9] Because of their simpler and more stable structures, peptides retain their activity even when coupled to biomaterial scaffolds [5,10,11].

Choosing the correct peptide sequence from a protein sequence is key to developing therapeutic peptides. Typically, peptides are derived from the binding domains of the proteins as these are the sequences that bind and activate the target receptor. BMP-2 has two binding domains that interact with its target receptors. The large wrist epitope binds BMPR-IA while the smaller knuckle epitope binds BMPR-II. Binding of the BMP-2 protein through these domains to its receptors triggers oligomerization of the receptors and activates downstream signaling such as Smad phosphorylation. The large size of the wrist epitope makes it an unideal target for peptide derivation, while the small size of the knuckle-epitope makes it an attractive target.

A sequence derived from the knuckle epitope of BMP-2, KIPKASSVPTELSAISTLYL (KIP) which corresponds to residues 73-92, induces osteogenic differentiation and ectopic bone formation when delivered on an alginate scaffold [7]. This discovery is important because the knuckle epitope peptide was able to induce bone formation independent of the wrist epitope. Further studies also demonstrated clinical utility of this sequence in promoting osteogenic differentiation, particularly when combined with cell binding peptides such as the RGD sequence [5,10].

While many integrin and cell binding peptides have been derived from the sequences of native proteins, screening techniques such as phage display have been increasingly used to discover novel cell binding sequences [12]. Phage display can also be used to discover sequences

with high affinity for specific material surfaces [13]. The hydroxyapatite (HA) binding sequence VTK (**VTK**HLNQISQSY), and the mesenchymal stem cell (MSC) binding sequence DPI (**DPI**YALSWSGMA) were discovered via phage display[13,14] Combining these two domains into the dual peptide DPI-VTK (GG**DPI**YALSWSGMAGGGS**VTK**HLNQISQSY) allows for the tethering of MSCs to mineralized materials. DPI-VTK increases the strength of adhesion and promotes bone and vascular regeneration in an ectopic transplantation model [13,14]. With the success of DPI-VTK, there is a possibility to use the VTK domain to tether other peptide domains to Ca-P biomaterials. For example, the knuckle-epitope BMP-2 peptide KIP could be combined with VTK to anchor it to mineralized scaffolds to induce bone formation. When combined with integrin binding peptides such as DPI-VTK, this effect on osteogenic differentiation could be further enhanced since crosstalk between integrin binding peptides/proteins and BMP signaling has been established and integrin activation has a synergistic effect on osteogenic gene expression [15–17].

By combining BMP derived peptides with biomaterial and MSC binding peptides, it could be possible to create dual-functional materials that are both osteoconductive and osteoinductive. Combining a peptide derived from the knuckle epitope of BMP-2 (KIPKASSVPTELSAISMLYL) with mineral binding peptide VTK could allow for the conjugation of mineralized films with BMP signals and provide a synergistic effect with DPI-VTK by combining the osteoconductive properties of DPI-VTK with the osteoinduction of BMP. The hypothesis of this work is that VTK will enhance the binding of KIP to mineral, and that the co-adsorption of KIP-VTK and DPI-VTK on mineral surfaces will enhance the osteogenic differentiation of human MSCs. To test this hypothesis, peptide KIP-VTK along with peptides

KIP, VTK, and DPI-VTK were tested to determine the effect of adding the material-binding anchor VTK on the absorption of KIP to Ca-P biomaterials. Then MSC differentiation was assessed by preparing bone-like mineral films functionalized with no peptide, DPI-VTK, KIP-VTK, and both DPI-VTK and KIP-VTK. Soluble rhBMP-2 was used as a positive control. Human MSCs were cultured on films for different time points (3, 7, and 14 days) and then analyzed for alkaline phosphatase activity as a marker of osteogenic differentiation or probed via western blotting for expression of osteogenic proteins Runx2, P-Smad, Osx, and Ocn to determine any synergistic effect between DPI-VTK and KIP-VTK. In order to test the effect of the peptides on mineralization, an alternative to mineralized films was developed due to the interference with the mineralized films on Alizarin Red Staining. A chemical coupling scheme was used to chemically conjugate the peptides to glass slides and MSCs were cultured for 21 days. Lastly, MSCs were cultured on films with or without DPI-VTK and with or without soluble rhBMP-2 to determine any synergistic effect between DPI-VTK and rhBMP-2.

4.3 Materials and methods

4.3.1 Peptides

Peptides were synthesized by the University of Michigan Peptide Core using solid phase peptide synthesis (Table 4,1). All peptides were verified at >95% purity with HPLC. Peptides were stored lyophilized at -20^{o}C until use. Stock solutions of peptides were prepared by dissolving peptides in distilled water followed by dilution in PBS before use. Fluorescently tagged peptides were obtained by reacting FITC or Rhodamine isothiocyanate with peptides in

pH 9 carbonate buffer overnight and then dialyzing for 48 hours. Fluorescently tagged peptides were lyophilized, dissolved in DMSO, and diluted in PBS before use. All peptides were sterile filtered with a 0.22 μm syringe filter before use in cell culture experiments.

4.3.2 Preparation of mineralized films

A 5% w/v solution of PLGA in chloroform was prepared and pipetted (250uL) onto 1.5 cm diameter circular glass coverslips. The films were loosely covered and allowed to evaporate overnight in a fume hood followed by placement in a vacuum chamber to complete evaporation of the solvent. Films were then functionalized by incubation in 0.5 M NaOH for 7 minutes followed by three washes with Milli-Q water. Fresh 2x modified simulated body fluid (mSBF) was prepared. 1x mSBF contains 141 mM NaCl, 4.0 mM KCl, 0.5 mM MgSO4, 1.0 mM MgCl2, 4.2 mM NaHCO3, 5.0 mM CaCl2•2H2O, and 2.0 mM KH2PO4 at pH 6.8. The films were incubated in 2x mSBF at 37°C for 48 hours, at which point a continuous layer of bone-like mineral had formed on the surface. The films were then washed with Mill-Q water, dried, and stored in a vacuum desiccator until use. When used for cell culture, the films were placed in sterile 24 well plates and sterilized with 70% ethanol for 15 minutes. The ethanol was aspirated and the films were washed with sterile water. Peptide solutions (100 μg/mL in PBS) or PBS for controls were pipetted (500 μL per well) into each well with a sterilized film. The plate was sealed with parafilm and placed in a 37°C incubator for 3 hours. The peptide solutions were removed, and the films were washed with PBS three times before seeding with cells.

4.3.3 Quantification of peptide absorption

Stock solutions of peptides (1 mg/mL) were prepared and used to make standard curves. Films were placed in 24 well plates and 500 µL of peptide solution (100 µg/mL) was placed in each well (n=3). Blank wells with PBS were also prepared. The plates were sealed with parafilm and placed in an incubator at 37^{o}C for 3 hours. Afterwards, the peptide solutions were collected from the wells and quantified with UV absorbance at 214 nm. The concentrations were calculated from the standard curve and the absorbed peptide was determined by subtracting the final concentrations from the initial concentrations.

4.3.4 Quantification of peptide co-adsorption

FITC-DPI-VTK or Rhodamine-KIP-VTK were combined at different ratios (100:0- 100 µg/mL DPI-VTK, 0 µg/mL KIP-VTK; 75:25- 75 µg/mL DPI-VTK, 25 µg/mL KIP-VTK; 50:50- 100 µg/mL DPI-VTK, 100 µg/mL KIP-VTK; 25:75- 25µg/mL DPI-VTK, 75 µg/mL KIP-VTK; 0:100- 0 µg/mL DPI-VTK, 100 µg/mL KIP-VTK) (n=3/ratio) and incubated with mineralized films for 3 hours. Peptide concentration was quantified by measuring absorbance of solutions following incubation with films and calculating concentration using a plate reader. The absorbed peptide was calculated by subtracting from initial concentration. Absorbed films (n=3/ratio) were mounted on slides with Vectashield and imaged for FITC (DPI-VTK) and rhodamine (KIP-VTK) fluorescence using a Nikon Ti-Eclipse confocal microscope with a 20x objective. 5 fields of view were obtained for each sample.

4.3.5 Cell Culture

Human mesenchymal stem cells were purchased from RoosterBio and used from passages 2-5. The cells were expanded in RoosterBio media. During experiments, the cells were switched to alpha-MEM with 10% FBS with antibiotics. Osteogenic media was prepared by adding 10−8 M Dexamethasone, 2×10^{-3} to 5×10^{-3} M β-glycerophosphate, 10^{-4} M ascorbic acid to complete media.

4.3.6 ALP activity assays

ALP assays were performed using a commercially available ALP assay from Abcam. Human MSCs were cultured on mineralized films (n=3/condition/time) with no peptide, absorbed DPI-VTK, absorbed KIP-VTK, both absorbed DPI-VTK and KIP-VTK, and no peptide films with soluble 100 ng/mL rhBMP-2 (R&D Systems) as a positive control for 3, 7, or 14 days. Media was aspirated from the mineralized films in the 24 well plates and the films were washed with PBS. Assay buffer was placed in each well and the cells were scraped off using a cell scraper along with the assay buffer into a centrifuge tube. The tubes were homogenized in an ultrasonic bath and then centrifuged at 13,000 rpm for 15 minutes. Samples were placed in a 96 well plate, reacted with pNPP for 60 minutes, and read on a plate reader at wavelength 405 nm. A standard curve was used to calculate the ALP activity (U/mL) which was then normalized to DNA content.

4.3.7 Western Immunoblotting

In each well (n=3/condition), the media was aspirated, and the cells were washed with sterile PBS followed by addition of RIPA buffer with protease inhibitors. Using a cell scraper,

the cells and lysis buffer were scraped and transferred to centrifuge tubes and homogenized in an ultrasonic bath for 5 minutes. This was followed by centrifugation at 13,000 rpm for 10 minutes. The protein concentrations were quantified using the Pierce BCA assay following the manufacturer's instructions. The samples were diluted with RIPA buffer to ensure equal protein concentrations, and then diluted with 5X Laemmli buffer before heating at 95^{o}C for 5 minutes. 10 ug of protein were loaded per well. SDS-PAGE gels were run at 225 V for 50 minutes in Tris-Glycine buffer. This was followed by transfer onto PVDF membranes at 50 V for 1.25 hours. Membranes were blocked with 3% BSA in TBST for 1 hour at room temperature and incubated overnight at 4^{o}C with primary antibodies. After 3 washes with TBST, the membranes were incubated with secondary antibodies for 1 hour at room temperature and washed 3 more times before development with ECL reagent. After imaging, the bands were quantified with Image-J and normalized to Actin as a loading control. Osteogenic factors analyzed include P-Smad, Runx2, Osx, Ocn, Opn, and Col1A. BMP signaling was quantified by normalizing phosphorylated Smad 1,5,8 to Smad.

4.3.8 Mineralization assay utilizing chemically coupled peptide

To perform an *in vitro* cell mineralization assay without interference from the mineralized films, a chemical coupling strategy was utilized. Circular glass coverslips (1.5 mm diameter) were cleaned by immersion in anhydrous ethanol and sonicated in an ultrasonic bath for 5 minutes. This was followed by three washes with MilliQ water. Piranha solution was prepared by adding 30% hydrogen peroxide to concentrated sulfuric acid dropwise in a 1:3 ratio. The container was immersed in an ice bath to control the temperature. The cleaned glass coverslips were immersed in the piranha solution for 2 hours. Afterwards, the piranha solution

was removed, and the coverslips were washed several times with water. Then the coverslips were submerged in an aqueous-ethanol solution of 3-aminopropyl-triethoxysilane for 2 hours. After drying in a vacuum oven, the coverslips were submerged in an acetone solution of DSC and washed with dry acetone. The functionalized coverslips were reacted with solutions of peptides (100 ug/mL) for 3 hours to create peptide coated coverslips. Peptide coupling efficiency was quantified with UV absorbance at 214 nm. The concentrations were calculated from the standard curve and the absorbed peptide was determined by subtracting the final concentrations from the initial concentrations. Cells were seeded onto coverslips (n=3/condition) in osteogenic media for 21 days. On day 21, the cells were washed with PBS and fixed in 4% PFA solution for 15 minutes before washing with distilled water. The coverslips were stained with Alizarin Red solution and imaged to qualitatively compare the amount of mineralization.

4.3.9 Statistics

Significant differences between groups in the ALP and western blotting assays were determined with One-way ANOVA with Tukey's multiple comparisons. Student's t test was used to determine significant differences between groups in the peptide absorption studies.

4.4 Results

4.4.1 Addition of VTK domain to peptide KIP enhances absorption to bone-like mineral

When absorbed on bone-like mineral, the absorption of peptide KIP-VTK is approximately double that of KIP and has similar absorption to peptide DPI-VTK (Figure 4.1). Both peptides KIP-VTK and DPI-VTK were significantly increase ($p>0.05$) compared to KIP.

4.4.2 DPI-VTK and KIP-VTK can be co-adsorbed onto bone-like mineral

When co-adsorbed, peptides DPI-VTK and KIP-VTK were both able to be conjugated onto BLM. At a 100:0 ratio of DPI-VTK to KIP-VTK, only DPI-VTK was absorbed (4.1 μg). At a 75:25 ratio, approximately equal DPI-VTK (2.4 μg) and KIP-VTK (2.7 μg) was absorbed. At a 1:1 ratio in the absorbing solution, more KIP-VTK (7.1 μg) was absorbed than DPI-VTK (4.4 μg). At a 25:75 ratio, KIP-VTK (8.3 μg) was absorbed but no DPI-VTK. At 0:100 ratio, only KIP-VTK was absorbed (11.9 μg). When analyzed with confocal microscopy, the peptides had an even distribution throughout the films, but formed clusters of either DPI-VTK or KIP-VTK (Figure 4.2).

4.4.3 Co-adsorbed DPI-VTK and KIP-VTK does not enhance ALP activity

Human MSCs were cultured on mineralized films functionalized with no peptide, DPI-VTK, KIP-VTK or both peptides. 100 ng/mL rhBMP-2 was used as a positive control. After culturing for 3, 7, and 14 days, there was no significant difference between peptide groups

(Figure 4.3). At the day 3, and 7 timepoint, there was no significant difference with the positive control BMP-2 and the no-peptide control. There was, however, a significant difference between BMP-2 and all other groups at the day 14 timepoint.

4.4.4 Co-adsorbed DPI-VTK and KIP-VTK does not enhance BMP signaling

Human MSCs were cultured on mineralized films functionalized with no peptide, DPI-VTK, KIP-VTK or both peptides for 3 hours before lysis. 100 ng/mL BMP-2 was used as a positive control. BMP signaling was quantified by normalizing phosphorylated Smad 1,5,8 to Smad. There was no significant increase in Smad phosphorylation with the co-adsoprtion of DPI-VTK and KIP-VTK (Figure 4.4).

4.4.5 Co-adsorbed DPI-VTK and KIP-VTK does not enhance expression of osteogenic factors

Human MSCs were cultured on mineralized films functionalized with no peptide, DPI-VTK, KIP-VTK or both peptides. 100 ng/mL rhBMP-2 was used as a positive control. Timepoints included 3, 7, and 14 days. At day 7, there was a significant difference between DPI-VTK+KIP-VTK and the control group, but no significant differences between DPI-VTK+KIP-VTK and each peptide alone. At Day 14, there was a significant difference between the KIP-VTK and the control group, but no difference between KIP-VTK and DPI-VTK+KIP-VTK (Figure 4.5).

4.4.6 Co-coupling of DPI-VTK and KIP-VTK does not enhance mineralization

Peptide coupling through published protocols coupled more peptide (Figure 4.6) than passive absorption on mineral (Figure 4.1). There was, however, less peptide coupled when peptides DPI and KIP were co-coupled compared to KIP alone (Figure 4.6). One-way ANOVA with multiple comparisons shows that there is a significant difference between KIP and DPI, and KIP and DPI+KIP, but no difference between DPI and DPI+KIP. After culturing human MSCs for 21 days in osteogenic media, there was no difference in mineralization between groups (Figure 4.7).

4.4.7 DPI-VTK does not enhance osteogenic effects of rhBMP-2

Human MSCs were cultured on mineralized films with or without DPI-VTK, with or without 100 ng/mL BMP-2 (4 groups total). The timepoints used were 3 days, 7 days, and 14 days. At day 3, there was a significant difference between the BLM BMP group and the BLM control for Runx2 expression, but no difference between BLM BMP and DPI-VTK BLM (Figure 4.8). For the Day 7 timepoint, there were significant differences between the BMP groups and non-BMP groups, but no difference between BLM BMP and DPI-VTK BMP groups for osterix expression. There were no significant differences for the other proteins probed, Runx2 and osteopontin (Figures 4.8, 4.9). For the Day 14 timepoints, there were significant differences between the BMP groups and non-BMP groups, but no difference between BLM BMP and DPI-VTK BMP groups for osterix expression. There were no significant differences for the other proteins probed, Runx2, osteocalcin, and collagen 1A (Figure 4.10). While BMP was expected to significantly increase all osteogenic markers versus the non-BMP controls, the only significant increase was for osterix expression.

4.5 Discussion

The BMP-2 knuckle-epitope derived peptide KIP has shown promising results in the field of bone tissue engineering [7]. For example, delivery of KIP in a scaffold caused ectopic bone formation in mice and coupling of KIP to an alginate scaffold resulted in enhance osteogenic differentiation of MSCs [7,10]. Also, these peptides act synergistically with adhesion peptides such as RGD by enhancing ALP activity and expression of osteogenic factors [5,10]. These studies motivated the hypothesis that KIP would act synergistically with dual-functional peptide DPI-VTK. The first experiments involved testing if the addition of the VTK domain would improve absorption of the KIP domain. Indeed, KIP-VTK had improved absorption to BLM films compared to KIP, and similar absorption to DPI-VTK (Figure 4.1). Both peptides could be co-adsorbed onto BLM films (Figure 4.2). These results verified the first hypothesis of this Aim that the VTK domain would enhance the binding of the KIP domain to mineral surfaces.

After culturing human MSCs on mineralized films functionalized with peptides, there was no difference in ALP expression between the films with a combination of DPI-VTK and KIP-VTK, versus each peptide alone at different timepoints (3,7,14 days; Figure 4.3). Likewise, similar non-significant differences between peptide groups were seen with Runx2. (Figure 4.5). No significant effect on BMP signaling was seen from the BMP derived peptides (Figure 4.4), which contradicts other results [5,10]. To test the effect of the peptides on mineralization, Alizarin Red staining was utilized. This was complicated by the fact that the existing mineral on the mineralized films would interfere with the staining of secreted mineral by the cells. Therefore, for it was not possible to test this using the mineral binding DPI-VTK and KIP-VTK peptides and a chemical coupling approach was used instead with the single peptides rather than

dual peptides. The chemical coupling was successful in coupling DPI, KIP, and DPI+KIP to glass slides. Interestingly, significantly more KIP was coupled when alone compared to DPI alone or KIP in combination with DPI (Figure 4.6). Also, a greater amount of peptide was coupled compared to the absorption onto mineralized films (Figure 4.1). Despite this, after culturing MSCs on the functionalized slides for 21 days in osteogenic media, there was no observable difference in mineral secretion by any of the groups, demonstrating that the peptides lacked any activity when chemically coupled (Figure 4.7).

The hypothesis that DPI-VTK and KIP-VTK would have a synergistic effect was not supported by the data. It is possible that although the VTK domain enhances absorption of KIP to the mineral, it is not available enough to bind to its receptor. KIP has induced osteogenesis when chemically coupled to alginate scaffolds. One study involved the use of KIP sequences modified with cysteine groups to create maleimide linkages, allowing more precise control of the orientation [10]. While the absorption mechanism of VTK to mineral has been investigated [18], the absorption mechanism of KIP or KIP-VTK has not been, so it is possible that the binding site is obscured when absorbed to mineral. The KIP-VTK does have a glycine spacer between the two sequences, a longer spacer made from a biocompatible polymer such as polyethylene glycol (PEG) may be necessary for sufficient activity. The KIP domain is connected to the VTK domain through the carboxy terminus, connecting it through the amino terminus instead could also create a more active confirmation. Also, compared to the full BMP-2 protein, the KIP peptide has significantly less activity (Figure 4.4) [10]. While KIP has been shown to induce osteogenesis despite binding only one of the two types of BMP receptors, it is possible that this significantly limits its effect on BMP signaling compared to the native BMP protein [7].

These results demonstrating the lack of activity of KIP-VTK led to the formation of another hypothesis, that DPI-VTK would enhance the osteogenic response of MSCs to rhBMP-2. This hypothesis was supported by previous studies that have shown synergistic effects between ECM proteins such as collagen and BMP-2 [14,19,20]. The data (Figures 4.8-4.10), however, showed that there was no effect of the DPI-VTK on osteogenesis when BMP-2 was administered. DPI-VTK does influence expression of osteogenic genes [17], but this work shows that this is minimal compared to the osteogenic effects of BMP-2 (Figure 4.8-4.10). The non-significant effect of DPI-VTK on osteogenic protein expression suggests that although DPI-VTK can recruit MSCs through chemotaxis and adhesion (Figure 3.1), it does not have osteogenic effects. Despite the lack of synergistic cell signaling seen in these experiments, DPI-VTK may still be useful in combination with recombinant BMP-2 because of its effects on cell recruitment. While the data presented here shows a lack of synergy on the molecular level when DPI-VTK is combined with rhBMP-2, these experiments did not account for the migratory effects of the DPI-VTK peptide which were seen in Chapter 3 (Figure 3.4). In effect, the DPI-VTK would bring more MSCs into a defect/scaffold while rhBMP-2 would act as the osteo-inductive agent.

4.6 Acknowledgements

Thank you to the University of Michigan Peptide Synthesis Core for helping with peptide synthesis for the peptides used in this study. Funding was provided by NIH T32 DE007057; R01 DE 026116; F30 DE028465.

Table 2 Peptides used in Chapter 4

Peptide	Sequence	Description	MW (g/mol)	Net Charge	Acidic Residues
DPI	DPIYALSWSGMA	MSC-binding peptide	1310.49	-1	3
VTK	VTKHLNQISQSY	Mineral-binding Peptide	1417.59	1	2
DPI-VTK	GGDPIYALSWSGMAGG GSVTKHLNQISQSY	Dual-functional MSC and mineral binding peptide	3025.35	0	5
KIP	KIPKASSVPTELSAISTLYL	Knuckle-epitope BMP-2 derived peptide	2118.47	1	1
KIP-VTK	GGKIPKASSVPTELSAIS TLYLGGGSVTKHLNQISQSY	Dual-functional BMP-2 derived peptide and mineral binding peptide	3890.35	2	1

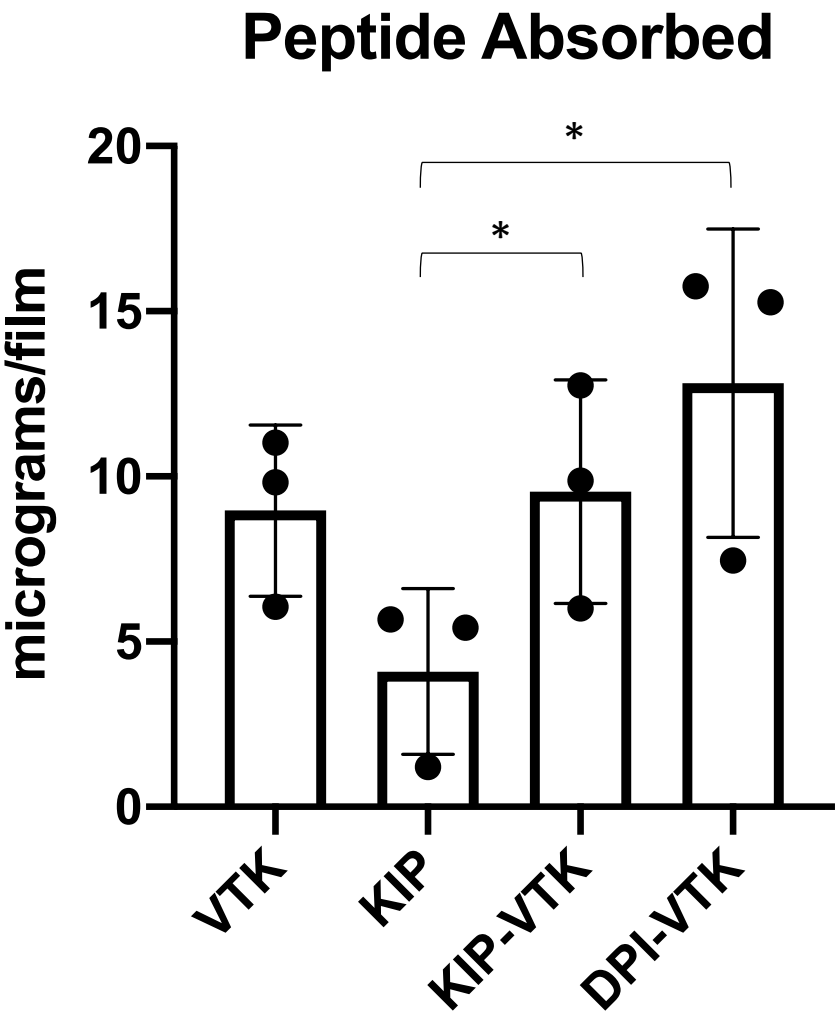

Figure 4.1 Peptide Absorption on Bone-like mineral

Quantification of peptides VTK, KIP, KIP-VTK, and DPI-VTK after absorption on BLM films for 3 hours. KIP-VTK and DPI-VTK had significantly higher absorption than KIP.

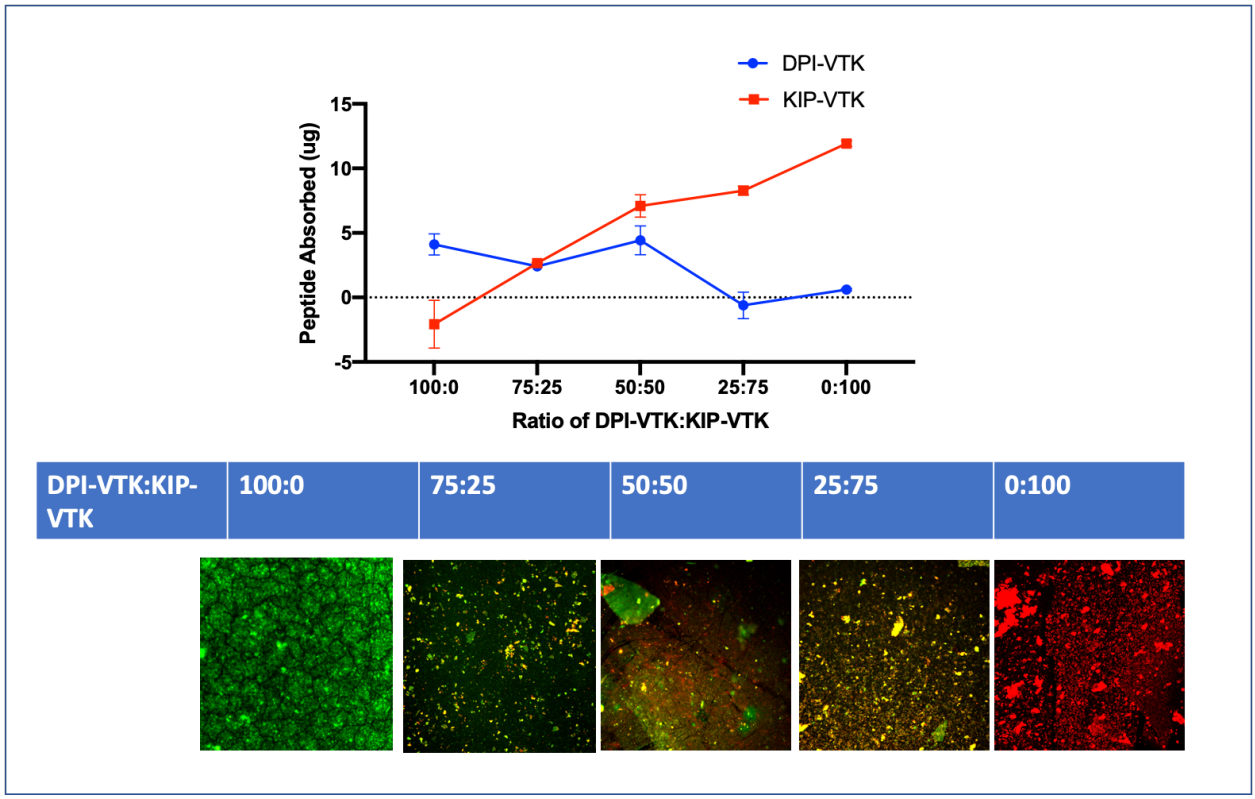

Figure 4.2 Co-Adsorption of Peptides DPI-VTK and KIP-VTK on bone like mineral

FITC-DPI-VTK and rhodamine-KIP-VTK were co-adsorpbed on BLM films at different ratios. Quantification showed that at equal ratios, more KIP-VTK was absorbed than DPI-VTK. Confocal images show presence of both peptides when co-adsorbed.

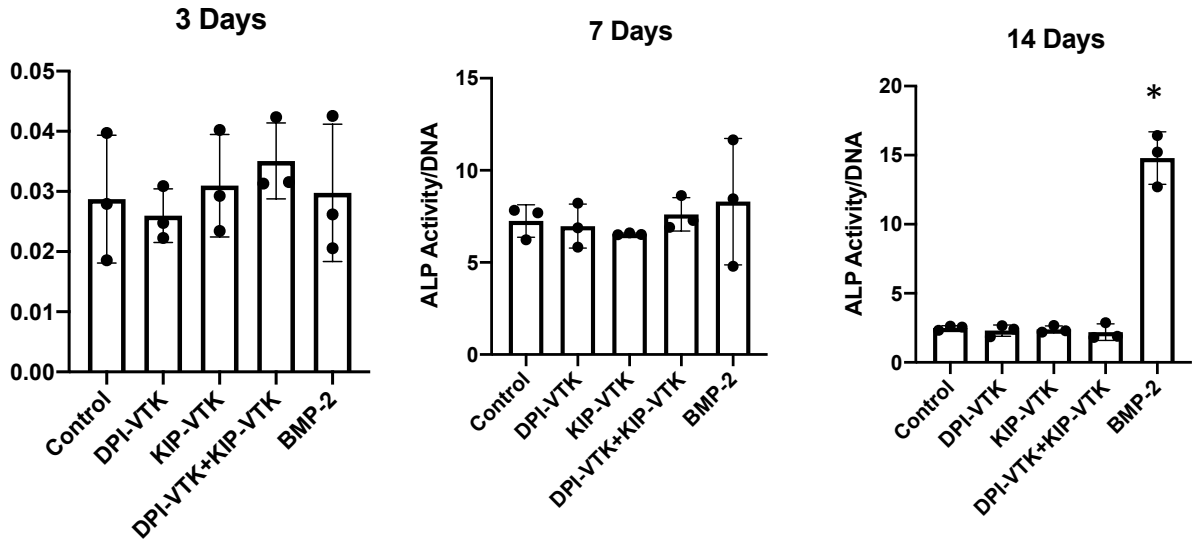

Figure 4.3 Effect of peptide functionalized mineral on alkaline phosphatase activity

ALP activity of human MSCs was quantified after 3, 7, or 14 days of culture on BLM films. Absorbed DPI-VTK, KIP-VTK, or DPI-VTK+KIP-VTK had no significant effect on ALP activity at any timepoint versus control. The positive control (100 ng/mL BMP-2) only significantly increased ALP activity at the 14 day timepoint.

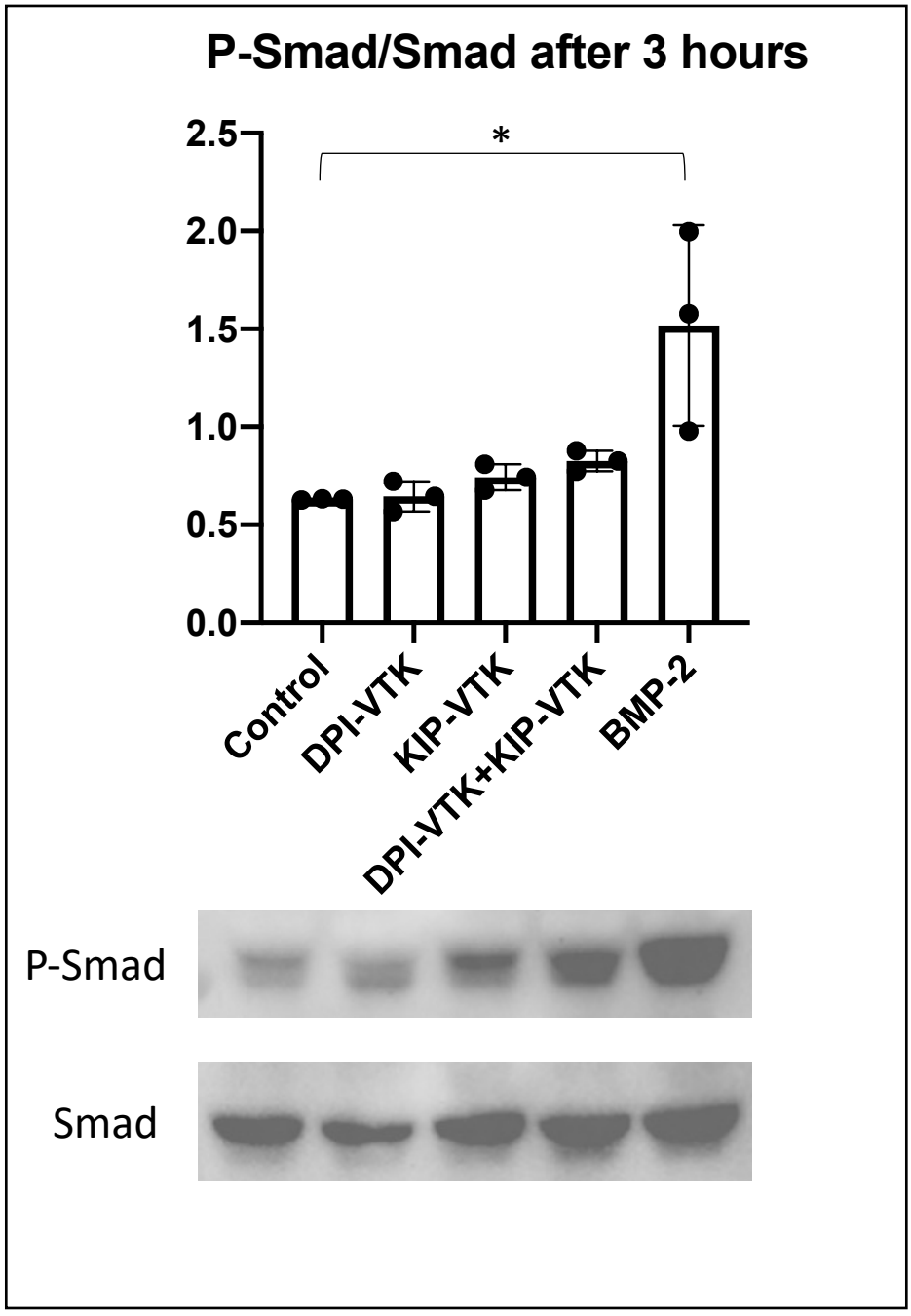

Figure 4.4 Effect of peptide functionalized mineral on BMP activity

Smad phosphorylation was quantified and normalized to unphosphorylated Smad in MSCs after 3 hours on mineralized films. The BMP-2 group was significantly increased compared to the no-peptide control but there was no other significant differences.

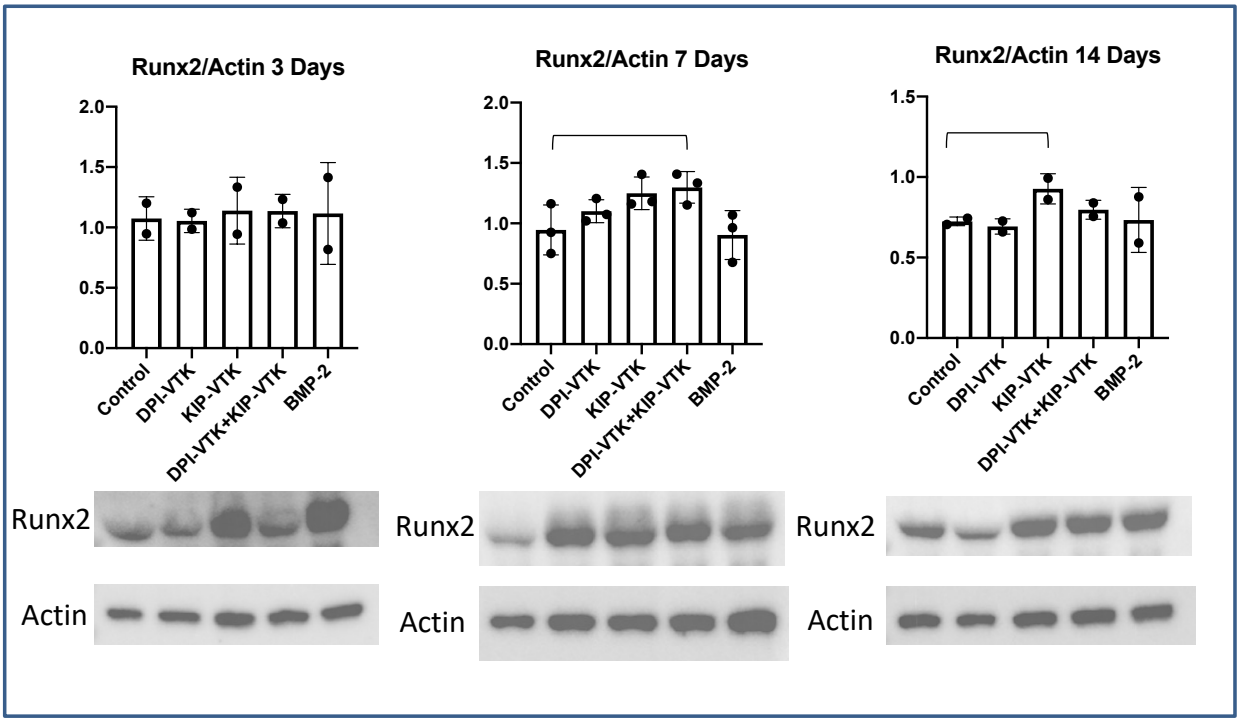

Figure 4.5 Effect of peptide functionalized mineral on Runx2 expression

Runx2 expression was quantified in MSCs after 3, 7, or 14 days of culture on mineralized films. There were significant differences between DPI-VTK+KIP-VTK and no-peptide control at Day7 and KIP-VTK and no peptide control at Day 14.

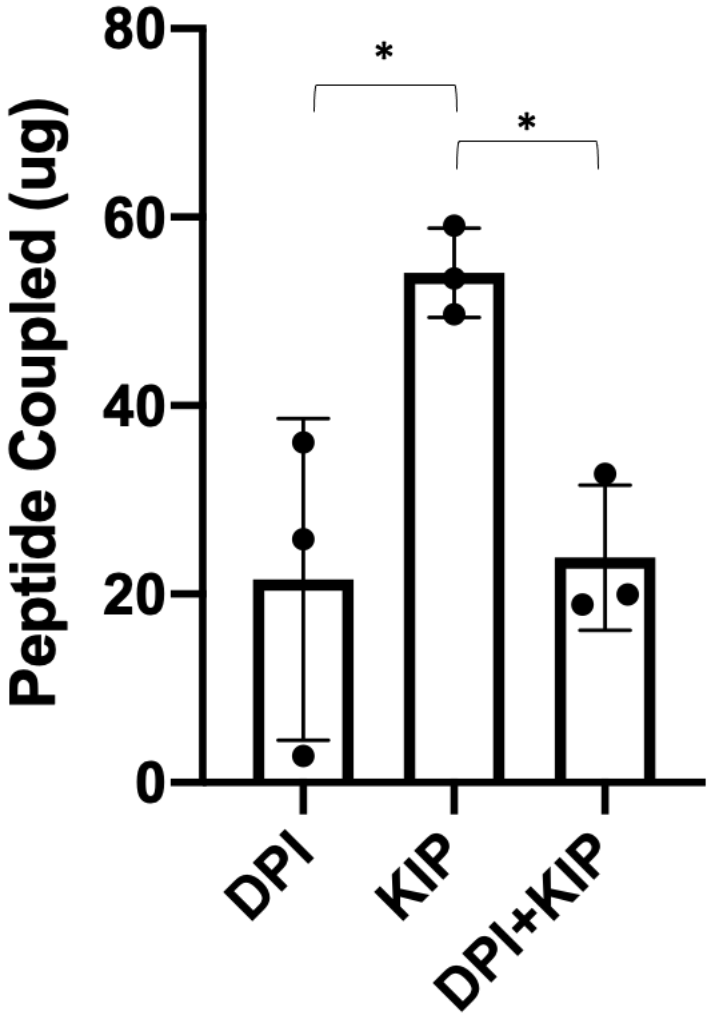

Figure 4.6 Chemical Coupling of peptides to glass coverslips

After chemically coupling peptides to glass coverslips, there was a significant increase in the amount of peptide KIP coupled compared to DPI and DPI+KIP.

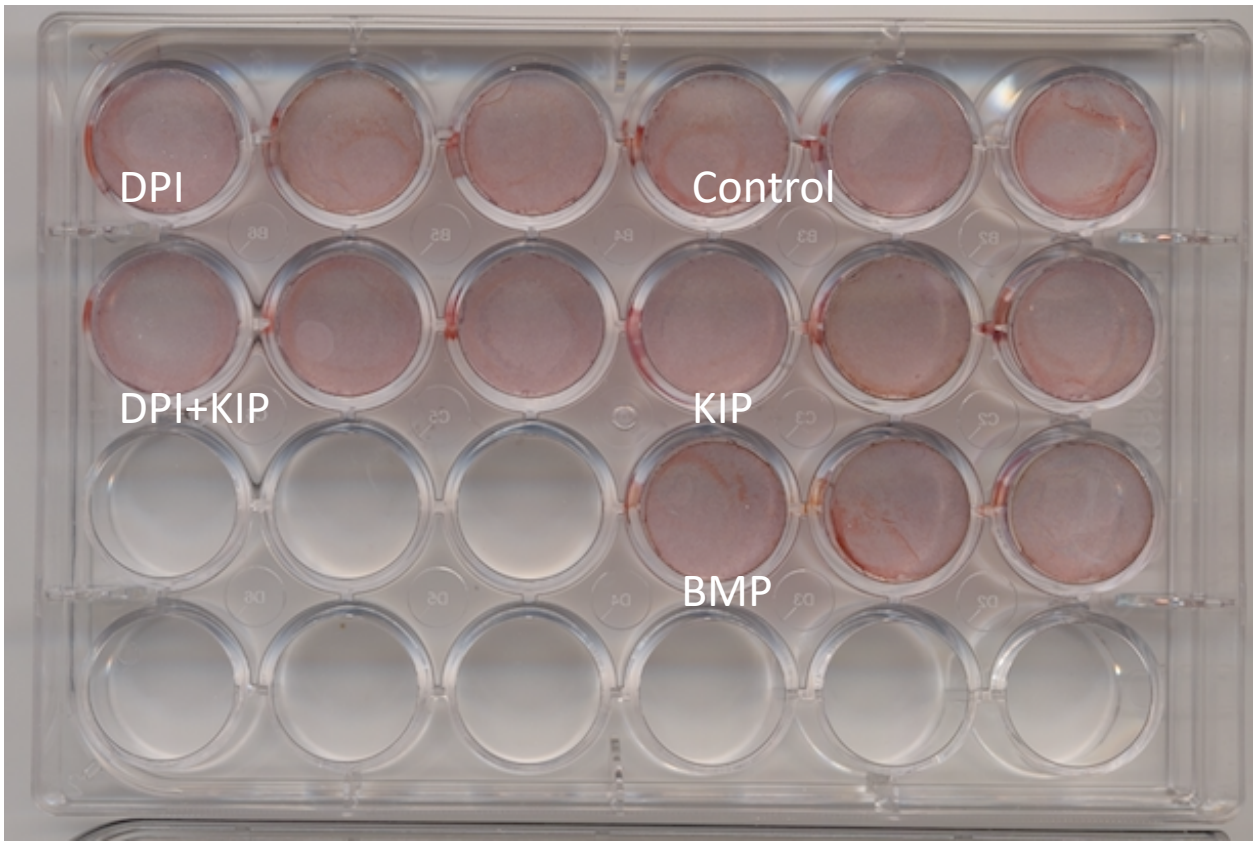

Figure 4.7 Mineralization of hMSCs after culture on peptide functionalized coverslips.

After 21 days of hMSC culture in osteogenic media on chemically functionalized coverslips, there was no qualitative difference in mineralization between groups.

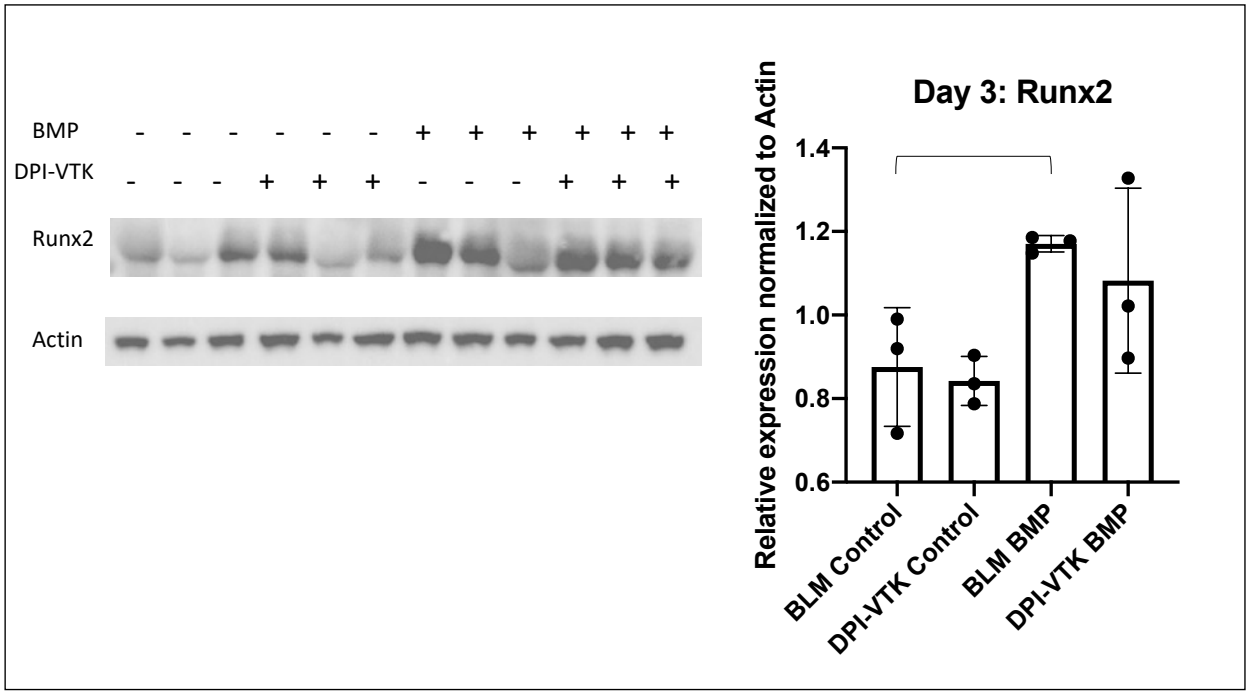

Figure 4.8 Effect of DPI-VTK and rhBMP-2 on osteogenesis after 3 days

After 3 days of culture on mineralized film, MSCs cultured on no-peptide BLM mineralized with BMP-2 had significantly increased Runx2 expression compared to the control. There was no significant difference between the BMP groups with or without DPI-VTK.

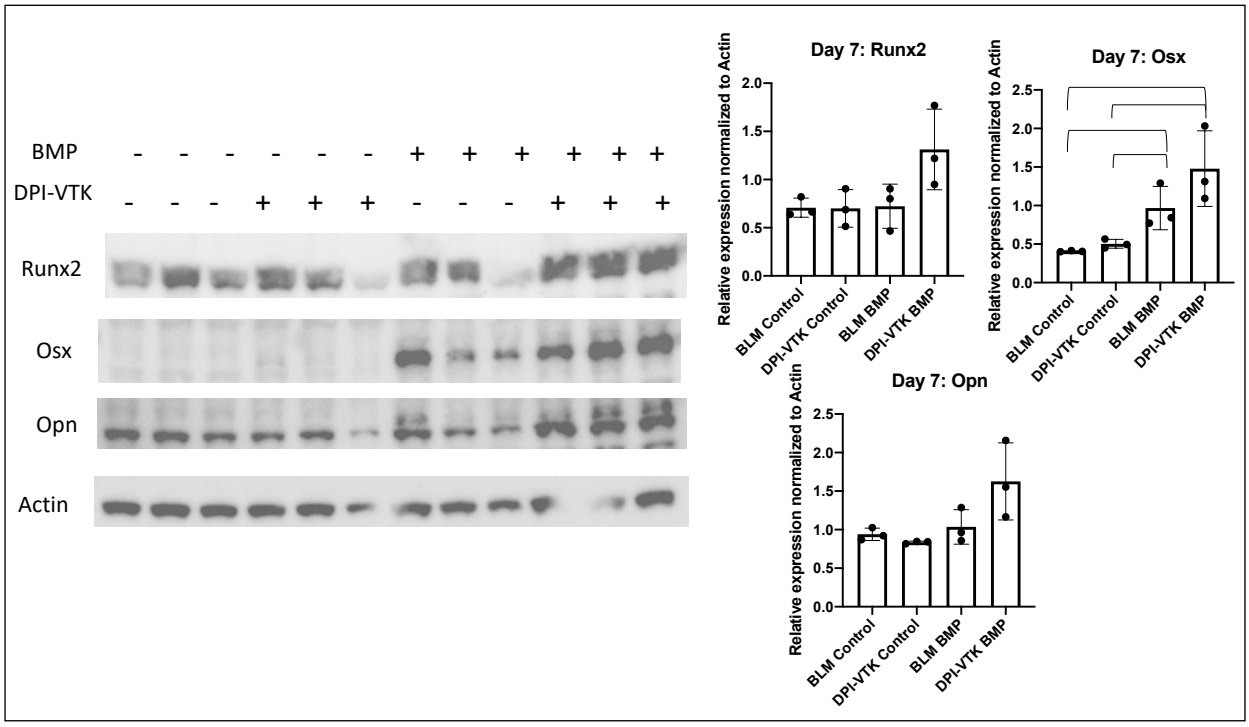

Figure 4.9 Effect of DPI-VTK and rhBMP-2 on osteogenesis after 7 days

After 7 days of culture on mineralized film, the groups exposed to BMP-2 had significantly increased osterix expression compared to the non-BMP groups, but no difference between BMP groups with or without DPI-VTK. There was no significant difference in Runx2 or OPN.

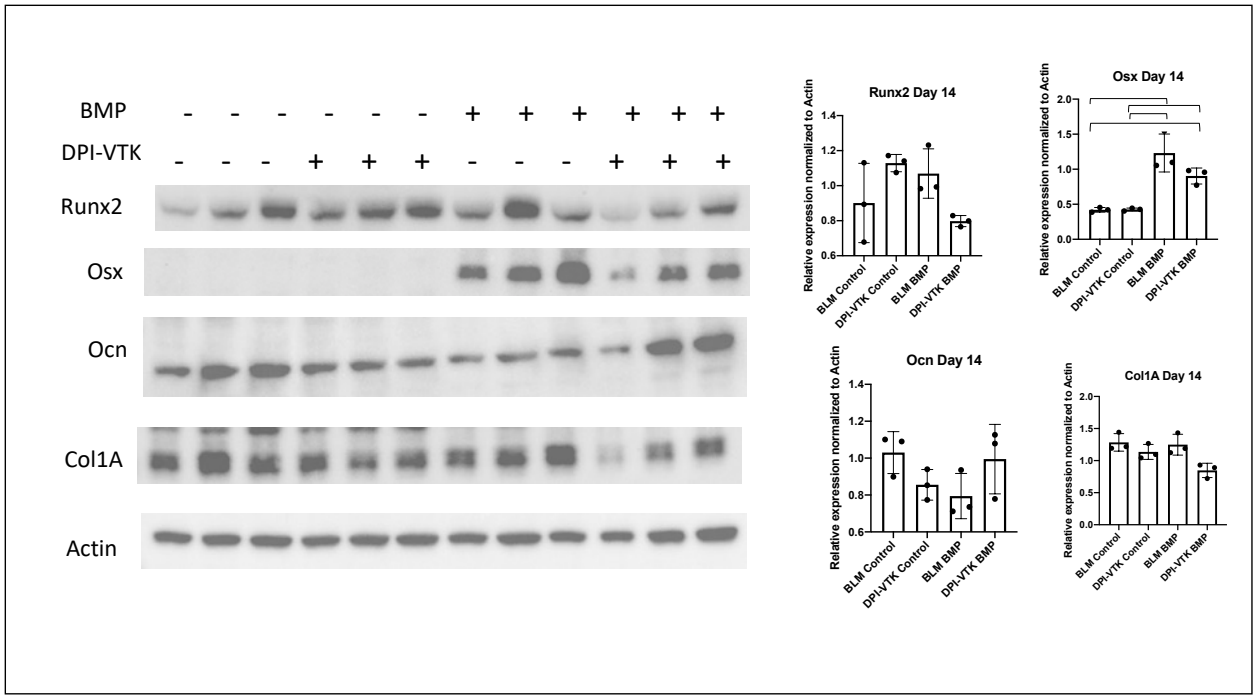

Figure 4.10 Effect of DPI-VTK and rhBMP-2 on osteogenesis after 14 days

After 14 days of culture on mineralized film, the groups exposed to BMP-2 had significantly increased osterix expression compared to the non-BMP groups, but no difference between BMP groups with or without DPI-VTK. There was no significant difference in Runx2, OCN, or Col1A.

4.7 References

[1] N.E. Epstein, Pros, cons, and costs of INFUSE in spinal surgery, Surg. Neurol. Int. 2 (2011) 10. https://doi.org/10.4103/2152-7806.76147.

[2] W.F. McKay, S.M. Peckham, J.M. Badura, A comprehensive clinical review of recombinant human bone morphogenetic protein-2 (INFUSE?? Bone Graft), Int. Orthop. 31 (2007) 729–734. https://doi.org/10.1007/s00264-007-0418-6.

[3] V. Campana, G. Milano, E. Pagano, M. Barba, C. Cicione, G. Salonna, W. Lattanzi, G. Logroscino, Bone substitutes in orthopaedic surgery: from basic science to clinical practice, J. Mater. Sci. Mater. Med. 25 (2014) 2445–2461. https://doi.org/10.1007/s10856-014-5240-2.

[4] E.J. Carragee, E.L. Hurwitz, B.K. Weiner, A critical review of recombinant human bone morphogenetic protein-2 trials in spinal surgery: Emerging safety concerns and lessons learned, Spine J. 11 (2011) 471–491. https://doi.org/10.1016/j.spinee.2011.04.023.

[5] I. Bilem, P. Chevallier, L. Plawinski, E.D. Sone, M.C. Durrieu, G. Laroche, RGD and BMP-2 mimetic peptide crosstalk enhances osteogenic commitment of human bone marrow stem cells, Acta Biomater. 36 (2016) 132–142. https://doi.org/10.1016/j.actbio.2016.03.032.

[6] I. Pountos, M. Panteli, A. Lampropoulos, E. Jones, G.M. Calori, P. V Giannoudis, The role of peptides in bone healing and regeneration: a systematic review., BMC Med. 14 (2016) 103. https://doi.org/10.1186/s12916-016-0646-y.

[7] A. Saito, Y. Suzuki, S.I. Ogata, C. Ohtsuki, M. Tanihara, Activation of osteo-progenitor cells by a novel synthetic peptide derived from the bone morphogenetic protein-2 knuckle epitope., Biochim. Biophys. Acta. 1651 (2003) 60–67. https://doi.org/10.1016/S1570-9639(03)00235-8.

[8] T.A. Wright, R.C. Page, D. Konkolewicz, Polymer conjugation of proteins as a synthetic post-translational modification to impact their stability and activity, Polym. Chem. 10 (2019) 434–454. https://doi.org/10.1039/c8py01399c.

[9] E.M. Pelegri-Oday, E.W. Lin, H.D. Maynard, Therapeutic protein-polymer conjugates: Advancing beyond pegylation, J. Am. Chem. Soc. 136 (2014) 14323–14332. https://doi.org/10.1021/ja504390x.

[10] C.M. Madl, M. Mehta, G.N. Duda, S.C. Heilshorn, D.J. Mooney, Presentation of BMP-2 mimicking peptides in 3D hydrogels directs cell fate commitment in osteoblasts and mesenchymal stem cells, Biomacromolecules. 15 (2014) 445–455. https://doi.org/10.1021/bm401726u.

[11] J.Y. Lee, J.E. Choo, Y.S. Choi, J.S. Suh, S.J. Lee, C.P. Chung, Y.J. Park, Osteoblastic differentiation of human bone marrow stromal cells in self-assembled BMP-2 receptor-binding peptide-amphiphiles, Biomaterials. 30 (2009) 3532–3541. https://doi.org/10.1016/j.biomaterials.2009.03.018.

[12] S.J. Segvich, D.H. Kohn, Phage Display as a Strategy for Designing Organic/Inorganic Biomaterials, in: B. R, D.A. Puleo (Eds.), Biol. Interact. Mater. Surfaces Underst. Control. Protein, Cell, Tissue Responses, Springer, New York, 2009: pp. 115–132.

[13] H. Ramaraju, S.J. Miller, D.H. Kohn, Dual-functioning peptides discovered by phage display increase the magnitude and specificity of BMSC attachment to mineralized biomaterials, Biomaterials. 134 (2017) 1–12. https://doi.org/10.1016/j.biomaterials.2017.04.034.

[14] S. Segvich, S. Biswas, U. Becker, D.H. Kohn, Identification of peptides with targeted adhesion to bone-like mineral via phage display and computational modeling, Cells Tissues Organs. 189 (2008) 245–251. https://doi.org/10.1159/000151380.
[15] L. Fourel, A. Valat, E. Faurobert, R. Guillot, I. Bourrin-Reynard, K. Ren, L. Lafanechère, E. Planus, C. Picart, C. Albiges-Rizo, β3 integrin-mediated spreading induced by matrix-bound BMP-2 controls Smad signaling in a stiffness-independent manner, J. Cell Biol. 212 (2016) 693–706. https://doi.org/10.1083/jcb.201508018.
[16] E. Migliorini, A. Valat, C. Picart, E.A. Cavalcanti-Adam, Tuning cellular responses to BMP-2 with material surfaces, Cytokine Growth Factor Rev. (2016). https://doi.org/10.1016/j.cytogfr.2015.11.008.
[17] S.-H. Oh, J.-W. Kim, Y. Kim, M.N. Lee, M.-S. Kook, E.Y. Choi, S.-Y. Im, J.-T. Koh, The extracellular matrix protein Edil3 stimulates osteoblast differentiation through the integrin α5β1/ERK/Runx2 pathway, PLoS One. 12 (2017) e0188749. https://doi.org/10.1371/journal.pone.0188749.
[18] W. Zhao, Z. Xu, Q. Cui, N. Sahai, Predicting the Structure-Activity Relationship of Hydroxyapatite-Binding Peptides by Enhanced-Sampling Molecular Simulation, Langmuir. 32 (2016) 7009–7022. https://doi.org/10.1021/acs.langmuir.6b01582.
[19] A. Shekaran, J.R. García, A.Y. Clark, T.E. Kavanaugh, A.S. Lin, R.E. Guldberg, A.J. García, Bone regeneration using an alpha 2 beta 1 integrin-specific hydrogel as a BMP-2 delivery vehicle, Biomaterials. 35 (2014) 5453–5461. https://doi.org/10.1016/j.biomaterials.2014.03.055.
[20] G. Xiao, R. Gopalakrishnan, D. Jiang, E. Reith, M.D. Benson, R.T. Franceschi, Bone morphogenetic proteins, extracellular matrix, and mitogen-activated protein kinase signaling pathways are required for osteoblast-specific gene expression and differentiation in MC3T3-E1 cells, J. Bone Miner. Res. 17 (2002) 101–110. https://doi.org/10.1359/jbmr.2002.17.1.101.

Chapter 5: Additional Data: Investigation of DPI-VTK binding mechanism

5.1 Introduction

Cell-matrix interactions are primarily mediated through integrin receptors. Integrins are present in the cell membrane as pairs of alpha and beta subunits [1]. Extracellular matrix proteins such as fibronectin and collagen have peptide motifs that bind to integrins [2]. Integrin binding peptides have received much interest in engineering biomaterials for bone regeneration due to the key role of integrins in osteoblast survival and differentiation [3]. Many of these peptides, however, are derived from extracellular matrix proteins and consequently have broad-spectrum cell binding [4]. The phage display derived peptide DPI-VTK, in contrast, shows specificity toward binding MSCs. In the presence of anti-integrin antibodies, the binding of DPI-VTK to MSCs is disrupted, suggesting a possible integrin mediated mechanism [5]. The high specificity of DPI-VTK to MSCs, however, may suggest that other types of proteins mediate the binding as well.

Identifying the mechanism of MSC binding to DPI-VTK is significant for several reasons. First, understanding mechanism could facilitate the enhancement of DPI-VTK's clinical capabilities. For example, the DPI-VTK sequence could be modified to have greater interactions with the target proteins, or recombinant target proteins could be expressed in cells to enhance the cells' interactions with DPI-VTK. Another reason for investigating this mechanism is that the specificity of DPI-VTK to unique to MSCs. This specificity would be important because MSCs are heterogeneous and the currently identified markers for MSCs are not specific enough. The

discovery of an MSC specific peptide could make it easier to identify and isolate MSCs, facilitating both basic science research and clinical translation. In Chapter 3, the target cell population of DPI-VTK was evaluated for expression of MSC markers. CD90 and CD200 are two MSC markers that were expressed by both the DPI-VTK binding population and the population induced to migrate into a calvarial defect. It is possible that these markers interact with DPI-VTK binding integrins or even be binding targets themselves. To advance our understanding of what types of binding targets on MSCs are required to create MSC-specific interactions, several pilot experiments were performed. To identify binding targets for DPI-VTK, an affinity purification protocol involving the labeling of DPI-VTK target probes with biotin followed by purification with magnetic beads and evaluation with western blotting was tested. A colocalization experiment testing the binding of DPI-VTK to focal adhesions was performed. Lastly, data from the flow cytometry experiment presented in Chapter 3 was analyzed for evidence of DPI-VTK binding to MSC markers. While Chapter 3 had focused on whether DPI-VTK binding cells express MSC markers, this chapter focuses on direct binding between DPI-VTK and the marker proteins.

5.2 Methods

5.2.1 Affinity purification of DPI-VTK target proteins

For the binding assay, DPI-VTK was conjugated with sulfo-SBED (Pierce) according to the manufacturer's instructions. Human iPS-MSCs were incubated with the peptides for 30 minutes and crosslinked for 10 minutes with UV. Cells were lysed with RIPA buffer and affinity purified with streptavidin Dynabeads. The purified proteins as well as the supernatants were

subjected to SDS-PAGE and western blotting. After affinity purification, the supernatants were removed from the Dynabeads. 2X Laemmli buffer was added to both the supernatants and the Dynabeads and the samples were heated at 95^{o}C for 5 minutes. Samples were loaded onto SDS-PAGE gels and run at 225 V for 50 minutes in Tris-Glycine buffer. This was followed by transfer onto PVDF membranes at 50 V for 1.25 hours. Membranes were blocked with 3% BSA in TBST for 1 hour at room temperature and incubated overnight at 4^{o}C with primary antibodies for integrin Alpha 5. After 3 washes with TBST, the membranes were incubated with HRP-tagged secondary antibodies for 1 hour at room tempura and washed 3 more times before development with ECL reagent.

5.2.2 Co-localization of DPI-VTK with focal adhesions

Human iPSC-MSCs were seeded on fibronectin coated glass slides for 24 hours in Alpha-MEM with 10% FBS and antibiotics. They were then fixed in 4% PFA for 15 minutes, washed with PBS, permealized with Triton X-100, and co-stained with FITC-DPI-VTK and anti-vinculin antibodies. They were then mounted with Vecta-shield and imaged with fluorescence microscopy. Co-localization was evaluated qualitatively.

5.2.3 Flow cytometry

Calvaria were dissected from 4–5-week-old male C57/BL6 mice (n=7) and digested in collagenase solution to yield a heterogenous cell suspension. The cells were resuspended in flow cytometry buffer and stained with primary antibodies for MSC markers CD29, CD45, CD73, CD90, CD105, CD106, Sca-1, CD31, CD44, and CD200 followed by APC tagged secondary

antibodies and FITC tagged DPI-VTK. The stained cells were submitted to the University of Michigan Flow Cytometry core for analysis on a BD LSRFortessa Cell Analyzer.

5.3 Results

5.3.1 Affinity purification of DPI-VTK target proteins

Western blotting for integrin alpha 5 showed that Alpha 5 protein was pulled down by the streptavidin beads when the Sulfo-SBED-DPI-VTK tagged the cells but not in the control group (Figure 5.1). The presence of bands in the supernatants for both the Sulfo-SBED and the control groups confirms that integrin Alpha 5 was present in both samples, but was only pulled down by the magnetic beads when Sulfo-SBED-DPI-VTK was added to the cells.

5.3.2 Co-localization of DPI-VTK with focal adhesions

Human MSCs were stained with vinculin as a marker for focal adhesions as well as FITC tagged DPI-VTK. Clusters of vinculin (red) and FITC-DPI-VTK (green) are seen throughout the cells. When merged, co-staining for vinculin and FITC-DPI-VTK showed co-localization (yellow), showing evidence that DPI-VTK targets focal adhesions.

5.3.3 Data from flow cytometry

When the cells were stained with CD90 and CD31 antibodies, the percentage of the total cell population that bound DPI-VTK decreased by more than 50%, indicating possible competitive binding between DPI-VTK and the antibodies.

5.4 Discussion

Blocking integrins α5, αV, β1, β3, β5, and α2β1 inhibited the adhesion of iPSC-MSC cells to DPI-VTK [5], suggesting that DPI-VTK targets integrins. Because of the promiscuous binding nature of integrins, a more targeted approach was used. Using the biotin transfer agent sulfo-SBED, DPI-VTK target proteins were labeled with biotin and purified with streptavidin functionalized magnetic beads. Western blotting for integrin alpha 5 showed that integrin alpha 5 was a binding target of DPI-VTK (Figure 5.1). This proof-of-concept experiment demonstrates the possibility of using this approach to identify the binding targets of DPI-VTK. Rather than using western blotting, the purified proteins could be analyzed using mass spectrometry to determine the peptide binding targets in a less biased approach.

Co-staining of DPI-VTK and vinculin demonstrated co-localization (Fig. 5.2). Vinculin is a key marker of focal adhesion complexes [6,7]. When binding the substrate, integrins cluster into focal adhesion complexes. The colocalization of DPI-VTK with these complexes supports the integrin binding hypothesis. In Chapter 3, a flow cytometry approach was used to determine which MSC markers were expressed by the DPI-VTK binding cell population. During the experiment, the samples were split into groups that were stained with antibodies for the different markers. All groups were stained with equivalent amounts of fluorescently tagged DPI-VTK. Although the percentage of the total cell population that bound the peptide should have been equivalent for all the groups, two of the groups were significantly lower, CD90 and CD31. An

explanation for this unexpected result is that the antibodies for CD90 and CD31 are acting as competitive inhibitors and blocking the binding of DPI-VTK. This suggests that CD90 and CD31 could be possible binding targets of peptide DPI-VTK, which would complicate the hypothesis that DPI-VTK targets just integrins.

In the Chapter 3 studies, CD90 was identified as a key marker of the cells that DPI-VTK recruits *in vivo*, so CD90 being a key binding target would explain the specificity. There have been several publications which have investigated interactions between CD90 and various integrins, particularly in the context of cellular migration [8–10]. CD90 can interact with integrins in both a *cis* (within the same cell) and *trans* (between different cells) manner [9]. CD90 and integrin interactions are important in trans-endothelial migration of leukocytes by allowing the leukocytes to bind to endothelial cells [8]. CD90 also induces migration of metastatic cancer cells in an integrin β3 dependent manner [10], although this has not been confirmed in MSCs. In addition, CD90 has been found to be important for regulating integrin activity through an integrin binding RLD motif [9]. These interactions could be key in explaining the cell-specific and chemotactic effects of DPI-VTK and warrant further investigation. Understanding the mechanism of DPI-VTK induced migration would not only reveal how DPI-VTK obtains cellular specificity, but could also result in insights into the molecular mechanisms of MSC migration that could be useful in the development of cell specific homing therapies.

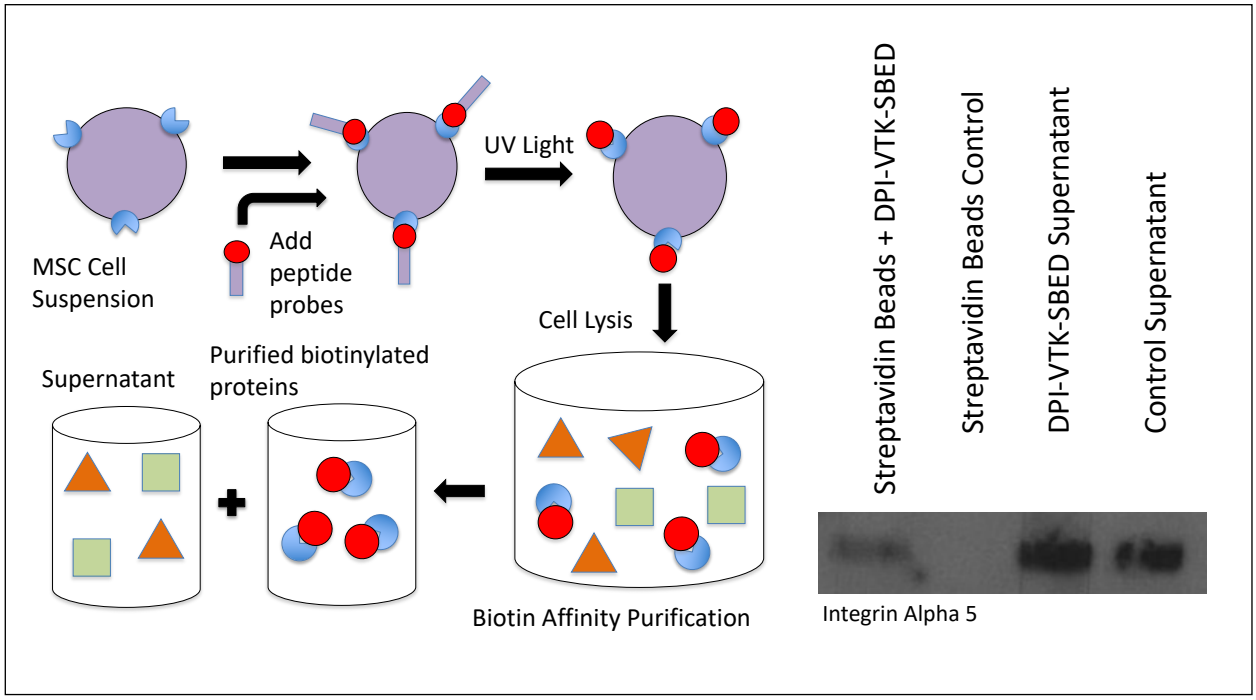

Figure 5.1 Affinity Purification Assay

Peptide DPI-VTK labeled with Sulfo-SBED was incubated with a suspension of human MSCs. Exposure to UV light coupled the biotin markers to DPI-VTK target proteins. After lysis, the biotinylated proteins were purified with magnetic streptavidin beads and analyzed wit western blotting for integrin Alpha 5. Control cells without the peptide probe were also lysed and purified. Supernatants of both biotinylated and control cells were analyzed to confirm presence of integrin Alpha 5.

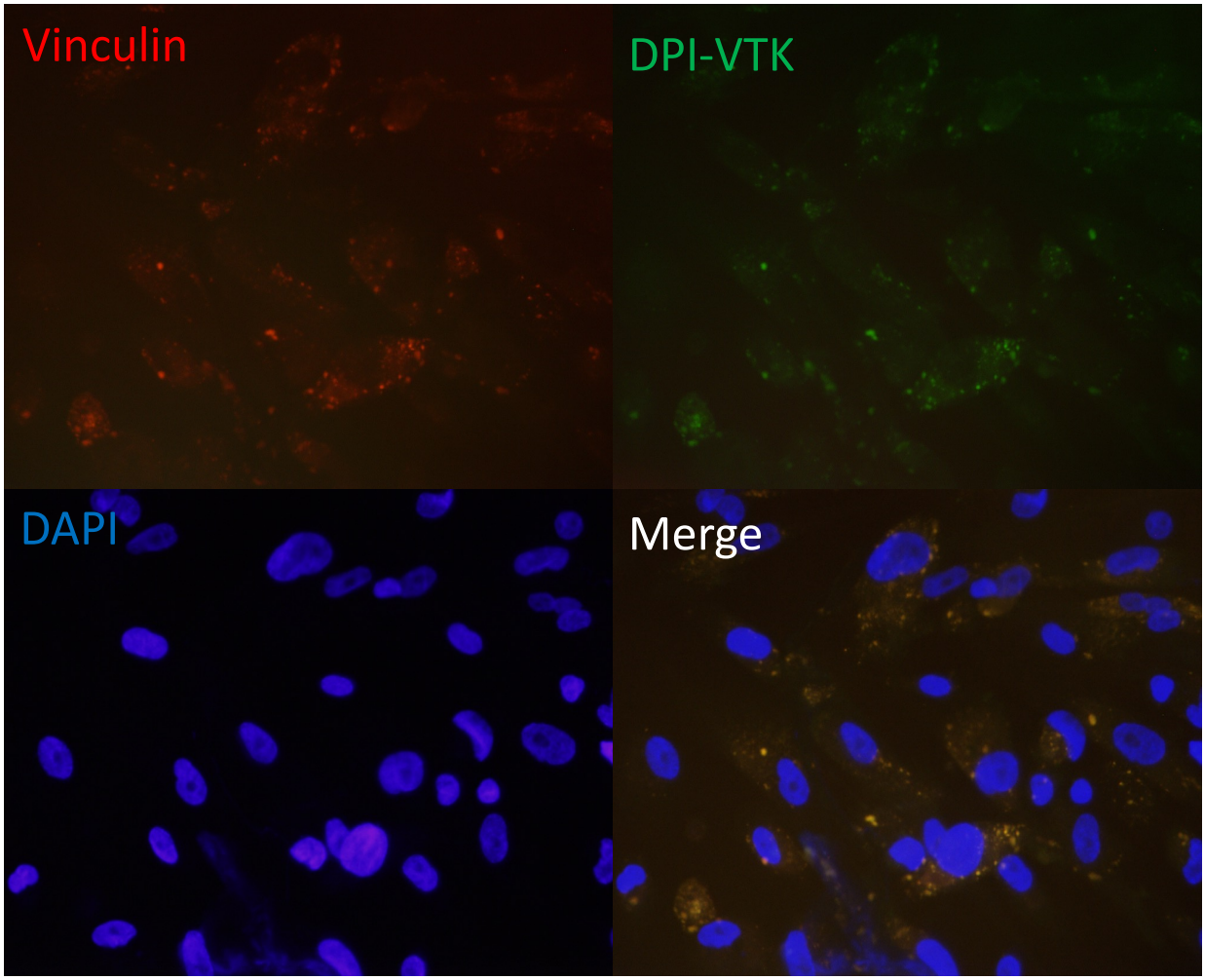

Figure 5.2 Co-localization of DPI-VTK with focal adhesions

Human MSCs were stained with anti-vinculin antibodies (red), FITC-DPI-VTK (Green), and DAPI (Blue). Merging images reveals colocalization (yellow) of vinculin (focal adhesions) with DPI-VTK.

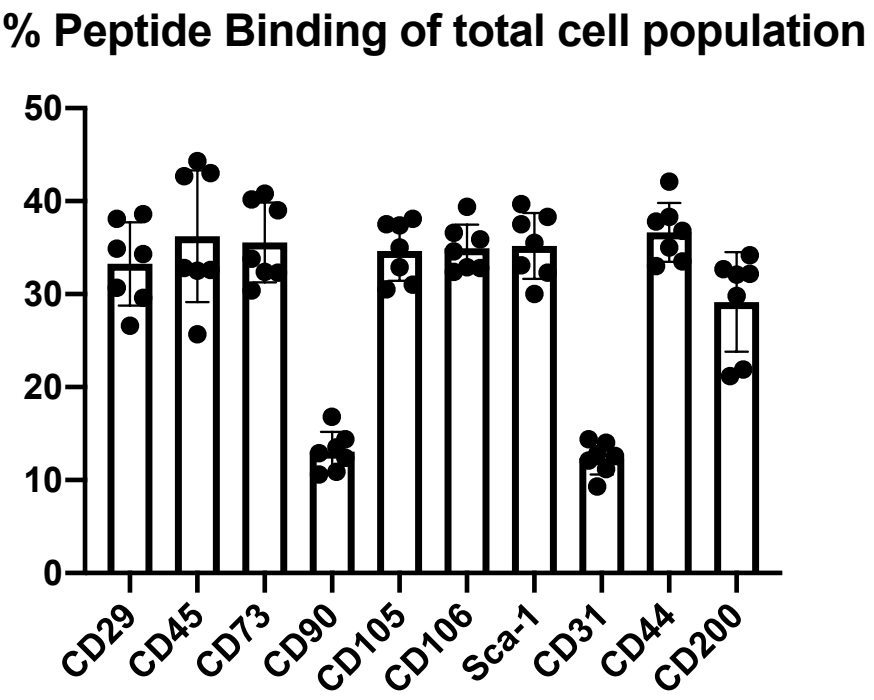

Figure 5.3 CD90 and CD31 antibodies disrupt binding of DPI-VTK

Mouse calvarial cells were stained with antibodies for MSC markers as well as FITC-DPI-VTK. CD90 and CD31 antibodies reduced the total percent of cells binding with DPI-VTK.

5.5 References

[1] R.O. Hynes, The emergence of integrins: A personal and historical perspective, Matrix Biol. 23 (2004) 333–340. https://doi.org/10.1016/j.matbio.2004.08.001.

[2] U. Hersel, C. Dahmen, H. Kessler, RGD modified polymers: Biomaterials for stimulated cell adhesion and beyond, Biomaterials. 24 (2003) 4385–4415. https://doi.org/10.1016/S0142-9612(03)00343-0.

[3] M. Kantlehner, P. Schaffner, D. Finsinger, J. Meyer, a Jonczyk, B. Diefenbach, B. Nies, G. Hölzemann, S.L. Goodman, H. Kessler, Surface coating with cyclic RGD peptides stimulates osteoblast adhesion and proliferation as well as bone formation., Chembiochem. 1 (2000) 107–114. https://doi.org/10.1002/1439-7633(20000818)1:2<107::aid-cbic107>3.0.co;2-4.

[4] H. Ramaraju, S.J. Miller, D.H. Kohn, Dual-functioning peptides discovered by phage display increase the magnitude and specificity of BMSC attachment to mineralized biomaterials, Biomaterials. 134 (2017) 1–12. https://doi.org/10.1016/j.biomaterials.2017.04.034.

[5] H. Ramaraju, D.H. Kohn, Cell and Material-Specific Phage Display Peptides Increase iPS-MSC Mediated Bone and Vasculature Formation In Vivo, Adv. Healthc. Mater. 1801356 (2019) 1–11. https://doi.org/10.1002/adhm.201801356.

[6] J.D. Humphries, P. Wang, C. Streuli, B. Geiger, M.J. Humphries, C. Ballestrem, Vinculin controls focal adhesion formation by direct interactions with talin and actin, J. Cell Biol. 179 (2007) 1043 LP-1057. https://doi.org/10.1083/jcb.200703036.

[7] B.G. Keselowsky, A.J. García, Quantitative methods for analysis of integrin binding and focal adhesion formation on biomaterial surfaces, Biomaterials. 26 (2005) 413–418. https://doi.org/10.1016/j.biomaterials.2004.02.050.

[8] L. Leyton, J. Díaz, S. Martínez, E. Palacios, L.A. Pérez, R.D. Pérez, Thy-1/CD90 a Bidirectional and Lateral Signaling Scaffold, Front. Cell Dev. Biol. 7 (2019) 1–11. https://doi.org/10.3389/fcell.2019.00132.

[9] P. Hu, L. Leyton, J.S. Hagood, T.H. Barker, Thy-1-Integrin Interactions in cis and Trans Mediate Distinctive Signaling, Front. Cell Dev. Biol. 10 (2022) 1–20. https://doi.org/10.3389/fcell.2022.928510.

[10] M. Brenet, S. Martínez, R. Pérez-Nuñez, L.A. Pérez, P. Contreras, J. Díaz, A.M. Avalos, P. Schneider, A.F.G. Quest, L. Leyton, Thy-1 (CD90)-Induced Metastatic Cancer Cell Migration and Invasion Are β3 Integrin-Dependent and Involve a Ca2+/P2X7 Receptor Signaling Axis, Front. Cell Dev. Biol. 8 (2021) 1–16. https://doi.org/10.3389/fcell.2020.592442.

[11] C.M. Madl, M. Mehta, G.N. Duda, S.C. Heilshorn, D.J. Mooney, Presentation of BMP-2 mimicking peptides in 3D hydrogels directs cell fate commitment in osteoblasts and mesenchymal stem cells, Biomacromolecules. 15 (2014) 445–455. https://doi.org/10.1021/bm401726u.

[12] A. Saito, Y. Suzuki, S.I. Ogata, C. Ohtsuki, M. Tanihara, Activation of osteo-progenitor cells by a novel synthetic peptide derived from the bone morphogenetic protein-2 knuckle epitope., Biochim. Biophys. Acta. 1651 (2003) 60–67. https://doi.org/10.1016/S1570-

9639(03)00235-8.
[13] L.N. Luong, S.I. Hong, R.J. Patel, M.E. Outslay, D.H. Kohn, Spatial control of protein within biomimetically nucleated mineral, Biomaterials. 27 (2006) 1175–1186. https://doi.org/10.1016/j.biomaterials.2005.07.043.

Chapter 6: Summary and Future Directions

6.1 Summary of Dissertation

The limitations of current bone grafting techniques have motivated the development of tissue engineering approaches to heal bone defects. As this field has developed, the need for more targeted approaches has become apparent. High-throughput screening methods such as phage display have allowed for the development of specific peptide sequences for both cellular and material substrates. This method creates the possibility of developing peptide functionalized materials with affinity for specific cell types. For example, the combination MSC binding and mineral binding DPI-VTK peptide was used to create mineralized scaffolds with enhanced adhesion of MSCs for bone tissue engineering applications. The early application of DPI-VTK, however, was limited to transplanted cells, which is complicated by logistical issues in cellular harvesting and expansion. Therefore, work in this dissertation investigated the use of DPI-VTK as a chemotactic agent for MSCs.

Transwell assays were first conducted to determine the effect of DPI-VTK on MSC migration. In transwell assays, DPI-VTK stimulated the migration of human iPS-MSCs. No effect was seen on the MC3T3s or MDFs (Figure 3.1A). Next, transwell assays using singular peptides DPI and VTK along with DPI-VTK demonstrated that DPI domain is responsible for the chemotactic effect independent of the VTK domain (Figure 3.1B). Additionally, a significant

migratory effect on mouse calvarial cells was shown (Figure 3.1C) when transwell assays were performed with primary mouse cells. To determine if DPI-VTK could be successfully delivered with mineralized scaffolds to induce migration of MSC *in vivo*, the minimum concentration required to induce migration was determined to be 50 μg/mL (Figure 3.2C). In order to ensure this concentration was achieved in vivo, a bolus of peptide was delivered with the scaffolds in a mouse calvarial defect model. One week following administration of DPI-VTK along with a mineralized scaffold, a significant increase in CD90 and CD200 positive cells was seen in the defect, providing evidence that DPI-VTK enhances migration of CD90 and CD200 cells in vivo (Figure 3.4). To better characterize the cells that DPI-VTK targets in the calvaria, flow cytometry analysis was used to confirm that the peptide binds calvarial cells with MSC markers. Additional analysis involving staining of calvarial sections with DPI-VTK showed that the peptide targets cells in the calvarial suture as well as periosteum with MSC markers Figure 3.3). Lastly, a bone regeneration study was performed to determine if DPI-VTK could increase bone regeneration *in vivo*. This experiment showed that DPI-VTK enhances bone formation versus an acellular control (Figure 3.5).

While DPI-VTK enhances the osteoconductivity of mineralized biomaterials through both migration and adhesion, it is not osteoinductive. BMPs have been used extensively in the clinic as osteoinductive agents. There are several limitations such as high cost and side effects that have not been completely addressed. BMP derived peptides could address some of these limitations through their cheaper cost and greater flexibility to be modified. Based on the success of the DPI-VTK peptide for anchoring MSCs to biomaterials, it was hypothesized that the coupling of VTK to the BMP derived KIP peptide could allow for more precise delivery of

osteoinductive BMP signals on mineralized materials and act synergistically with MSC binding DPI-VTK.

While VTK enhanced the mineral binding of KIP compared to KIP alone (Figure 4.1), and could be co-adsorbed with DPI-VTK (Figure 4.2), there was no significant effect on osteogenesis from the combination of DPI-VTK and KIP-VTK. There was significant difference in Runx2 expression between the KIP-VTK group and the control group at day 14 as well as the KIP-VTK+DPI-VTK group at the day 7 timepoints, suggesting the KIP peptide does have a weak effect on osteogenesis (Figure 4.5). There was, however, no effect on Smad phosphorylation when the peptide was absorbed on mineralized films (Figure 4.4). Other studies found KIP to have significant effects on osteogenesis when coupled to an alginate scaffold [11,12]. It is possible that the KIP's efficacy is dependent on its presentation. While coupling to the VTK peptide did improve the absorption of KIP to mineral, the absorbed peptide had no significant effect on osteogenesis. There is a possibility that when absorbed to the mineral surface, the KIP domain is not displayed in a way to effectively bind with its receptor. This work demonstrates that when designing dual-functional peptides, one must consider the structure-function relationships that are affected when coupling different domains together. For example, the linker must be sufficiently long and flexible enough to allow each domain to act independently of the other. Also, when absorbed to materials, it is critical that anchoring domain is interacting with the material surface while the cell-binding domain is available to bind to its receptor. When delivered along with BMP-2 there was also no effect with the addition of absorbed DPI-VTK. Although DPI-VTK and other integrin binding domains enhance osteogenic

differentiation, this data demonstrates the effect is not strong enough to yield synergistic results in biochemical outcomes.

6.2 Future Directions

Following the completion of this work, there are several interesting directions that can be taken to build upon the results. With the discovery that DPI-VTK can act as a chemotactic agent, more investigation should be done on how to utilize this clinically. While the bolus delivery method was effective, more sophisticated delivery methods could be used. For example, controlled release systems involving encapsulation of the peptides within biodegradable polymers or bioceramics could help maintain effective concentrations of the peptide over a longer period of time. Previous work on co-precipitation of biomolecules within BLM using SBF could be applied to peptide DPI-VTK [13]. To better optimize the delivery of DPI-VTK, its biological half-life *in vivo* as well as its other pharmacokinetic properties should be investigated.

Although KIP-VTK was not effective at inducing osteogenic differentiation with or without DPI-VTK, there is additional work that could be done. For example, the glycine linker in the KIP-VTK peptide may not be long and flexible enough to allow the peptide to fully interact with the BMP receptors while absorbed to the surface. Using chemical bioconjugation techniques, it could be possible to link the KIP and VTK domains with a flexible PEG linker. This may allow the KIP domain to fully interact with the BMP receptors on the cells and induce osteogenic effects. Since PEG is available in many different lengths/molecular weights, it would be possible to test different PEG linker sizes to optimize the ideal length for stimulating activity.

While no synergistic effect between DPI-VTK and BMP-2 was found on the molecular level, it is possible that these two bioactive agents could act synergistically when delivered together in an *in vivo* system. This is because the chemotactic and adhesive effect of the DPI-VTK would improve the migration of MSCs into a defect, while BMP-2 would provide the osteoinductive signals. Thus, DPI-VTK would recruit more MSCs that would be induced to differentiate by the BMP-2, resulting in greater bone regeneration.

Of particular importance to this work is the specificity of DPI-VTK to MSCs. Previous work had identified the cell-specific adhesion of the peptide *in vitro* [4], but this dissertation provided further insight into the *in vivo* population that the peptide targets. The definition of MSCs is a controversial issue that is subject to debate. Therefore, determining if a bioactive agent such as DPI-VTK specifically targets MSCs is a significant challenge. Many cellular populations have been described as MSCs, so it is better to consider MSCs as a broad classification of different cells with a common phenotype rather than a specific type of cell. Flow cytometry analysis of the calvarial cells binding DPI-VTK showed that the DPI-VTK binding cells expressed known MSC markers, but not CD45, a negative marker. While this work has provided evidence that DPI-VTK targets a population of MSCs within the calvaria, more work can be done to further elucidate this population. Flow cytometry done with more sophisticated gating strategies could more precisely define this population. Also, these studies could be done with cells derived from other anatomical locations, such as bones from the axial skeleton. This is particularly interesting due to the different embryonic origins of craniofacial bones versus axial bones. Data showed a more significant effect on migration for the calvarial cells versus bone

marrow cells form the long bones (Figure 3.1AC), suggesting that DPI-VTK may especially suited for craniofacial applications.

The development of an MSC specific chemotactic and adhesive agent also has broader implications for the field of tissue engineering. Since MSCs are capable of multi-potent differentiation into bone, cartilage, adipose and other tissue types, this peptide could be applied to tissue engineering of other tissue types as well. It may also be useful for establishing interfaces between different tissues. For example, DPI-VTK could stimulate the migration and attachment of MSCs to dentin to regenerate the periodontal-tooth interface.

The use of a phage-display derived peptide as a chemotactic agent is a novel concept. While phage display has traditionally been used to develop adhesive agents, this work serves as a proof of principle that it could also be used to develop a new generation of cell-specific chemotactic agents. This could be done by screening cells with peptide libraries while performing transwell assays to isolate sequences that can improve migration.

The fact that DPI-VTK acts as both a chemotactic and adhesive agent demonstrates the potential in developing other novel combination chemotactic and adhesive peptides. Although the coupling of VTK to the KIP peptide failed to work as expected in the conditions tested, there remains the potential in coupling other peptide sequences to VTK to functionalize the surface of mineralized materials. VTK could also be coupled to synthetic polymers and even larger molecular weight proteins. For example, rather than using the KIP peptide coupled to VTK, VTK could be coupled to the BMP-2 protein to enhance its absorption to apatite. Overall, the capabilities of phage-display to develop novel peptide sequences has the potential to significantly impact the field of tissue engineering. Discovering different peptide domains and combining

them in a modular manner such as DPI-VTK has potential to create custom-tailored biomaterials for numerous applications. With the relative ease of functionalizing mineralized materials with mineral binding peptides such as VTK, along with the common usage of mineralized materials in clinical settings, peptides could be easily added to materials depending on the clinical needs. For example, in patients with compromised vasculature, vascularization promoting peptides could be added; in situations where cell transplantation is not possible, migration promoting peptides could be utilized. This could also allow for adding multiple peptides to the same graft material, and different combinations could be studied to determine the optimal formulations. Using phage-display derived peptides in this manner would be translatable to a clinical setting and allow for progress in bone grafting techniques. In addition, more advanced delivery methods could be incorporated to deliver the peptides in a stepwise manner to create more sophisticated peptide-functionalized biomaterials.

6.3 Concluding Remarks

The work presented in this dissertation demonstrates the cell-specific chemotactic effects of the dual-functional MSC-binding and mineral-binding peptide DPI-VTK and its applications in bone tissue engineering. Findings resulting from these experiments demonstrate the potential for developing cell-specific biomolecule functionalized materials using phage display technology. Future work with the DPI-VTK peptide can help further understand the specific-cell population that it attracts and help expand knowledge on osteogenic stem cells for bone tissue engineering. Although the dual-functional BMP-derived and mineral binding peptide KIP-VTK failed to show any synergistic relationship with DPI-VTK, the studies presented in this work can

help guide design of future dual-functional peptides by understanding the limitations of this approach. Overall, this thesis furthers our understanding of dual-functional peptides for the application of bone tissue engineering by demonstrating the capabilities of phage display to develop novel cell-specific peptides that can promote both migration and adhesion of mesenchymal stem cells.

6.4 References

[1] R.O. Hynes, The emergence of integrins: A personal and historical perspective, Matrix Biol. 23 (2004) 333–340. https://doi.org/10.1016/j.matbio.2004.08.001.

[2] U. Hersel, C. Dahmen, H. Kessler, RGD modified polymers: Biomaterials for stimulated cell adhesion and beyond, Biomaterials. 24 (2003) 4385–4415. https://doi.org/10.1016/S0142-9612(03)00343-0.

[3] M. Kantlehner, P. Schaffner, D. Finsinger, J. Meyer, a Jonczyk, B. Diefenbach, B. Nies, G. Hölzemann, S.L. Goodman, H. Kessler, Surface coating with cyclic RGD peptides stimulates osteoblast adhesion and proliferation as well as bone formation., Chembiochem. 1 (2000) 107–114. https://doi.org/10.1002/1439-7633(20000818)1:2<107::aid-cbic107>3.0.co;2-4.

[4] H. Ramaraju, S.J. Miller, D.H. Kohn, Dual-functioning peptides discovered by phage display increase the magnitude and specificity of BMSC attachment to mineralized biomaterials, Biomaterials. 134 (2017) 1–12. https://doi.org/10.1016/j.biomaterials.2017.04.034.

[5] H. Ramaraju, D.H. Kohn, Cell and Material-Specific Phage Display Peptides Increase iPS-MSC Mediated Bone and Vasculature Formation In Vivo, Adv. Healthc. Mater. 1801356 (2019) 1–11. https://doi.org/10.1002/adhm.201801356.

[6] J.D. Humphries, P. Wang, C. Streuli, B. Geiger, M.J. Humphries, C. Ballestrem, Vinculin controls focal adhesion formation by direct interactions with talin and actin, J. Cell Biol. 179 (2007) 1043 LP-1057. https://doi.org/10.1083/jcb.200703036.

[7] B.G. Keselowsky, A.J. García, Quantitative methods for analysis of integrin binding and focal adhesion formation on biomaterial surfaces, Biomaterials. 26 (2005) 413–418. https://doi.org/10.1016/j.biomaterials.2004.02.050.

[8] L. Leyton, J. Díaz, S. Martínez, E. Palacios, L.A. Pérez, R.D. Pérez, Thy-1/CD90 a Bidirectional and Lateral Signaling Scaffold, Front. Cell Dev. Biol. 7 (2019) 1–11. https://doi.org/10.3389/fcell.2019.00132.

[9] P. Hu, L. Leyton, J.S. Hagood, T.H. Barker, Thy-1-Integrin Interactions in cis and Trans Mediate Distinctive Signaling, Front. Cell Dev. Biol. 10 (2022) 1–20. https://doi.org/10.3389/fcell.2022.928510.

[10] M. Brenet, S. Martínez, R. Pérez-Nuñez, L.A. Pérez, P. Contreras, J. Díaz, A.M. Avalos, P. Schneider, A.F.G. Quest, L. Leyton, Thy-1 (CD90)-Induced Metastatic Cancer Cell Migration and Invasion Are β3 Integrin-Dependent and Involve a Ca2+/P2X7 Receptor Signaling Axis, Front. Cell Dev. Biol. 8 (2021) 1–16. https://doi.org/10.3389/fcell.2020.592442.

[11] C.M. Madl, M. Mehta, G.N. Duda, S.C. Heilshorn, D.J. Mooney, Presentation of BMP-2 mimicking peptides in 3D hydrogels directs cell fate commitment in osteoblasts and mesenchymal stem cells, Biomacromolecules. 15 (2014) 445–455. https://doi.org/10.1021/bm401726u.

[12] A. Saito, Y. Suzuki, S.I. Ogata, C. Ohtsuki, M. Tanihara, Activation of osteo-progenitor cells by a novel synthetic peptide derived from the bone morphogenetic protein-2 knuckle epitope., Biochim. Biophys. Acta. 1651 (2003) 60–67. https://doi.org/10.1016/S1570-

9639(03)00235-8.
[13] L.N. Luong, S.I. Hong, R.J. Patel, M.E. Outslay, D.H. Kohn, Spatial control of protein within biomimetically nucleated mineral, Biomaterials. 27 (2006) 1175–1186. https://doi.org/10.1016/j.biomaterials.2005.07.043.

Appendix

Appendix A

Bioceramics[2]

Introduction

The clinical goal when using ceramic biomaterials, as with any biomaterial, is to replace lost tissue structure and/or function. The rationale for using ceramics in medicine and dentistry was initially based upon the relative biological inertness of ceramic materials compared to metals. However, in the past 30 years, emphasis has shifted towards the use of bioactive ceramics, materials that elicit normal tissue formation and also form an intimate bond with tissue through partial dissolution of the material surface. Bioceramics are also used in conjunction with biological therapies, where the ceramic delivers cells, proteins and/or genes, with an end-goal of regenerating functional tissue.

Ceramic biomaterials are processed to yield one of four types of surfaces and associated mechanisms of tissue attachment (Kohn and Ducheyne, 1992): (1) fully dense, relatively inert crystalline ceramics that attach to tissue by either a press fit, tissue growth onto a roughened surface, or via a grouting agent; (2) porous, relatively inert ceramics, where tissue grows into the pores, creating a mechanical attachment between the implant and tissue; (3) fully dense, surface

[2] Published as Madsen, E; Kohn, D. Biomedical Engineering Fundamentals, 3rd Edition, M. Kutz, McGraw-Hill, New York, 2019

reactive ceramics, which attach to tissue via a chemical bond; and (4) resorbable ceramics that integrate with tissue and eventually are replaced by new or existing host tissue. Ceramics may therefore be classified by their macroscopic surface characteristics (smooth, fully dense, roughened or porous) or their chemical stability (inert, surface reactive or bulk reactive/resorbable). The integration of biological (i.e. inductive) agents with ceramics further expands the clinical potential of these materials.

Relatively inert ceramics elicit minimal tissue response and lead to a thin layer of fibrous tissue adjacent to the ceramic surface. Surface-active ceramics are partially soluble, resulting in ion-exchange and the potential to lead a direct chemical bond with tissue. Bulk bioactive ceramics are fully resorbable, have greater solubility than surface-active ceramics, and may be replaced by an equivalent volume of regenerated tissue. The relative level of bioactivity mediates the thickness of the interfacial zone between the biomaterial surface and host tissue (Fig. 1). There are no standardized measures of "reactivity", but the most common are pH changes, ion solubility, tissue reaction, and assays for cell function.

Five main ceramics are used for musculoskeletal reconstruction and regeneration: carbon (Christel et al. 1987, More et al., 2004), alumina (Al_2O_3) (Kohn and Ducheyne 1992, Popat & Desai 2013, Hannouche et al. 2013), zirconia (ZrO_2) (Kohn and Ducheyne 1992, Cales and Stefani 1995), bioactive glasses and glass ceramics (Kohn and Ducheyne 1992, Ducheyne 1985, Hench & Best 2013) and calcium-phosphates (Kohn and Ducheyne 1992, Van Raemdonck et al. 1984).

In this Chapter, 3 types of bioceramics (bioinert, surface bioactive, bulk bioactive) are discussed, with a focus on musculoskeletal and dental applications. A materials science approach is taken to address design issues of importance to a biomedical engineer; the processing-structure-composition-property synergy is discussed for each material, then properties important to the

design and clinical success of each class of bioceramic are presented. Within the framework of discussing the processing-composition-structure synergy, issues of material selection, service conditions, fabrication routes and characterization methodologies are discussed.

Bioinert Ceramics

Ceramics are fully oxidized materials and are therefore chemically stable and less likely to elicit an adverse biological response than metals, which only oxidize at their surface. Three types of "inert" ceramics are of interest in musculoskeletal applications: carbon, alumina and zirconia.

Carbon

The benign biological reaction to carbon-based materials, along with the similarity in stiffness and strength between carbon and bone, made carbon a candidate material for musculoskeletal reconstruction almost 50 years ago (Bokros et al. 1972). Carbon has a hexagonal crystal structure that is formed by covalent bonds. Graphite has a planar hexagonal array structure, with a crystal size of approximately 1000Å (Bokros 1978). The carbon-carbon bond energy within the planes is large (114 kcal/mol), whereas the bond between the planes is weak (4 kcal/mol) (Hench and Ethridge 1982). Therefore, carbon derives its strength from the strong in-plane bonds, whereas the weak bonding between the planes results in a low modulus, near that of bone (Bokros 1978).

Isotropic carbon, on the other hand, has no preferred crystal orientation and therefore possesses isotropic material properties. Pyrolytic carbons are formed by the deposition of carbon from a fluidized bed onto a substrate. The fluidized bed is formed from pyrolysis of hydrocarbon gas (Hench and Ethridge 1982). Low temperature isotropic (LTI) carbons are formed at temperatures below 1500°C. LTI pyrolytic carbon possesses good wear resistance and

incorporation of silicon can further increase wear resistance (Bokros 1978). Vitreous carbon is a fine-grained polycrystalline material formed by slow heating of a polymer. Upon heating, the more volatile components diffuse from the structure and only carbon remains (Hench and Ethridge 1982). Properties of all three forms of carbon are summarized in Table 1.

Deposition of LTI coatings onto metal substrates is limited by the brittleness of the coatings . Carbon may also be vapor deposited onto a substrate by the evaporation of carbon atoms from a high temperature source and subsequent condensation onto a low temperature substrate (Hench and Ethridge 1982). Vapor deposited coatings are ~ 1□m thick, allowing properties of the substrate to be retained. Diamond-like carbon (DLC) coatings also improve fixation to bone (Koistinen et al. 2005, Reikeras et al. 2004) and wear resistance (Allen et al. 2001). Carbon-based thin films are produced from solid carbon or liquid/gaseous hydrocarbon sources, using ion beam or plasma deposition techniques, and have properties intermediate to those of graphite and diamond (Allen et al. 2001).

With the advent of nanotechnology, interest in carbon has been rekindled, in the form of carbon nanotubes (CNTs). CNTs have been proposed as scaffolds to support osteoconductivity (Zanello et al. 2006) and as a second phase in polymer scaffolds (Shi et al. 2006). Carbon nanotubes can guide the spatial deposition of mineral in hydrogels (Cancian et al. 2016). Carbon nanotubes have also been combined with hydroxyapatite and collagen to make composites. . CNT/collagen/HA composites exhibit increased stiffness, MSC proliferation, spreading, osteogenic gene expression, and bone formation (Jing et al. 2017). Despite these many uses, there are concerns about toxicity. Several mechanisms of toxicity have been proposed, including trace metals generating reactive oxygen species, membrane rupture, and disruption of biochemical processes. Smaller sized carbon nanotubes are especially toxic due to increased surface area. The

toxic effects are greatest when the carbon nanotubes are dispersed or in suspension, and minimized when bound to a substrate (Newman et al. 2013).

Alumina

High density, high purity, polycrystalline alumina is used for femoral stems, femoral heads, acetabular components and dental implants (Kohn and Ducheyne 1992, Boutin et al. 1988, Heimke et al. 2002, Nizard et al. 2008, Tateiwa et al. 2008, Hannouche et al. 2011, Popat & Desai 2013). Ion-modified and nanostructured Al_2O_3 have been synthesized, to increase strength and bioactivity (Webster et al. 2000, Zreiqat et al. 1999). In addition to chemical stability another attribute of alumina is wear resistance. A main motivation for using alumina in orthopaedic surgery is to increase tribological properties, and many total hip replacements are now designed as modular devices – i.e. an alumina femoral head is press-fit onto the neck of a metal femoral stem.

High purity alumina powder is isostatically compacted and shaped. Sintering (1600-1800°C) transforms a preform into a dense polycrystalline solid having a grain size < 5□m (Boutin et al. 1988). Single crystals (sapphire) may be grown by feeding powder onto a seed and allowing build up.

The mechanical properties of alumina are a function of purity, grain size, grain size distribution, porosity and inclusions (Kohn and Ducheyne 1992, Boutin et al. 1988, Dorre and Dawihl 1980) (Table 1). The elastic modulus of dense alumina is 2-4 fold greater than that of metals used in bone and joint reconstruction. Both grain size (d) and porosity (P, $0 \leq P \leq 1$) affect strength (□) via power law and exponential relations, respectively (Eqs. 1,2), where $□_0$ is the strength of the dense ceramic, A, n and B are material constants, experimentally determined, and n is ~ 0.5.

$$□ = Ad^{-n} \quad (1)$$

$$\square_P = \square_0 e^{-BP} \quad (2)$$

Decreasing grain size of from 7 to 4□m increases strength by ~ 20% (Dorre and Dawihl 1980). It is now possible to fabricate alumina with grain sizes ~ 1□m increasing strength further. Wear in alumina-alumina bearing couples can be 10 times less than in metal-polyethylene systems (Hannouche et al. 2011, Lusty et al. 2007).

The major limitation of alumina is its low fracture toughness. As a consequence, alumina is sensitive to stress concentrations and overloading. Retrieved alumina total hip replacements exhibit damage caused by fatigue, impact or overload (Walter and Lang 1986).

Zirconia

Yttrium oxide partially stabilized zirconia (YPSZ) is an alternative to alumina, and there are > 500,000 zirconia components in clinical use (Mantripragada et al. 2013). YPSZ has a higher toughness than alumina, since it can be transformation toughened, and is used in bulk form or as a coating (Filiaggi et al. 1996).

At room temperature, pure zirconia has a monoclinic crystal symmetry. Upon heating, it transforms to a tetragonal phase at ~ 1000-1100ºC, and then to a cubic phase at approximately 2000°C (Fig. 2). A partially reversible volumetric shrinkage (density increase) of 3-10% occurs during the monoclinic to tetragonal transformation (Christel et al. 1989). The volumetric changes resulting from the phase transformations can lead to residual stresses and cracking. Because of the large volume reduction, pure zirconia cannot be sintered. However, sintering and phase transformations can be controlled via the addition of stabilizing oxides. Yttrium oxide (Y_2O_3) stabilizes the tetragonal phase such that upon cooling the tetragonal crystals are maintained in a

metastable state and do not transform back to a monoclinic structure. The tetragonal to monoclinic transformation and volume change are also prevented by neighboring grains inducing compressive stresses on one another (Christel et al. 1989).

The modulus of partially stabilized zirconia is approximately half that of alumina, while the bending strength and fracture toughness are 2-3 times greater (Table 1). The strength and toughness result from transformation toughening, where crack nucleation and propagation lead to locally elevated stresses and energy in the tetragonal crystals surrounding the crack-tip (Fig. 3). The elevated energy induces the metastable tetragonal grains to locally transform into monoclinic grains. Since the monoclinic grains are larger than the tetragonal grains, there is a local volume increase, compressive stresses are induced, more energy is needed to advance the crack, and crack blunting occurs.

The wear rate of YPSZ on UHMWPE is variable, but can be less than the wear rate of alumina on UHMWPE (Chen et al. 2016). Wear resistance is a function of grain size, surface roughness and residual compressive stresses induced by the phase transformation. The increased mechanical and tribological properties of zirconia may allow for smaller diameter femoral heads to be used in comparison to alumina.

Partially stabilized zirconia is typically shaped by cold isostatic pressing and then densified by sintering. The material is usually presintered until 95% dense and then HIP-ed to remove residual porosity (Christel et al. 1989). Sintering can be performed without inducing grain growth, and final grain sizes can be less than 1 □m.

Zirconia has seen increasing use in dentistry as a material for crown restorations, bridges and onlays/inlays. CAD/CAM systems that can mill such restorations from a ceramic block make zirconia attractive compared to full cast metal and porcelain fused to metal restorations that require

time-consuming casting techniques to fabricate (Bona et al. 2015). Zirconia dental implants have also received much attention as an alternative to titanium due to improved aesthetics. Despite good osseointegration, zirconia implants have ncreased risk of fracture, although there is a lack of long-term clinical studies (Cionca et al. 2017).

Critical Properties of Bioinert Ceramics

Properties of bioinert ceramics important for their long-term clinical function include stiffness, strength, toughness, wear resistance and biological response. Stiffness represents a gauge of the mechanical interaction between an implant and surrounding tissue. Stiffness is a determinant of the magnitude and distribution of stresses at a biomaterial/tissue interface, and dictates the potential for stress shielding. Load-bearing biomaterials must also be designed to ensure that they maintain their structural integrity – i.e. designed to be fail-safe at stresses above peak in-service stresses for a lifetime greater than the expected service life of the prosthesis. Thus, the static (tensile, compressive and flexural strength), dynamic (high cycle fatigue) and toughness properties of ceramics, in physiological media, under a multitude of loading conditions and rates must be well-characterized.

Although knowledge of these properties is an important aspect of bioceramic design, the mechanical integrity of a bioceramic is also dependent on its processing, size and shape. Failure of ceramics usually initiates at a critical defect, at a stress level that depends on the geometry of the defect. To account for these variables and minimize the probability of failure, fracture mechanics and statistical distributions are used to predict failure probability at different load levels (Soltesz and Richter 1984).

Bioactive Ceramics

The concept of bioactivity originated with bioactive glasses via the hypothesis that the biocompatibility of an implant is optimal if it elicits the formation of normal tissues at its surface, and if it establishes a contiguous interface capable of supporting the loads which occur at the site of implantation (Hench et al. 1972). Three classes of ceramics may fulfill these requirements: bioactive glasses and glass ceramics, calcium phosphate ceramics and composites of gasses and ceramics. Incorporation of inductive factors into each of these ceramics may enhance bioactivity. These different classes of ceramics (and biological constituents) are used in a variety of applications, including: bulk implants (surface active), coatings on metal or ceramic implants (surface active), permanent bone augmentation devices/scaffold materials (surface active), temporary scaffolds for tissue engineering (surface or bulk active), fillers in cements or scaffolds (surface or bulk active), and drug delivery vehicles (bulk active).

The nature of the biomaterial/tissue interface and reactions (e.g. ion-exchange) at the ceramic surface dictate mechanical, chemical, physical and biological properties. For resorbable materials, additional design requirements include: the need to maintain strength and stability of the material/tissue interface during material degradation and host tissue regeneration; material resorption and tissue repair/regeneration rates should be matched; and the resorbable material should consist only of metabolically acceptable species.

Bioactive Glasses and Glass Ceramics

Bioactive glasses are used as bulk implants, coatings on metal or ceramic implants, and scaffolds for guiding biological therapies (Kohn and Ducheyne 1992, Hench & Best 2013, Brauer et al. 2015, Jones 2015) (Table 2). Chemical reactions are limited to the surface (~300-500□m) of the glass, and bulk properties are not affected by surface reactivity. The degree of activity and

physiologic response are dependent on the chemical composition of the glass, and may vary by over an order of magnitude.

Ceravital, a variation of Bioglass^{R}, is a glass-ceramic. The seed material is quench melted to form a glass, then heat-treated to form nuclei for crystal growth and transformation from a glass to a ceramic. Ceravital has a different alkali oxide concentration than bioglass – small amounts of alkaline oxides are added to control dissolution rates (Table 2) - but the physiological response to both glasses is similar (Gross and Strunz 1980). A glass-ceramic containing crystalline oxyapatite, fluorapatite and □-wollastonite in a glassy matrix, denoted glass-ceramic A-W, is another bioactive glass ceramic (Kitsugi et al. 1986, Kokubu et al. 1990, Nakamura et al. 1985). A-W glass-ceramic bonds to bone through a thin calcium and phosphorus-rich layer which is formed at the surface of the glass-ceramic (Kitsugi et al. 1986, Nakamura et al. 1985). *In-vitro*, if the physiological environment is correctly simulated in terms of ion concentration, pH and temperature, this layer consists of small carbonated hydroxyapatite (HA) crystallites with a defective structure, and the composition and structural characteristics are similar to those of bone (Kokubu et al. 1990).

Glass and glass-ceramics interact with the physiological microenvironment because ceramics are susceptible to surface changes in an aqueous media. Lower valence ions segregate to surfaces and grain boundaries, leading to concentration gradients and ion exchange. These reactions are dependent on the local pH and can be biologically beneficial or adverse.

When placed in physiological media, bioactive glasses leach Na^{+} ions, and subsequently K^{+}, Ca^{2+}, P^{5+}, Si^{4+} and Si-OH. These ionic species are replaced with H_3O^{+} ions from the media through an ion exchange reaction which produces a silica-rich gel surface layer. The depletion of H^{+}/H_3O^{+} ions in solution causes a pH increase, which further drives dissolution of the glass

surface. The high surface area silica-rich surface gel chelates calcium and phosphate ions, and a Ca-P-rich, amorphous apatite layer forms on top of the silica-rich layer. The amorphous Ca-P layer eventually crystallizes and CO_3^{2-} substitutes for OH^- in the apatite lattice, leading to the formation of carbonated apatite. Bioactive glasses have also been prepared with added strontium, and Sr-doped glassdownregulates RANKL while upregulating OPG, demonstrating the potential to modulate both bone resorption and formation (Fiorilli et al. 2018).

In parallel with these physical/chemical-mediated reactions, in an *in-vivo* setting, proteins adsorb/desorb from the silica gel and carbonate layers. The bioactive surface and preferential protein adsorption can enhance attachment, differentiation and proliferation of osteoblasts and secretion of an extracellular matrix (ECM). Crystallization of carbonated apatite within an ordered collagen matrix leads to an interfacial bond.

The rate of change of the glass surface, R, is quantified as the sum of the reaction rates of each stage of the reaction (Hench & Best 2013):

$$R = -k_1 t^{0.5} - k_2 t^{1.0} + k_3 t^{1.0} + k_4 t^{y} + k_5 t^{z} \quad (3)$$

where: k_i is the rate constant for each stage, i and represents, respectively, the rate of exchange between alkali cations in glass and H^+/H_3O^+ in solution (k_1), interfacial SiO_2 network dissolution (k_2), repolymerization of SiO_2 (k_3), carbonate precipitation and growth (k_4), and other precipitation reactions (k_5). Using these rates, the following design criterion may be established: the kinetics of each stage, especially Stage 4, should match the rate of biomineralization *in-vivo.* For R >> *in-vivo* rates, resorption will occur, whereas if R << *in-vivo* rates, the glass will be non-bioactive (Hench & Best 2013).

The degree of activity and physiological response (e.g. rates of formation of the Ca-P surface and glass/tissue bond) therefore depend on the glass composition and time, and are

mediated by the biomaterial, solution and cells. The dependence of reactivity and rate of bond formation on glass composition is defined by the ratio of network former to network modifier: $SiO_2/[CaO + Na_2O + K_2O]$ (Hench and Clark 1982). The higher this ratio, the less soluble the glass, and the slower the rate of bone formation. A SiO_2-Na_2O-CaO ternary diagram (Fig. 4) is useful to quantify the relationship between composition and biological response (Hench and Best 2004). The diagram may be divided into 3 zones: Zone A - bioactive bone bonding: glasses are characterized by CaO/P_2O_5 ratios > 5 and $SiO_2/[CaO + Na_2O] < 2$; Zone B – nearly inert: bone bonding does not occur (only fibrous tissue formation occurs), because the SiO_2 content is too high and reactivity is too low - these high SiO_2 glasses develop only a surface hydration layer or too dense of a silica-rich layer to enable further dissolution and ion exchange; Zone C – resorbable glasses: no bone bonding occurs because reactivity is too high and SiO_2 undergoes rapid selective alkali ion exchange with protons or H_3O^+, leading to a thick but porous unprotected SiO_2-rich film that dissociates at a high rate.

The level of bioactivity is related to bone formation via an Index of Bioactivity, I_B, which is related to the amount of time it takes for 50% of the interface to be bonded (Hench & Best 2013):

$$I_B = 100/t_{0.5BB} \quad (4)$$

The compositional dependence of the biological response may be understood by iso-I_B contours superposed onto the ternary diagram (Fig. 4). The cohesion strength of the glass/tissue interface will be a function of surface area, thickness and stiffness of the interfacial zone, and is optimum for $I_B \sim 4$ (Hench & Best 2013).

Calcium-Phosphate Ceramics

Among the calcium phosphates (Ca-P), the apatites, defined by the chemical formula $M_{10}(XO_4)_6Z_2$, are most relevant to biomaterials Apatites form a range of solid solutions as a result

of ion substitution at the M^{2+}, XO_4^{3-} or Z^- sites. The M^{2+} species is typically a bivalent metallic cation, such as Ca^{2+}or Sr^{2+}, the XO_4^{3-} species is typically PO_4^{3-}, and the monovalent Z^- ions are usually OH^- or F^- (Van Raemdonck et al. 1984). More complex ionic structures may also exist. For example, replacing the two monovalent Z^- ions with a bivalent ion, such as CO_3^{2-}, results in the preservation of charge neutrality, but one anionic position becomes vacant. The M^{2+} positions may also have vacancies; in this case, charge neutrality is maintained by vacancies at the Z^- positions or by substitution of trivalent PO_4^{3-} ions with bivalent ions (Shin et al. 2007).

The most common apatite used in medicine and dentistry is hydroxyapatite, $Ca_{10}(PO_4)_6(OH)_2$ (Fig. 5). Hydroxyapatite has ideal weight percents of: 39.9% Ca, 18.5% P and 3.38% OH and an ideal Ca/P ratio of 1.67. The crystal structure and crystallization behavior of HA are affected by ionic substitutions.

The impetus for using synthetic HA as a biomaterial stems from the hypothesis that a material similar to the mineral phase in bone and teeth will have superior binding to mineralized tissues and is therefore advantageous for replacing these tissues. Additional advantages include elastic properties similar to bone, control of *in-vivo* degradation rates through control of material properties, and the potential for ceramic to function as a barrier when coated onto a metal.

Most synthetic hydroxyapatites contain substitutions for the PO_4^{3-} and/or OH^- groups and vary from the ideal stoichiometry and Ca/P ratios. Oxyhydroxyapatite, tricalcium phosphate, tetracalcium phosphate and octocalcium phosphate have all been detected in commercially available apatite implants (Table 3) (Segvich et al. 2008b).

Synthetic apatites are processed via hydrolysis, hydrothermal synthesis and exchange, sol-gel techniques, wet chemistry, and conversion of natural bone and coral (Koeneman et al., 1990). Differences in the structure, chemistry and composition arise from differences in processing

techniques, time, temperature and atmosphere. Understanding the processing-composition-structure-processing synergy for calcium phosphates is therefore critical to understanding the *in-vivo* function of these materials. For example, at temperatures above 1050°C, HA decomposes into □-TCP and tetracalcium phosphate (Van Raemdonck et al. 1984), and at temperatures above 1350°C, □-TCP transforms into □-TCP.

Bone bonding to calcium phosphates occurs by osteoblasts secreting a mineralized matrix at the ceramic surface, resulting in a narrow, amorphous electron-dense band ~3-5□m thick. Collagen bundles form between this zone and cells. Bone mineral crystals nucleate within this amorphous zone in the form of an octocalcium phosphate precursor phase and undergo a conversion to HA. As the healing site matures, the bonding zone shrinks to ~0.05-0.2□m, and bone attaches through a thin epitaxial layer as the growing bone crystals align with apatite crystals of the material (de Brujin et al. 1995).

Calcium-phosphates are used as coatings on dense and porous implants to accelerate fixation to tissue (Kohn and Ducheyne 1992, Ducheyne et al. 1980, Oonishi et al. 1994, Ong & Chan 2017). Bond strength to bone, solubility and *in-vivo* function vary, suggesting a window of material variability in parallel with a window of biological variability.

Processing techniques used to bond Ca-P powders to substrates include plasma and thermal-spraying, sintering, ion-beam and other sputter techniques, electrophoretic deposition , sol-gel techniques, pulsed laser deposition and chemical vapor deposition (de Groot et al. 1987, Ducheyne et al. 1990, Wolke et al. 1994, Chai et al. 1998, Garcia et al. 1998). Different structures and compositions result from different processing approaches, and modulate biological reactions. For example, increased Ca/P ratios, fluorine and carbonate content, and crystallinity lead to greater stability. Ca/P ratios in the range 1.5 - 1.67 yield the most beneficial tissue response.

Much interest exists in creating synthetic apatites with altered stoichiometries. For example, strontium doped apatites increase osteoblastgenesis, while inhibiting osteoclastgenesis, and have been used as a pharmaceutical agent to treat osteoporosis. This provides a mechanism for strontium apatite to enhance bone formation (Chandran et al. 2016, Schumacher, et al. 2016).

Bioactive ceramics exhibit low strength and toughness, as the design requirement of bioactivity supercedes mechanical property requirements. Bioceramic composites have been synthesized as a means of increasing the mechanical properties of bioactive materials. Three approaches are used in developing bioceramic composites: (1) utilize the beneficial biological response to bioceramics, but reinforce the ceramic with a second phase, (2) utilize bioceramics as the second phase to achieve strength and toughness, and (3) synthesize transient scaffold materials for tissue (re)generation.

Critical Properties of Bioactive Ceramics

Important needs in bioactive ceramics research and development include: characterization of the processing-composition-structure-property synergy, characterization of *in-vivo* function, and establishing predictive relationships between *in-vitro* and *in-vivo* outcomes. Understanding reactions at the ceramic surface and increasing ceramic/tissue bond strength depend on: (1) characterization of surface activity, including surface analysis, biochemistry and ion transport, (2) physical-chemistry, pertaining to strength and degradation, stability of the tissue/ceramic interface and tissue resorption, and (3) biomechanics, as related to strength, stiffness, design, wear and tissue remodeling.

Physical/chemical properties that are important to characterize and relate to biological response include: powder particle size and shape, pore size, shape and distribution, specific surface

area, phases present, crystal structure and size, grain size, density, coating thickness, hardness and surface roughness (Table 4).

An additional factor that should be considered in evaluating chemical stability and surface activity of bioceramics is the aqueous microenvironment. The type and concentration of electrolytes in solution and the presence of proteins or cells influence how the ceramic surface changesA solution with constituents, concentrations and pH equivalent to human plasma most accurately reproduces surface changes observed *in-vivo*, whereas standard buffers do not reproduce these changes (Kokubo et al. 1990).

Surface analyses can be accomplished with solution chemical methods, such as atomic absorption spectroscopy; physical methods, such as x-ray diffraction (XRD), electron microprobe analysis (EMP), energy dispersive x-ray analysis (EDXA), Fourier transform infrared spectroscopy (FTIR); and surface sensitive methods, such as AES, x-ray photoelectron spectroscopy (XPS), and secondary ions mass spectroscopy (SIMS) (Fig. 6).

The major factors limiting expanded use of bioactive ceramics are their low tensile strength and fracture toughness. The use of bioactive ceramics in bulk form is therefore limited to applications in which service loads are compressive. Approaches that may allow ceramics to be used in sites subjected to tensile stresses include: use of the bioactive ceramic as a coating on a metal or ceramic substrate, strengthening the ceramic via crystallization or nanotechnology, and reinforcing the ceramic with a second phase (Ducheyne et al. 1980, Gross et al. 1981, Kitsugi et al. 1986, Li et al. 1995, Zhao et al. 2018, Siddiqui et al. 2018).

No matter which of these strategies is used, the ceramic must be stable, both chemically and mechanically, until it fulfills its intended function(s). The property requirements depend upon the application. For example, if a metallic total hip prosthesis is to be fixed to bone by coating the

stem with a Ca-P coating, then the ceramic/metal bond must remain intact throughout the service-life of the prosthesis. However, if the coating will be used on a porous coated prosthesis to accelerate bone ingrowth into the pores of the metal, then the ceramic/metal bond need only be stable until tissue ingrowth is achieved. A number of interfacial bond tests are available, including: pull-out, lap-shear, 3 and 4 point bending, double cantilever beam, double torsion, indentation, scratch tests, and interfacial fracture toughness tests.

Ceramics for Tissue Engineering and Biological Therapies

An ideal tissue substitute would possess the biological advantages of an autograft and supply advantages of an allograft, but alleviate the complications each of these grafts is subject to. Such a construct would also satisfy design requirements of: (1) biocompatibility, (2) osteoconductivity – it should provide an appropriate environment for attachment, proliferation and function of osteoblasts or their progenitors, leading to secretion of a new bone ECM, (3) ability to incorporate osteoinductive factors to direct and enhance new bone growth, (4) allow for ingrowth of vascular tissue to ensure survival of transplanted cells and regenerated tissue, (5) mechanical integrity to support loads at the implant site, (6) degradability, with controlled, predictable, and reproducible rate of degradation into non-toxic species that are easily metabolized or excreted, and (7) be easily processed into irregular 3D shapes. Particularly difficult is the integration of criteria (4) and (5) into one design, since transport is maximized by maximizing porosity, while mechanical properties are maximized by minimizing porosity.

One strategy to achieve these design goals is to create a composite graft in which autogenous or allogenic cells (primary cells, cell lines, genetically modified cells or stem cells) are seeded into a degradable biomaterial (scaffold) that serves as an ECM analogue and supports cell adhesion, proliferation, differentiation and secretion of a natural ECM. Following cell-seeding, cell/scaffold constructs may be immediately implanted or cultured further and then implanted. In the latter case, the cells proliferate and secrete new ECM and factors necessary for tissue growth, *in-vitro*, and the biomaterial/tissue construct is implanted as a graft. Once implanted, the scaffold is also populated by cells from host tissue. Ideally, for bone regeneration, secretion of a calcified ECM by osteoblasts and occurs concurrently with scaffold degradation. In the long-term, a functional ECM and tissue are regenerated, and are devoid of any residual synthetic scaffold.

Bone regeneration can be achieved by culturing cells capable of expressing the osteoblast phenotype onto synthetic or natural materials that mimic aspects of natural ECMs. Bioceramics that satisfy the design requirements listed above, include bioactive glasses and glass ceramics (Reilly et al. 2007, El-Rashidy et al. 2017), HA, TCP and coral (Kruyt et al. 2004, Holtorf et al. 2005, Bouler et al. 2017, Denry & Kuhn 2018), HA and HA/TCP + collagen (Kuznetsov et al. 1997, Cholas et al. 2016), and polymer/apatite composites (Shin et al. 2007, Segvich et al. 2008a, Thomson et al. 1998, Guillaume et al. 2017, Ramaraju et al. 2017, 2019**).** Varying biomaterial properties leads to a variation in biological outcome (e.g. osteoblast or progenitor cell attachment and proliferation, collagen and non-collagenous protein synthesis, RNA transcription) (Leonova et al. 2006, Puleo et al. 1991, Ducheyne et al. 1994, El-Ghannam et al. 1997, Thomson et al. 1998, Zreiqat et al. 1999, Chou et al. 2005). The nature of the scaffold also affects *in-vivo* response (e.g. progenitor cell differentiation to osteoblasts, amount and rate of bone formation, intensity or duration of any transient or sustained inflammatory response) (Ohgushi et al. 1990, Kuznetsov et al. 1997, Krebsbach et al. 1997,1998, James et al. 1999, Hartman et al. 2005, Rossello et al., 2014).

Biomimetic Ceramics

Biomimetic materials, or man-made materials that mimic select aspects of biology, are hypothesized to lead to a superior biological response. Compared to synthetic materials, natural biominerals reflect a remarkable level of control in their composition, size, shape and organization at all levels of hierarchy (Lowenstein and Weiner 1989). A biomimetic mineral surface could therefore promote preferential absorption of proteins that regulate adhesion of osteogenic precursors and cell-mediated biomineralization. The rationale for using biomimetic mineralization as a material design strategy is based on the mechanisms of biomineralization (Lowenstein and Weiner 1989, Mann and Ozin 1996) and bioactive material function (Section III). Bioactive ceramics bond to bone through a layer of bone-like apatite, which forms on the surfaces of these materials *in-vivo*, and is characterized by a carbonate-containing apatite with small crystallites and defective structure (Nakamura et al. 1985, Combes and Rey 2002, Kokubo and Takadama 2006). This type of apatite is not observed at the interface between non-bioactive materials and bone and it has been suggested, but not universally agreed upon, that non-bioactive materials do not exhibit surface-dependent cell differentiation (Ohgushi and Caplan 1999). It is therefore hypothesized that a requirement for a biomaterial to bond to bone is the formation of a biologically active bone-like apatite layer (Ducheyne 1987, Nakamura et al. 1985, Kokubo and Takadama 2006).

A bone-like apatite layer can be formed *in-vitro* at STP conditions (Murphy et al. 2000, Shin et al. 2007, 2017, Bunker et al. 1994, Wen et al. 1997, Kokubo & Yamaguchi 2019), providing a strategy to control the *in-vivo* response to a biomaterial. The basis for synthesizing bone-like mineral in a biomimetic fashion lies in the observation that in nature, organisms use macromolecules to control mineral nucleation and growth (Weiner 1986, Bunker et al. 1994). Macromolecules usually contain functional groups that are negatively charged at the crystallization pH (Weiner 1986), enabling them to chelate ions present in the surrounding media which stimulate

crystal nucleation (Bunker et al. 1994). The key requirement is to chemically modify a substrate to induce heterogeneous nucleation of mineral from a solution (Bunker et al. 1994). Biomimetic processes are guided by the pH and ionic concentration of the microenvironment, and conditions conducive to heterogeneous nucleation will support epitaxial growth of mineral (Fig. 7).

Surface functionalization may be achieved via hydrolysis, grafting, self-assembled monolayers, irradiation or alkaline treatment (Murphy et al. 2000, Shin et al. 2007, Tanahashi et al. 1995, Yamamoto et al. 1997, Wu et al. 1997, Hanawa et al. 1998, Kokubo & Yamaguchi 2019). This biomimetic strategy has been used with metals to accelerate osseointegration (Kohn 1998, Campbell et al. 1996, Wen et al. 1997, Hanawa et al. 1998, Kokubo & Yamaguchi 2016) as well as glasses, ceramics and polymers (Murphy et al. 2000, Shin et al. 2007, Segvich et al. 2008a, Hong et al. 2008, Tanahashi et al. 1995, Yamamoto et al. 1997, Wu et al. 1997, Kamei et al. 1997, Du et al. 1999, Taguchi et al. 1999, Chou et al. 2005).

As an example of this biomimetic strategy, porous polyester scaffolds incubated in a simulated body fluid (SBF, a supersaturated salt solution with a composition and ionic concentrations approximating those of plasma), exhibit coordinated surface functionalization, nucleation and growth of a continuous bone-like apatite layer on the polymer surfaces and within the pores (Fig. 8) after relatively short incubation times (Murphy et al. 2000, Shin et al. 2007, Segvich et al. 2008a). FTIR analyses confirm the nature of the bone-like mineral, and ability to control mineral composition via controlling the ionic activity product (IP) of the SBF (Fig. 9). As IP increases, more mineral grows on the scaffold pore surfaces, but the apatite is less crystalline and the Ca/P molar ratio decreases. Since mineral composition and structure affect cell function, the IP of the mineralization solution is an important modulator of both material properties and biological outcomes. Mineralization of the polymer substrate also results in a 5-fold increase in

compressive modulus, without a significant reduction in scaffold porosity (Murphy et al. 2000). The increase in mechanical properties with the addition of only a thin sheath of mineral is important in light of the competing design requirements of transport and mechanics, which frequently may only be balanced by choosing an intermediate porosity.

The self-assembly of mineral within the pores of a polymer scaffold enhances cell adhesion, proliferation and osteogenic differentiation, as well as modulates cytoskeletal organization and cell motility *in-vitro* (Rossello & Kohn 2014, Leonova et al 2006). When progenitor cells are transplanted on these materials, a larger and more spatially uniform volume of bone is regenerated, compared to unmineralized templates (Rossello & Kohn 2014). An additional benefit of biomimetic processing (room temperature, atmospheric pressure) is that growth factors and plasmid DNA can be incorporated into the mineral without concern for denaturing (Fig. 10) (Luong et al. 2006, 2009, 2012, Segvich et al. 2008a). Biomineralized materials can serve as a platform for conductive, inductive and cell transplantation approaches to regeneration, and fulfill the majority of the design requirements outlined above.

Inorganic/Organic Hybrid Biomimetics

Mineral-organic hybrids consisting of bone like apatites combined with inductive factors, can increase cell proliferation, differentiation, and bone formation. The method of combining inorganic mineral with organic factors can influence the release profile and, therefore, influence the response of cells. The most basic method of incorporating proteins into ceramics is adsorption, where the factor is loosely bound to the ceramic surface by submersion or pipetting. A second way of incorporating protein with apatite is to create microcarriers that allow HA crystals to form in the presence of protein or allow protein to adsorb to the HA (Ijntema et al. 1994) Barroug and

Glimcher 2002, Matsumoto et al. 2004). A third method of protein incorporation is coprecipitation, in which protein is added to SBF and becomes incorporated into the bone-like apatite during calcium phosphate precipitation. Organic/inorganic hybrids combine the osteoconductive properties provided by the apatite with the osteoinductive potential provided by growth factors, DNA, and peptides.

Through coprecipitation, BMP-2 has been incorporated into biomimetic coatings deposited on titanium, and biological activity has been retained (Liu et al. 2004). Biomolecules can be incorporated at different stages of calcium phosphate nucleation and growth (Fig. 10) (Luong et al. 2006, Azevedo et al. 2005), enabling spatial localization of the biomolecule through the apatite thickness, and controlling its release. With spatial localization, there is also the potential for delivery of multiple biomolecules.

Techniques used to incorporate growth factors into bone-like mineral can also be used to incorporate genes. One of the most common methods of gene delivery is to encapsulate DNA within a Ca-P precipitate (Jordan et al 1996). This method protects DNA from degradation and encourages cellular uptake, but DNA is released in a burst. By utilizing coprecipitation to incorporate plasmid DNA into a biomimetic apatite layer, more sustained release can be achieved (Luong et al., 2009). The mineral increases substrate stiffness, which also enhances cellular uptake of plasmid DNA (Kong et al. 2005).

Following co-precipitation, the release of biological factors and resultant biological responses are influenced by many variables, including the concentration of the factor, the expression of the receptors that are affected by the presence of the factor, the physical characteristics of the delivery substrate and mineral/organic coating, and the site of implantation. Release kinetics can be controlled via diffusion of the biological factor, dissolution/degradation of

the carrier and/or osmotic effects. For delivery systems based on co-precipitation of a biological molecule with a biomineral, the dissolution mechanisms of mineral are the most important.

Mineral dissolution is controlled by factors associated with the solution (pH, saturation), bulk solid (solubility, chemical composition), and surface (adsorbed ions, phases). The apatite that is typically formed from a supersaturated ionic solution is carbonated (Shin et al. 2007). The presence of carbonate in an apatite lattice influences crystallinity and solubility (McElderry et al. 2013). The dissolution rate of carbonated HA depends pH, and occurs with the protonation of the carbonate or phosphate group to form either carbonic acid or phosphoric acid (Hankermeyer et al. 2002).

Proteins simply adsorbed to an apatite surface are released in a burst, with most of the protein released within the first 6 hours. In comparison, less than 1% of the protein incorporated within bone-like apatite is released after 5 days (Liu et al. 2001). With coprecipitation, a sustained release occurs because protein is incorporated within the apatite matrix, rather than just a superficial association (Liu et al. 2001). The affinity a protein has for apatite influences the dissolution rate of the mineral and, therefore, the release rate. Since protein release is proportional to apatite dissolution, the possibility of temporally controlling the release profile, as well as developing multi-factor delivery systems is possible due the ability to spatially localize the protein within the biomimetically nucleated mineral (Luong et al. 2006, 2012).

In addition to controlling cell function via biomolecular incorporation within apatite, another strategy is to present biomolecules on a biomimetic surface. While the objective of coprecipitation is to control spatial and temporal release of biomolecules, the objective of presenting peptides with conformational specificity on a material surface is to recruit a population of cells that can initiate the early stages of bone regeneration. Proteins, growth factors, and peptides have been ionically

or covalently attached to biomaterial surfaces to increase cell adhesion, and ultimately, the amount of tissue regeneration. Proteins are prone to degradation and can change conformation because they possess domains with varying hydrophobicities. On the other hand, peptides can mimic the same response as a protein while being smaller, cheaper, and less susceptible to degradation. Peptides have a greater potential for controlling initial biological activity, because they can contain specific target amino acid sequences and can permit control of hydrophilic properties through sequence design (Ladner et al. 2004).

Identification of cell recognition sequences has motivated the development of bioactive materials that can recruit cells to adhere to a material surface via specific integrin mediated bonding. One peptide sequence that interacts with a variety of cell adhesion receptors is the RGD (Arg-Gly-Asp) sequence. Other peptide sequences have been designed to mimic sections of the ECM proteins bone sialoprotein, osteopontin, fibronectin, statherin, elastin and osteonectin (Fujisawa et al. 1997, Gilbert et al. 2000, Simionescu et al. 2005). Peptide sequences with preferential affinity to HA and bone-like mineral have been discovered using phage display libraries (Segvich et al. 2009).

Non-specific adsorption of peptides onto the surface of bioceramics can be a simple but sufficient method for inducing a biological reaction. An excellent example of this is the P15 peptide, a collagen derived peptide that supports bone formation when adsorbed onto HA. Pepgen-P15, is a commercially available product that consists of P15 peptide adsorbed onto bovine derived bone particles (Gomar et al. 2007). RGD peptides have also been adsorbed onto HA, but reduce cell adhesion due to competing interactions with serum proteins such as fibronectins (Hennessy et al. 2008).

The lack of affinity of many of these peptides to apatite results in poor adsorption or non-optimal orientation, the development of more effective ways to functionalize ceramic surfaces. One strategy is to use chemical crosslinking to covalently couple the active domains of the peptide onto the ceramic the surface. For example, silane agents can react with hydroxyl groups on the surface of zirconia to functionalize the surface with chemically active groups such as amines, carboxylates, or alkyl halides. Subsequently, proteins and peptides can be coupled via amino and carboxyl groups with the aid of crosslinking agents (Fernandez-Garcia et al. 2015).

Covalent coupling is not effective for calcium phosphate ceramics such as hydroxyapatite due to their ionic nature. Another strategy is to use peptide sequences with preferential affinity for apatite. Polyglutamate sequences have high affinity for HA via electrostatic binding due to their strong negative charge and are found in naturally occurring bone-binding proteins such as osteonectin (Fujisawa et al. 1997). Phage display, a high throughput screening technique, has been used to identify peptides with strong affinity for apatite. These peptides include the VTKHLNQISQSY (VTK) sequence, which has preferential affinity for the biomimetic carbonated apatite found in bone like mineral (BLM) versus highly crystalline stoichiometric HA (Segvich et al. 2009) and SVSVGMKPSPRP (Roy et al. 2008).

While these mineral binding sequences have no inherent cell-binding capabilities, they can be coupled to cell binding sequences. For example, the sequence EEEEEEEPRGDT contains both polyglutamate and RGD, and increases osteoblast attachment and differentiation on mineral substrates (Fujisawa et al. 1997, Itoh et al. 2002). Collagen derived peptide DGEA has also been combined with polyglutamate, resulting in 9 times greater loading onto allograft and significantly increased peptide density (Culpepper et al. 2012). The VTK peptide was coupled to a mesenchymal stem cell binding peptide DPIYALSWSGMA (DPI) and the dual-peptide DPI-VTK

enhanced attachment of MSCs to mineralized scaffolds (Ramaraju et al 2017). Interestingly, this dual peptide retains its high affinity for hydroxyapatite despite containing no net charge. DPI-VTK mediates both the magnitude and specificity of MSC attachment to biomimetic apatite (Ramaraju et al. 2017). When adsorbed onto 3-dimentional mineralized scaffolds and seeded with iPS-MSCs, DPI-VTK increased bone and vasculature formation in vivo (Ramaraju et al. 2019).

Hydroxyapatite nanoparticles are another application of inorganic/organic hybrid materials. Different preparation methodologies have been used, including chemical precipitation, emulsions, electrospraying, vapor deposition, and hydrothermal methods (Haider et al. 2017). Bioactive molecules can be incorporated into nanoparticles through encapsulation, co-precipitation, and surface adsorption (Munir et al. 2018, Xie et al. 2010). Growth factors such as BMP-2 have been incorporated into these particles for controlled delivery (Xie et al. 2010). Another potential application of nanoparticles is a controlled release system for antibiotics for the treatment of bone infections (Munir et al. 2018). HA nanoparticles have also been used to fabricate larger and more complex constructs such as microspheres (Bi et al. 2019).

Summary

Bioceramics have a long clinical history, especially in skeletal reconstruction and regeneration. Bioceramics are classified as relatively inert (a minimal tissue response is elicited and a layer of fibrous tissue forms adjacent to the implant), surface-active (partially soluble, resulting in surface ion exchange with the microenvironment and leading to a direct chemical bond with tissue), and bulk bioactive (fully resorbable, with the potential to be completely replaced with *de-novo* tissue). Ceramics are processed via conventional materials science strategies, as well as strategies inspired by nature. The biomimetic approaches discussed above, along with all other

strategies to reproduce the design rules of biological systems, do not completely mimic nature. Instead, just selected biological aspects are mimicked. However, if the selected biomimicry is rationally designed into biomaterial, then the biological system will be able to respond in a more controlled, predictable and efficient manner, providing an exciting new arena for biomaterials research and development.

References

Allen M, Myer B, Rushton N, *J Biomed Mater Res (Appl Biomat)* 58: 319-328, 2001.
Azevedo HS, Leonor IB, Alves CM, Reis RL, *Mat Sci Eng C – Bio S*, 25: 169, 2005.
Barroug A, Glimcher MJ, *J Orthop Res* 20: 274, 2002.
Bi Y, Lin Z, Deng S, *Mater. Sci. Eng. C* 100**:** 576–583, 2019.
Bokros JC, *Trans. Biomed. Mater. Res. Symp*. 2: 32-36, 1978.
Bokros JC, LaGrange LD, Schoen GJ, In: *Chemistry and Physics of Carbon*, Walker PL, Ed, New York: Dekker, Vol. 9, pp. 103-171, 1972.
Bona, A. Della, Pecho, O. E. & Alessandretti, R. *Materials (Basel).* 8**:** 4978–4991, 2015.
Bouler JM, Pilet P, Gauthier O, Verron E. *Acta Biomater.* 53: 1-12, 2017.
Boutin P, Christel P, Dorlot JM, Meunier A, de Roquancourt A, Blanquaert D, Herman S, Sedel L, Witvoet J, *J Biomed Mater Res* 22: 1203-1232, 1988.
Brauer DS. *Angew Chem Int,* 54: 4160-4181, 2015.
Bunker BC, Rieke PC, Tarasevich BJ, Campbell AA, Fryxell GE, Graff GL, Song L, Liu J, Virden JW, McVay GL, *Science* 264: 48-55, 1994.
Cales B, Stefani Y, In: *Biomedical Engineering Handbook*, Bronzino JD, Ed, CRC Press, Boca Raton, FL, pp. 415-452, 1995.
Campbell AA, Fryxell GE, Linehan JC, Graff GL, *J Biomed Mater Res* 32: 111-118, 1996.
Cancian G, Tozzi G, Hussain, A. A. Bin, De Mori, A. & Roldo, M. *J. Mater. Sci. Mater. Med.* 27: 1–10 (2016).
Chandran S, Suresh Babu S, Hari Krishnan VS, Varma HK, John A, *J. Biomater. Appl.* 31, 499–509. 2016.
Chai CS, Gross KA, Ben-Nissan B, *Biomat* 19: 2291-2296, 1998.
Chen YW, Moussi J, Drury JL, Wataha JC, *Expert Rev Med Devices*. 13: 945-963, 2016.
Cholas R, Kunjalukkal Padmanabhan S, Gervaso F, Udayan G, Monaco G, Sannino A, Licciulli A, *Mater Sci Eng C Mater Biol Appl,* 63: 499-505, 2016.
Chou YF, Huang W, Dunn JCY, Miller TA, Wu BM, *Biomat* 26: 285-295, 2005.
Christel P, Meunier A, Leclercq S, Bouquet P, Buttazzoni B, *J Biomed Mater Res: Appl Biomat* 21(A2): 191-218, 1987.
Christel P, Meunier A, Heller M, Torre JP, Peille CN, *J Biomed Mater Res* 23: 45-61, 1989.
Cionca N, Hashim D, Mombelli A, *Periodontology 2000,* 73**,** 241–258, 2017.
Combes C, Rey C, *Biomat* 23: 2817-2823, 2002.
Culpepper BK, Bonvallet PP, Reddy MS, Ponnazhagan S, Bellis SL *Biomaterials* 34**,** 1506–1513, 2013.
de Bruijn JD, van Blitterswijk CA, Davies JE, *J Biomed Mater Res* 29: 89-99, 1995.
de Groot K, Geesink RGT, Klein CPAT, Serekian P, *J Biomed Mater Res* 21: 1375-1381, 1987.
Denry I, Kuhn LT, *Dent Mater,* 32: 43-53, 2016.
Dorre E, Dawihl W, In: *Mechanical Properties of Biomaterials*, Hastings GW, Williams DF, Eds, New York, Wiley, pp. 113-127, 1980.
Du C, Cui FZ, Zhu XD, de Groot K, *J Biomed Mater Res* 44: 407-415, 1999.
Ducheyne P, *J Biomed Mater Res* 19: 273-291, 1985.
Ducheyne P, *J Biomed Mater Res: Appl Biomat*, 21(A2): 219-236, 1987.
Ducheyne P, Hench LL, Kagan A, II, Martens M, Bursens A, Mulier JC, *J Biomed Mater Res* 14: 225-237, 1980.
Ducheyne P, Radin S, Heughebaert M, Heughebaert JC, *Biomat* 11: 244-254, 1990.

Ducheyne P, El-Ghannam A, Shapiro I, *J Cell Biochem* 56: 162-167, 1994.
El-Ghannam A, Ducheyne P, Shapiro IM, *J Biomed Mater Res* 36: 167-180, 1997.
El-Rashidy AA, Roether JA, Harhaus L, Kneser U, Boccaccini AR. *Acta Biomater,* 62: 1-28, 2017.
Fernandez-Garcia E, *et al.*, *J. Dent.* 43, 1162–1174, 2015.
Filiaggi MJ, Pilliar RM, Yakubovich R, Shapiro G, *J Biomed Mater Res (Appl Biomat)* 33: 225-238, 1996.
Fiorilli S, *et al., Materials (Basel).* 11, 2018.
Fujisawa R, Mizuno M, Nodasaka Y, Kuboki Y, *Matrix Biol* 16: 21, 1997..
Garcia F, Arias JL, Mayor B, Pou J, Rehman I, Knowles J, Best S, Leon B, Perez-Amor M, Bonfield W, *J Biomed Mater Res (Appl Biomat)* 43: 69-76, 1998.
Gilbert M, Shaw WJ, Long JR, Nelson K, Drobny GP, Giachelli CM, Stayton PS, *J Biol Chem* 275: 16213, 2000.
Gomar F, Orozco R, Villar JL, Arrizabalaga F, *Int. Orthop.* 31**,** 93–99, 2007.
Gross U, Strunz V, *J Biomed Mater Res* 14: 607-618, 1980.
Gross U, Brandes J, Strunz V, Bab I, Sela J, *J Biomed Mater Res* 15: 291-305, 1981.
Guillaume O, Geven MA, Sprecher CM, Stadelmann VA, Grijpma DW, Tang TT, Qin L, Lai Y, Alini M, de Bruijn JD, Yuan H, Richards RG, Eglin D. *Acta Biomater,* 54: 386-398, 2017.
Haider A, Haider S, Han SS, Kang IK, *RSC Adv.* 7**,** 7442–7458, 2017.
Hanawa T, Kon M, Ukai H, Murakami K, Miyamoto Y, Asaoka K, *J Biomed Mater Res* 41: 227-236, 1998.
Hankermeyer CR, Ohashi KL, Delaney DC, Ross J, Constantz BR, *Biomat* 23: 743, 2002.
Hannouche D, Zaoui A, Zadegan F, Sedel L, Nizard R, *Int Orthop*. 35: 207-213, 2011.
Hartman EHM, Vehof JWM, Spauwen PHM, Jansen JA, *Biomat* 26: 1829-1835, 2005.
Heimke G, Leyen S, Willmann G. *Biomaterials*. 23: 1539-1551, 2002.
Hench LL, Best SM, In: *Biomaterials Science: An Introduction to Materials in Medicine, 3rd Ed,* Ratner BD, Hoffman AS, Schoen FJ, Lemons JE, Eds, London, Elsevier Academic Press, pp. 128-151, 2013.
Hench LL, Clark AE, In: *Biocompatibility of Orthopaedic Implants*, Vol II, Williams DF, Ed, Boca Raton, FL, CRC Press, pp. 129-170, 1982.
Hench LL, Ethridge EC, *Biomaterials An Interfacial Approach*, New York, Academic Press, 1982.
Hench LL, Splinter RJ, Allen WC, Greenlee TK Jr, *J Biomed Mater Res Symp*, 2: 117-141, 1972.
Hennessy KM, Pollot BE, Clem WC, et al., *Biomaterials*. 2009;30(10):1898-1909, 2008.
Holtorf HL, Sheffield TL, Ambrose CG, Jansen JA, Mikos AG, *Ann Biomed Eng* 33: 1238-1248, 2005.

Hong SI, Lee KH, Outslay ME, Kohn DH, *J Mater Res* 23: 478-485, 2008.

Ijntema K, Heuvelsland WJM, Dirix C, Sam AP, **Int J Pharm** ***112: 215, 1994.***
Itoh D, *et al., J. Biomed. Mater. Res.* 62: 292–298, 2002.

James K, Levene H, Parson JR, Kohn J, **Biomat** ***20: 2203-2212, 1999.***
Jing, Z. *et al., Ann. Biomed. Eng.* 45: 2075–2087, 2017.
Jones JR *Acta Biomater,* Suppl: S53-82, 2015.
Jordan M, Schallhorn A, Wurm FM, *Nucleic Acids Res* 24: 596, 1996..
Kamei S, Tomita N, Tamai S, Kato K, Ikada Y, *J Biomed Mater Res* 37: 384-393, 1997.
Kitsugi T, Yamamuro T, Nakamura T, Higashi S, Kakutani Y, Hyakuna K, Ito S, Kokubo T, Takagi M, Shibuya T, *J Biomed Mater Res* 20: 1295-1307, 1986.
Koeneman J, Lemons J, Ducheyne P, Lacefield W, Magee F, Calahan T, Kay J, *J Appl Biomat* 1: 79-90, 1990.
Kohn DH, *Curr Opin Solid State Mater Sci* 3: 309-316, 1998.
Kohn DH, Ducheyne P, Materials for Bone, Joint and Cartilage Replacement, In: *Medical and Dental Materials*, DF Williams Ed, VCH Verlagsgesellschaft, FRG, 29-109, 1992.
Koistinen A, Santavirta SS, Kroger H, Lappalainen R, *Biomat* 26: 5687-5694, 2005.
Kokubo T, Ito S, Huang ZT, Hayashi T, Sakka S, Kitsugi T, Yamamuro T, *J Biomed Mater Res* 24: 331-343, 1990.
Kokubo T, Takadama H, *Biomat* 27: 2907-2915, 2006.
Kokuno T, Yamaguichi S, *Acta Biomater* 44:16-30, 2016.
Kokubo T, Yamaguichi S, *J Biomed Mater Res A* 107: 968-977, 2019.
Kong HJ, Liu JD, Riddle K, Matsumoto T, Leach K, Mooney DJ, *Nat Mater* 4: 460, 2005..
Krebsbach PH, Kuznetsov SA, Satomura K, Emmons RVB, Rowe DW, Gehron-Robey P, *Transplantation* 63: 1059-1069, 1997.
Krebsbach PH, Mankani MH, Satomura K, Kuznetsov SA, Gehron-Robey P, *Transplantation*, 66: 1272-1278, 1998.
Kruyt MC, Dhert WJA, Yuan H, Wilson CE, van Blitterswijk CA, Verbout AJ, de Bruijn JD, *J Orthop Res* 22: 544-551, 2004.
Kuznetsov SA, Krebsbach PH, Satomura K, Kerr J, Riminucci M, Benayahu D, Gehron-Robey P, *J Bone Min Res* 12: 1335-1347, 1997.
Ladner RC, Sato AK, Gorzelany J, de Souza M, *Drug Discov Today* 9: 525, 2004.
Leonova EV, Pennington KE, Krebsbach PH, Kohn DH, *J Biomed Mater Res*, *Part A* 79A: 263-270, 2006.
Li J, Fartash B, Hermansson L, *Biomat* 16: 417-422, 1995.
Liu YL, Hunziker EB, Layrolle P, de Bruijn JD, de Groot K, *Tissue Eng* 10: 101, 2004.
Liu YL, Layrolle P, de Bruijn J, van Blitterswijk C, de Groot K, *J Biomed Mater Res* 57: 327, 2001.
Lowenstein HA, Weiner S, *On Biomineralization*, Oxford Univ. Press, Oxford, 1989.
Luong LN, Hong SI, Patel RJ, Outslay ME, Kohn DH, *Biomat* 27: 1175-1186, 2006.
Luong LN, McFalls KM, Kohn DH, *Biomater* 30: 6996-7004, 2009.
Luong LN, Ramaswamy J, Kohn DH, *Biomater* 33: 283-294, 2012.
Lusty PJ, Watson A, Tuke MA, Walter WL, Walter WK, Zicat B, *J Bone Joint Surg* 89B: 1158-1164, 2007.
Mann S, Ozin GA, *Nature* 382: 313-318, 1996.

Mantripragada VP, Lecka-Czernik B, Ebraheim NA, Jayasuriya AC, *J Biomed Mater Res A*. 101: 3349–3364, 2013.
Matsumoto T, Okazaki M, Inoue M, Yamaguchi S, Kusunose T, Toyonaga T, Hamada Y, Takahashi J, *Biomat* 25: 3807, 2004.
McElderry JD, Zhu P, Mroue KH, Xu J, Pavan B, Fang M, Zhao G, McNerny E, Kohn DH, Franceschi RT, Banaszak Holl MM, Tecklenburg MM, Ramamoorthy A, Morris MD, *J Solid State Chem* 206: 192-198, 2013.
Miller RA, Smialek RG, Garlick, In: Advances in Ceramics Vol. 3, *Science and Technology of Zirconia*, Westerville, OH, American Ceramic Society, 1981, p. 241.
More RB, Haubold AD, Bokros JC, Pyrolytic Carbon for Long Term Medical Implants, In: *Biomaterials Science: An Introduction to Materials in Medicine, 2nd Ed.,* BD Ratner, AS Hoffman, FJ Schoen, JE Lemons, Eds., Elsevier Academic Press, London, pp 171–180, 2004.

Munir M, U. *et al. Int. J. Pharm.* 544**:** 112–120, 2018.

Murphy WL, Kohn DH, Mooney DJ, *J Biomed Mater Res* 50: 50-58, 2000.
Nakamura T, Yamamuro T, Higashi S, Kokubo T, Ito S, *J Biomed Mater Res* 19: 685-698, 1985.
Newman P, Minett A, Ellis-Behnke R, Zreiqat H, *Nanomedicine Nanotechnology, Biol. Med.* 9**:** 1139–1158. 2013.
Nizard R, Pourreyron D, Raould A, Hannouche D, Sedel L, *Clin Orthop Rel Res* 466: 317-323, 2008.
Ohgushi H, Caplan AI, *J Biomed Mater Res (Appl Biomat)* 48: 913-927, 1999.
Ohgushi H, Okumura M, Tamai S, Shors EC, Caplan AI, *J Biomed Mater Res* 24: 1563-1570, 1990.
Ong JL, Chan DCN. *Crit Rev Biomed Eng*. 45: 411-451, 2017.
Oonishi H, Noda T, Ito S, Kohda A, Ishimaru H, Yamamoto M, Tsuji E, *J Appl Biomat* 5: 23-37, 1994.
Popat KC, Desai TA, Alumina, In: In: *Biomaterials Science: An Introduction to Materials in Medicine, 3rd Ed.,* BD Ratner, AS Hoffman, FJ Schoen, JE Lemons, Eds., Elsevier Academic Press, London, pp 162-166, 2013.
Puleo DA, Holleran LA, Doremus RH, Bizios R, *J Biomed Mater Res* 25: 711-723, 1991.
Ramaraju H, Miller SJ, Kohn DH, *Biomaterials* 134**:** 1–12, 2017.
Ramaraju H, Kohn, DH, *Adv. Healthc. Mater.* 1801356**:** 1–11, 2019.
Reikeras O, Johansson CB, Sundfeldt M, *J Long Term Effects of Med Impl* 14: 443-454, 2004.
Reilly GC, Radin S, Chen AT, Dycheyne P, *Biomat* 28: 4091-4097, 2007.
Rossello RA, Kohn DH, *J Tissue Sci Eng* S1: 005, 2014.
Roy MD, Stanley SK, Amis E. J. & Becker, M. L. *Adv. Mater.* 20**,** 1830–1836, 2008.
Schumacher, M. *et al.* 37**,** 184–194, 2016.
Segvich SJ, Smith HC, Luong LN, Kohn DH, *J Biomed Mater Res, Part B,* 84B: 340-349, 2008.
Segvich SJ, Smith HC, Kohn DH, *Biomater* 30: 1287-1298, 2009.
Segvich SJ, Luong LN, Kohn DH, Biomimetic approaches to synthesize mineral and mineral/ organic biomaterials, In: *Biomaterials and Biomedical Engineering*, W Ahmed, N Ali, A Öchsner, Eds, Trans Tech Publications, Ltd, UK, 2008b.
Shi, X, Hudson JL, Spicer PP, Tour JM, Krishnamoorti R, Mikos AG, *Biomacromol* 7: 2237-2242, 2006.

Shin K, Acri T, Geary S, Salem AK. *Tissue Eng Part A*. 19-20: 1169-1180, 2017.
Shin K, Jayasuriya AC, Kohn DH, *J Biomed Mater Res Part A,* 83A: 1076-1086, 2007.
Siddiqui HA, Pickering KL, Mucalo MR. *Materials* 11: E1813, 2018.
Simionescu A, Philips K, Vyavahare N, *Biochem Biophys Res Commun*, 334:524–532, 2005.
Soltesz U, Richter H, In: *Metal and Ceramic Biomaterials Volume II Strength and Surface*, Ducheyne P, Hastings GW, Eds, Boca Raton, FL, CRC Press pp. 23-61, 1984.
Taguchi T, Shiraogawa M, Kishida A, Arashi M, *J Biomater Sci Polymer Edn* 10: 19-31, 1999.
Tanahashi M, Yao T, Kokubo T, Minoda T, Miyamoto T, Nakamura T, Yamamuro T, *J Biomed Mater Res* 29: 349-357, 1995.
Tateiwa T, Clarke IC, Williams PA, Garino J, Manaka M, Shishido T, Yamamoto K, Imakiire A. *Am J Orthop*, 37: E26-31, 2008.
Thomson RC, Yaszemski MJ, Powers JM, Mikos AG, *Biomat* 19: 1935-1943, 1998.
Van Raemdonck W, Ducheyne P, De Meester P, In: *Metal and Ceramic Biomaterials Volume II Strength and Surface*, Ducheyne P, Hastings GW, Eds, Boca Raton, FL, CRC Press pp. 143-166, 1984.
Walter A, Lang W, In: *Biomedical Materials* - Mater. Res. Soc. Symp. Proc. Vol. 55,. Williams JM, Nichols MF, Zingg W, Eds, Materials Research Society, Pittsburgh, PA, pp. 181-190, 1986.

Webster TJ, Ergun C, Doremus RH, Siegel RW, Bizios R, **J Biomed Mater Res** ***51: 475-483, 2000.***
Weiner S, *CRC Crit Rev Biochem* 20: 365-408, 1986.
Wen HB, de Wijn JR, Cui FZ, de Groot K, *J Biomed Mater Res* 35: 93-99, 1997.

Wolke JGC, van Dijk K, Schaeken HG, de Groot K, Jansen JA, *J Biomed Mater Res* 28: 1477-1484, 1994
Wu W, Zhuang H, Nancollas GH, *J Biomed Mater Res* 35: 93-99, 1997.
Xie G, Sun J, Zhong G, Liu C, Wei J, *J. Mater. Sci. Mater. Med.* 21: 1875–1880. 2010.
Yamamoto M, Kato K, Ikada Y, *J Biomed Mater Res* 37: 29-36, 1997.
Yang S *et al, Biomed. Mater.* 12: 2017.
Zanello LP, Zhao B, Hu H, Haddon RC, *Nano Letters* 6: 562-567, 2006.
Zhao X, Yang J, Xin H, Wang X, Zhang L, He F, Liu Q, Zhang W, *Mater Sci Eng C Mater Biol Appl.* 91: 135-145, 2018.
Zreiqat H, Evans P, Howlett CR, *J Biomed Mater Res* 44: 389-396, 1999.

Acknowledgements:

Parts of the authors' research discussed in this Chapter were supported by NIH/NIDCR R01 DE 026116 and F30 DE 028